

AUTOMATED APPROACHES FOR THE EARLY-STAGE DISTINGUISHING OF PALMER  
AMARANTH FROM WATERHEMP

A Thesis  
Submitted to the Graduate Faculty  
of the  
North Dakota State University  
of Agriculture and Applied Science

By  
Akhil Venkataraju

In Partial Fulfillment of the Requirements  
for the Degree of  
MASTER OF SCIENCE

Major Department:  
Computer Science

August 2022

Fargo, North Dakota

North Dakota State University  
Graduate School

---

**Title**

AUTOMATED APPROACHES FOR THE EARLY-STAGE  
DISTINGUISHING OF PALMER AMARANTH FROM WATERHEMP

---

**By**

Akhil Venkataraju

---

The Supervisory Committee certifies that this *disquisition* complies with North Dakota  
State University's regulations and meets the accepted standards for the degree of

**MASTER OF SCIENCE**

SUPERVISORY COMMITTEE:

Dr. Ravi Kiran Yellavajjala

---

Chair

Dr. Thomas Peters

---

Dr. Simone Ludwig

---

Approved:

11/02/2022

---

Date

Dr. Simone Ludwig

---

Department Chair

## **ABSTRACT**

Palmer amaranth is an invasive pigweed species, possessing rapid growth, posing a threat to the economy of crops including corn. Its early detection and mitigation are of utmost importance; however, it is visually similar to waterhemp in the early growth stages. In this study, automated approaches are employed to distinguish palmer amaranth from waterhemp, within two weeks after emergence, from their RGB images. Morphological characteristics of these weeds are estimated and fed to several Machine Learning (ML) models. To improve classification accuracy, RGB images are augmented, and a Convolutional neural network is trained on 16000 images. Validated on images embedded with gaussian noise, it produced a better accuracy compared to ML approaches. Finally, YOLOv5, an object detection algorithm based on transfer learning, is successfully prepared. Tested on synthetic images consisting of both weeds, YOLOv5 successfully detected a significantly high number of palmer amaranth objects while also distinguishing it from waterhemp.

## ACKNOWLEDGMENTS

I would like to thank the Divine Grace for always guiding me and providing for me.

I would like to express my sincere gratitude and deep appreciation to my advisor Dr. Ravi Kiran Yellavajjala for the guidance, and the assistance provided throughout my research. The motivation provided by him has been phenomenal and has constantly inspired me to perform better and to think higher.

I would like to thank the members of my dissertation committee, Dr. Thomas Peters and Dr. Simone Ludwig for generously offering their precious time, valuable suggestions, and guidance throughout my tenure here at NDSU. I would also like to thank all the members of Damage in Materials and Structures (DAMS) Research Group for the moral support and the helpful discussions.

Finally, I would like to acknowledge with gratitude my inspiration, my parents, and the continued support and love of my sister, and friends throughout my career, and my graduate program in particular.

## **DEDICATION**

To my family and teachers.

## TABLE OF CONTENTS

ABSTRACT.....	iii
ACKNOWLEDGMENTS .....	iv
DEDICATION.....	v
LIST OF TABLES .....	viii
LIST OF FIGURES .....	ix
1. INTRODUCTION .....	1
1.1. Motivation .....	1
1.2. Research gaps.....	5
1.3. Research objectives .....	6
1.4. Dissertation organization.....	6
2. A REVIEW OF MACHINE LEARNING TECHNIQUES FOR IDENTIFYING WEEDS IN CORN.....	7
2.1. Introduction .....	7
2.2. Machine Learning .....	9
2.3. Support Vector Machines.....	12
2.4. Neural networks .....	19
2.5. Miscellaneous models for identification of weeds.....	30
2.6. Dataset size, data augmentation, transfer learning, and performance metrics .....	48
2.7. Conclusion and future research directions for the identification of weeds in corn .....	53
3. DISTINGUISHING PALMER AMARANTH FROM WATERHEMP IN THE FIRST TWO WEEKS .....	61
3.1. Palmer amaranth and waterhemp image acquisition.....	62
3.2. Morphological characteristics .....	66
3.3. Machine Learning .....	72
3.4. Convolutional Neural Networks (CNN) .....	75

3.5. Object detection and transfer learning .....	82
3.6. Results .....	87
4. CONCLUSIONS.....	90
5. FUTURE RESEARCH DIRECTION.....	92
REFERENCES .....	94

## LIST OF TABLES

<u>Table</u>	<u>Page</u>
1.1. Comparison between the morphological characteristics of palmer amaranth and waterhemp. ....	5
2.1. Summary of studies that employed SVMs for the identification of weeds. ....	17
2.2. Summaries of studies that employed Neural networks for the identification of weeds.....	28
2.3. Summaries of studies that employed miscellaneous models for the identification of weeds. ....	45
2.4. Definitions of a classifier predictions. ....	51
2.5. Mathematical definitions of performance metrics. ....	51
3.1. Experiment details. ....	64
3.2. Performance comparison of different ML algorithms employed in the study.....	74
3.3. Augmentation techniques applied to original images of palmer amaranth.....	77
3.4. The network structure of CNN configured for the classification of palmer amaranth and waterhemp. ....	80
3.5. Tuned hyperparameters for the employed CNN model.....	81
3.6. Actual and predicted class labels of palmer amaranth and waterhemp. ....	81
3.7. Summary of results obtained for Object detection using YOLO V5.....	87
3.8. Object detection results summary.....	87



## LIST OF FIGURES

<u>Figure</u>	<u>Page</u>
1.1. Workflow of ML models. ....	10
2.2. Confusion matrix for a binary classification.....	52
2.3. Receiver-Operating characteristic (ROC) curves. ....	53
2.4. Frequency distribution of different ML approaches used in the reviewed articles.....	54
2.5. Frequency distribution of different ML problems focused on the reviewed articles.....	55
2.6. Frequency distribution of different data types used in the reviewed articles. ....	56
3.1. Palmer amaranth captured 8 days after emergence: (a) 25 centimeters from the soil surface; (b) 20 centimeters from the soil surface, and (c) close to the soil surface. ....	63
3.2. Waterhemp captured 8 days after emergence: (a) 25 centimeters from the soil surface; (b) 20 centimeters from the soil surface, and (c) close to the soil surface. ....	64
3.3. (a) Original image of palmer amaranth, (b) Palmer amaranth after background removal.....	65
3.4. (a) Original image of waterhemp, (b) Waterhemp after background removal. ....	66
3.5. Evolution of aspect ratio for palmer amaranth (8 to 14 DAE). ....	67
3.6. Evolution of circularity for palmer amaranth (8 to 14 DAE). ....	68
3.7. Evolution of roundness for palmer amaranth (8 to 14 DAE).....	68
3.8. Comparison of evolution of aspect ratio of palmer amaranth with that of waterhemp (8 to 14 DAE). ....	69
3.9. Comparison of evolution of circularity of palmer amaranth with that of waterhemp (8 to 14 DAE). ....	69
3.10. Comparison of evolution of roundness of palmer amaranth with that of waterhemp (8 to 14 DAE).....	70
3.11. Aspect ratios of palmer amaranth and waterhemp (8 to 14 DAE).....	71
3.12. Circularity of palmer amaranth and waterhemp (8 to 14 DAE). ....	71
3.13. Roundness of palmer amaranth and waterhemp (8 to 14 DAE). ....	72

3.14. Architecture of CNN employed in the study for the classification of palmer amaranth and waterhemp. ....	75
3.15. Types of pooling operations used after convolution operations. ....	76
3.16. (a) Palmer amaranth after addition of Gaussian noise, (b) Waterhemp after addition of Gaussian noise. ....	79
3.17. General architecture of Transfer learning. ....	84
3.18. Samples of palmer amaranth and waterhemp from original images randomly distributed to construct images for object detection. ....	85
3.19. Labelled images of individual samples of palmer amaranth and waterhemp obtained from the trained YOLO V5 model. YOLO V5 uses bounding boxes to localize individual image objects. ....	86

# 1. INTRODUCTION

## 1.1. Motivation

Palmer amaranth and waterhemp J. D. Sauer are two dioecious pigweed species [1, 2] which pose a severe threat to the productivity of several row crops, especially corn (*Zea mays* L.) and soybean (*Glycine max* (L.) Merr. [3–6]. Both these weeds are characterized by rapid growth under ideal growing conditions [7–10], competing with crops for essential resources namely, light, water, and nutrients thereby causing a drastic reduction in their yields [11–14]. However, palmer amaranth has shown to exhibit more aggressive growth or over 5 centimeters per day and up to 6 feet in 2 months [15] as compared to 3 centimeters of waterhemp [16], and up to 5 feet [17]. Waterhemp can produce about 250,000 seeds per plant [10] while on the other hand and owing to its rapid growth, palmer amaranth is more aggressive, capable of producing between 100,000 and 500,000 seeds per plant [18]. In addition, *Amaranth* species seeds are very small and easily dispersed within and across fields using equipment in a weed-infested fields, thus sowing seeds in uninfested areas. As a result, palmer amaranth has been found in the Midwestern states since 2014 [19–21]. Palmer amaranth can reduce corn yields by 91% [11] and soybean yields by 79% [22] while waterhemp causes a reduction in corn yield ranging between 8 and 36% [23] and a reduction of 43% in soybean yield [24]. Finally, palmer amaranth has developed resistance to various herbicide mechanisms.

Jonathon and Christy [25] reported palmer amaranth resistant to six herbicide sites of action, including glyphosate. According to the study by Amit et. al. [26], palmer amaranth is one of the very few weeds in the United States to have evolved resistance to herbicide groups with multiple mechanisms of action including 5-enol-pyruvylshikimate-3-phosphate synthase

inhibitors (EPSPS), microtubule assembly inhibitors, acetolactate synthase inhibitors (ALS)-, hydroxyphenylpyruvate dioxygenase inhibitors (HPPD) and photosystem (PS) II inhibitors [27].

Hence, for the above reasons discussed, weed identification, management, and eradication in agronomic fields, especially palmer amaranth, is of paramount importance. As a management strategy for palmer amaranth, [26] suggested chemical control where i.e., pre-plant burndown should be followed by a PRE residual herbicide and one or two POST herbicide treatments or POST herbicide mixtures with a residual herbicide in order to minimize the development of palmer amaranth later in the growing season. Travis and Bill et.al. [28] reported that PRE corn herbicides with one or more active ingredients including atrazine, fluthiacet-methyl, acetochlor, mesotrione, saflufenacil, alachlor, *S*-metolachlor, dimethenamid-P, flumioxazin, pyroxasulfone, or isoxaflutole can provide effective control of emerging palmer amaranth resistant to both glyphosate and ALS-inhibitors. Grichar et.al. [29] showed that atrazine, acetochlor, and flufenacet combined with isoxaflutole provided 78%, 95%, and 44% palmer amaranth control, respectively, 10–12 weeks after planting. HPPD inhibitors (mesotrione, tembotrione, and topramezone), auxin mimics (2, 4-D, dicamba, and diflufenzopyr), and PS II inhibitors (atrazine) are all common active components in POST herbicides. Acetochlor or *S*-metolachlor mixtures with a POST herbicide serve as an effective tank-mixing option and will also aid in the control of palmer amaranth in the later stages of growth. The authors also suggested the use of cover crops and tillage as non-chemical control management strategies and the use of herbicide-resistant technologies namely, Enlist™ or the XtendiMax® weed control system to effectively control glyphosate-resistant (GR) palmer amaranth. Wiggins et.al. [30] assessed the effect of POST herbicides used after cover crops on the control of palmer amaranth and determining which pesticide and cover crop combination provided the most efficient palmer

amaranth control for corn growers. The study by Crow et.al. [31] evaluated the control of GR palmer amaranth in corn through the use of non-atrazine herbicides treatments alone and in combination with dicamba plus diflufenzopyr. Janak et.al. [32] evaluated the crop tolerance and efficacy of several preemergence herbicides applied alone and in mixtures for weed control in field corn. The study indicated control of palmer amaranth was at least 90% with the use of preemergence herbicides.

Steckel and Sprague [33] reported a 50% reduction in corn yield when waterhemp emerged at the V6 [34] corn stage of growth. The efficiency of various postemergence herbicides in controlling triazine-resistant waterhemp was assessed by Anderson et.al. [35]. They reported atrazine plus bromoxynil or atrazine plus bentazon controlled less than 75% waterhemp while primisulfuron, 2,4-D ester, atrazine plus dicamba, dicamba, bentazon plus metribuzin, or dicamba plus primisulfuron controlled over 85% waterhemp. Shoup et al. [36] assessed the efficacy of herbicides mixtures for control protoporphyrinogen oxidase inhibitor-resistant waterhemp in corn. They found that all the herbicides provided 90% waterhemp control 8 WAPT (week after the postemergence herbicide treatment). Schuster et.al. [37] evaluated waterhemp control from herbicides alone or in mixtures at various timings in corn. Preemergence herbicides controlled waterhemp 7 to 34 days longer than the untreated control whereby strategies deploying multiple application timings controlled 84 to 100% waterhemp as compared to single herbicide treatment strategies which controlled 21 to 99 waterhemp. Waterhemp control from S-metolachlor, atrazine, mesotrione, and bicyclopyrone mixtures sprayed PRE or POST in GR corn at two stages was evaluated by Amit et.al. [38]. The researchers concluded that herbicide mixtures applied PRE or early POST in GR corn successfully aided in the control of waterhemp, even at lower doses, however, this pesticide should not be used late in the season to avoid

waterhemp interference and probable corn yield loss. A similar study was conducted by Legleiter et.al. [39] that aimed at determining herbicide strategies for use in conventional, GR, or glufosinate-resistant corn for the management of GR waterhemp.

The above studies have been successful in the management of these weeds in their later stages of growth, however, at this stage, they may have already produced mature seeds that may have been transported to other parts of the field or to other locations. Thus, it is important to manage weeds in the early stages of growth i.e., within the first two weeks of emergence. An important step in the management of weeds is identification as palmer amaranth possesses a striking resemblance with waterhemp, especially in the early stages. As a result, it is difficult to tell them apart, leading to a possibility of misidentification. [40–43] describe the most commonly used morphological characteristics that aid in distinguishing palmer amaranth from waterhemp. These characteristics are summarized in Table 1.1 and aid in distinguishing between the two weeds i.e., weeks after emergence. However, in the first two weeks, they exhibit very similar morphological characteristics thereby making it very hard to distinguish between the two. Hence, This dissertation focuses on the drawbacks of the existing approaches and develops a novel approach for distinguishing between palmer amaranth and waterhemp in the first two weeks after emergence.

Table 1.1. Comparison between the morphological characteristics of palmer amaranth and waterhemp.

<b>Characteristic features</b>	<b>Palmer amaranth</b>	<b>Waterhemp</b>
Leaf shape	Wide, oval leaves	Long, slender leaves
Petiole length	Petiole i.e., the stalk that connects the leaf blade to the stem is longer in palmer amaranth	The petiole length in waterhemp is shorter
Watermark	Leaves sometimes possess a V-shaped watermark	No presence of watermark
Leaf-tip hair	Leaves sometimes possess tiny hair at their tip	No presence of leaf-tip hair
Bracts	Presence of spiny bracts (female plants)	No presence of spiny bracts

## 1.2. Research gaps

The research gaps identified for this research are as follows.

1. Palmer amaranth is a noxious weed posing a major threat to corn's productivity and possesses an aggressive growth. It is important to identify the weed in cornfields especially in the early stage in order to reduce the spread of seeds to other parts of the field. It is essential to observe how the morphological characteristics of palmer amaranth evolve in the early stage of growth for successful identification.

2. Palmer amaranth and waterhemp possess similar morphological characteristics in the early stages of growth. It would be interesting to see how the morphological characteristics of waterhemp evolve in the early stage and how different they are from palmer amaranth.

3. Visual observation cannot aid in distinguishing between palmer amaranth and waterhemp, especially in the early stages due to similar morphological characteristics. Hence, automated approaches i.e., ML can be used to draw inferences from the morphological characteristics and aid in distinguishing palmer amaranth from waterhemp.

### **1.3. Research objectives**

The objectives of the research are as follows.

1. To quantify the evolution of morphological characteristics of palmer amaranth and waterhemp in the early stages.
2. To distinguish between palmer amaranth and waterhemp in the early stages.

### **1.4. Dissertation organization**

This dissertation is organized into two chapters. Chapter 1 provides a brief overview of the background required for the current research and lists the specific research objectives.

Chapter 2 reviews the various ML methods used for identification of weeds in Corn. Chapter 3 demonstrates the efficacy of ML and Deep Learning methods in distinguishing palmer amaranth and waterhemp within the first two weeks after emergence using a custom dataset. Chapter 4 provides the conclusions while Chapter 5 discusses the future work.



## **2. A REVIEW OF MACHINE LEARNING TECHNIQUES FOR IDENTIFYING WEEDS IN CORN**

### **2.1. Introduction**

Corn is one of the most consumed commodities in the world including in the United States. The United States accounted for 26% of the world's corn consumption during 2020-2021 [44]. Likewise, the United States is the world's largest corn producer, accounting for 345 million metric tons in 2019-2020 [44]. Corn is considered a highly productive crop because of its wide array of industrial and agricultural uses such as animal feeds, biofuels, and food sweeteners. According to the 2020 US corn usage issued by USDA (United States of Agricultural Department), a major proportion of the produced corn (roughly 46%) was used as animal feed and roughly 27% was used for biofuel production. A significant portion of the rest (roughly 18%) was exported, the majorly to countries including Colombia, South Korea, Japan, and Mexico. South Korea and Japan rely on corn from the United States for their animal feed. The rest of the production (roughly 9%) was used in making products such as corn syrup, sweeteners, corn starch, cereals, and beverages. Corn-based deicing materials [46, 47], corrosion inhibitors [47-49], and coating materials [49-51] are recently being developed and these products can further expand corn usage in the domestic market. Corn being a highly productive crop plays a major role in the US economy. The corn refining industry alone featured 47.5 billion dollars in economic output in the United States in 2020 according to a study conducted by Corn Refiners Association [52].

One of the major challenges in achieving higher corn productivity is the control and management of weed growth. Weeds, in addition to competing with the corn for the nutrients and crop resources, introduce harmful bacteria, viruses, and other microorganisms which results

in significant yield loss. According to a study [53] based on the USDA-NASS (United States Department of Agriculture -National Agricultural Statistics Service) 2014 corn yield report, the interference of weeds in corn production resulted in an average 50% yield loss annually from 2007 to 2013. In this period, weed interference resulted in an average loss of \$26.7 billion annually in terms of economic value. Weeds are commonly controlled through the application of herbicides or removal through mechanical, thermal, and electrical means. Out of these two broad approaches, the application of herbicides is most common. However, the use of herbicides involves several drawbacks. Applying herbicides to the entire field is very expensive. Herbicides cost roughly \$60 per acre which is 10% of the expected market revenue of the corn as per the 2021 Purdue Crop Cost and Return Guide [54]. Excessive use of herbicides is also detrimental to soil fertility, the aquatic ecosystem, and human health. Furthermore, weeds develop resistance to herbicides over time. Selective spraying of herbicides would address these shortcomings and also cut down the cost of the herbicides. Selective spraying of herbicides or the removal of weeds requires precise identification of weeds. Hence, the identification of weeds plays an important role in the management and control of weeds. Given the scale of the problem, manual identification of weeds is either untenable or impractical in many situations. ML techniques are successfully applied for the precise identification of weeds. The use of ML techniques also made the automation of weed control and management possible.

This review surveyed the various ML approaches that were applied over the years for the identification of weeds in cornfields. We also describe in full technical detail, the type of ML problem solved (classification, object detection etc.), the type of weeds identified, the type of data used, the type of error metrics used to evaluate the performances of these approaches. These ML approaches are grouped into three major categories namely, Support Vector Machines,

Neural Networks, and Miscellaneous. The rest of this chapter is organized as follows: Section 2.2 explains Machine Learning; Section 2.3 discusses work corresponding to the first category, SVM; Section 2.4 discusses Neural Network approaches; and Section 2.5 elaborates on the miscellaneous ML techniques used in the past for the identification of weeds in cornfields; Section 2.6 explains the importance of data for the performance of the ML techniques and the various metrics that are used to evaluate the performance of these techniques; finally, Section 2.7 briefly discusses the conclusion and future research directions of ML-based identification of weeds.

## **2.2. Machine Learning**

ML is a class of Artificial Intelligence (AI) that focuses on aiding the computers in learn the underlying relationship between inputs and outputs from the given data and make accurate predictions [55]. ML algorithms employ statistical methods to learn from the exposed data without any explicit programming instructions [56]. The workflow of a typical ML model is as depicted in Fig. 1 and consists of the following phases:

Data acquisition – gathering data (open-source datasets, sensors, etc.)

Data pre-processing – involves cleaning the data, making the data suitable to be used by the model

Dataset creation – involves splitting the data into training, validation, and testing sets

Model training – the training set is used to train the model and the model learns appropriate input-output relationships

Model testing and performance evaluation – the trained model is employed on the testing set and performance metrics are used to quantify the model's accuracy

Model deployment – making the model available to the users via web/software application

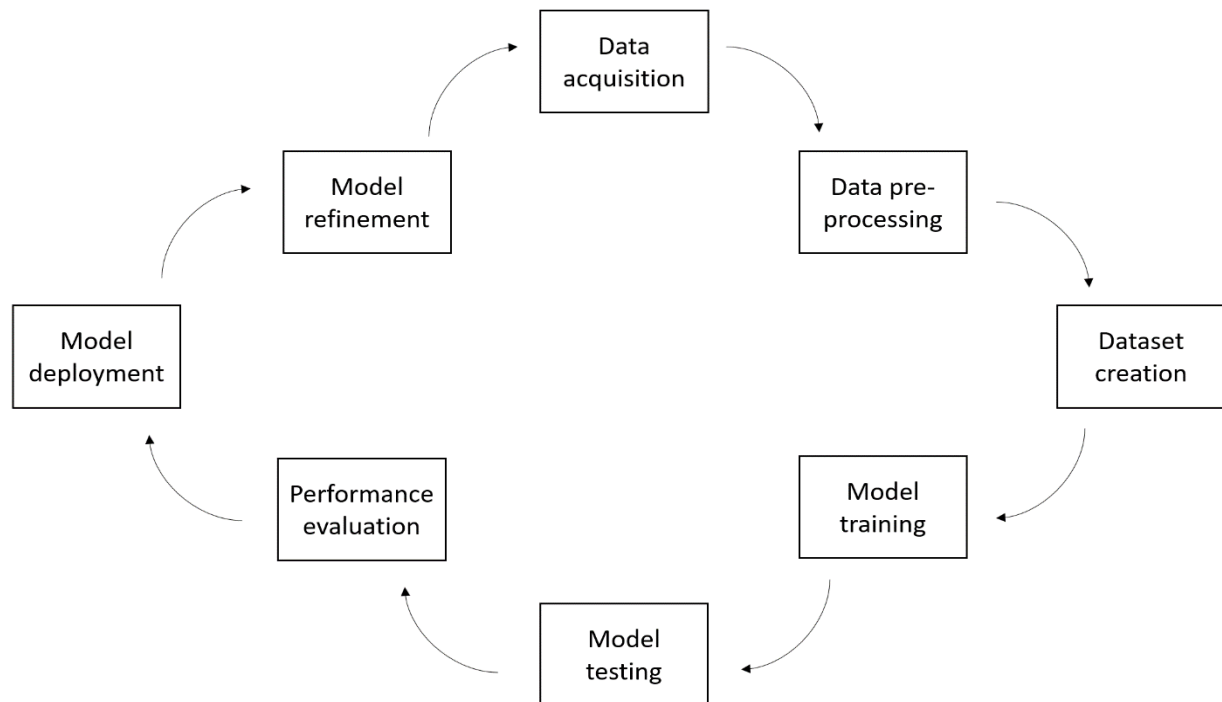


Fig. 1.1. Workflow of ML models.

During the process of model training, the model’s performance may degrade due to seasonal/abrupt changes in data patterns that may occur over time, hence, the model must be updated, and the workflow cycle must be completed by returning to the data acquisition phase. Also, the parameters whose values are set before the start of a learning process i.e., hyperparameters need to be tuned to better the positive results achieved during the process of model evaluation. This is mainly done to control the overall behavior of the model. Model deployment has become an important element in the modern practice as it focuses on the production standpoint of the ML models. MLOps offer comprehensive steps and methodology to address the deployment aspect of the ML models. More details about MLOps can be found here

[57–60]. ML is split into the following categories depending on the sort of learning response accessible to a learning system:

**Supervised learning:** Supervised learning includes training the ML algorithms with labeled data to perform tasks like classification or regression. Labeled datasets contain both the causal factors (input features) and their target responses or outcomes (output variables). The causal factors are the input features, and the target responses are the output variables. The objective of supervised learning is to identify the underlying relationship between input features and output variables so that they can predict the target responses for future unforeseen input features. Some of the applications of supervised learning in precision agriculture can be found in [61–63].

**Unsupervised learning:** Unsupervised ML algorithms are trained on an unlabeled dataset to identify patterns and structures in the given data. They are mainly used for tasks such as clustering and features association. K-means clustering, Principal Component Analysis (PCA), and Gaussian Mixture Models are popular unsupervised learning algorithms. Davis et al. [64–66] show some of the practical applications of unsupervised learning in precision agriculture.

**Reinforcement learning:** Reinforcement learning is a paradigm of ML which involves a sequential decision-making process to achieve the end goal. In reinforcement learning, a computer agent learns to reach a defined goal optimally by navigating through the environment by choosing actions that yield higher rewards. SARSA, and Deep Q networks are some of the widely used algorithms for reinforcement learning. The application of reinforcement learning in precision agriculture can be found here [67–69]

In the following three sections, we provide a brief introduction of popular ML methods and extensively analyze the use of these methods for identification of weeds in corn.

### 2.3. Support Vector Machines

Support Vector Machines (SVMs) is a non-heuristic classification method that was initially introduced as a linear classifier by Vapnik and Chervonenkis in 1963 [70]. SVMs construct hyperplanes to classify the given data set. The most defining aspect of it is it tends to identify a hyperplane that maximizes the margin between the support vectors. The support vectors are planes that pass through the nearest data points of the individual classes. This maximization of margin leads to a reduction in the generalization error. SVMs can use two types of margins: hard margin and soft margin. Hard margin is employed when the given data is linearly separable and noiseless. However, the use of a hard margin often leads to the overfitting of the data so, the soft margin is used to improve the generalization of the noisy data set. In the soft margin approach, overlapping data points are weighed down to allow slack in the classification. Cortes and Vapnik [71] introduced the soft margin approach in 1995 and successfully applied it to recognize handwritten images. In 1992, Boser et al [72] further developed SVMs to solve non-linear classification problems using an approach called ‘Kernel Trick’. Kernel trick maps the inputs into a higher dimensional space so that it becomes separable by linear hyperplanes. SVMs are also extended to solve regression and multi-class classification problems [72, 73]. SVMs have now become a highly dependable tool for digital image classification, text categorization, character recognition, and many other AI-related tasks. Some of its recent advancements in SVMs can be found in [74-82].

SVMs are popularly used for the identification of weeds [84, 85]. Karimi et al. [61] evaluated the application of SVM for the detection of weed and nitrogen stress in corn. The weeds involved in the study were dominant grassy weeds namely, crabgrass (*Digitaria ischaemum* Schreb.), barnyardgrass (*Echinochloa crusgalli* (L.) P.Beauv.), yellow nutsedge

(*Cyperus esculentus* L. ), and dominant broad-leaves namely, common lambsquarters (*Chenopodium album* L.), canada thistle (*Cirsium arvensis* (L.) Scop.), redroot pigweed (*Amaranthus retroflexus* L.) and sow thistle (*Sonchus oleraceus* L.). The data contains 72 narrow bands ranging between 408.73 and 947.07 nm. The major factor considered was weed treatment while the sub-factors were three nitrogen application rates. The classification accuracy of the employed SVM model with RBF kernel yielded an accuracy of 69.2% when the nitrogen rates and weed infestation levels were combined, interestingly when the weed control and nitrogen rates are considered separately the classification accuracy was improved to be more than 80%.

Wu and Wen [86] investigated SVM as a classifier to identify corn and weed seedlings with the use of texture features. The weeds were chinese sprangletop (*Leptochloa chinensis* (L.) Nees), yerbadetajo (*Ecliptaprostrata* L.), rice galangale (*Cyperus iria* L.), and copperleaf (*Acalypha australis* L.). The dataset comprising 66 color images (30 images of corn and 36 images of weeds respectively) was transformed to gray-level following which their statistical properties were obtained from their histograms. These, along with GLCM were used to extract the following texture features: smoothness (R); mean (m); entropy (e); third moment ( $\mu_3$ ); contrast (F1); energy (F2); homogeneity (F3); and correlation (F4); uniformity (u) and standard deviation (s). The features were replaced by their means i.e., mean of contrast (f1), mean of energy (f2), mean of homogeneity (f3), and mean of correlation (f4). 60% of the data was used to train the SVM while the remaining 40% was used for testing it. SVM with the following features as input vectors yielded the following results: 92.59% testing accuracy for F4 (consisting of f1, f2, f3, and f4) as input vector; 92.31% testing accuracy for F6 (consisting of m, s, R,  $\mu_3$ , u and e); 100% testing accuracy for F8 (features selected by PCA, not mentioned) and 100% testing accuracy for F10 (all texture features). When the SVM was input with F8 as the input vector and

compared with a BP network, the results showed that the SVM with an accuracy of 100% outperformed the BP network that could only produce an accuracy of 80%.

In a later study, Wu et al. [87] demonstrated the use of shape features as SVM inputs for the classification of corn and weed seedlings. The dataset consisted of 64 RGB images (40 used for training and 24 used for testing). The specific number of images of corn and weeds was not mentioned. The authors transformed the RGB images to HIS space, citing the images had better features in HIS space than in an RGB space as the reason. From these images, the following leaf shape parameters were obtained: R; M; L, and Roundness. These parameters were input to the SVM with three different kernel functions namely, RBF, sigmoid and polynomial. The classification accuracies read: 96.50% for RBF-SVM; 67.67% for sigmoid-SVM; 90.00% for polynomial-SVM and 83.20% for ANN (Artificial Neural Network) respectively.

Ahmed et al. [88] demonstrated a texture-based weed classification in which LBP was used to obtain textural features. Broadleaf and grassy categories of weeds were studied. For the dataset consisting of 200 color images (100 of each category), ten-fold cross-validation was performed, and the dataset was randomly partitioned into 10 subsets where one of them was used for testing and the remaining nine for training. The LBP operator was used to compute the LBP code for each pixel of the input image thereby resulting in the formation of an encoded representation of the image. With the use of this, a histogram was obtained and used as the feature vector, this feature vector represented the image's texture information. SVM with RBF kernel was used for classification and produced a classification accuracy of 98.5%.

The study by Wong et al. [89] aimed at classifying weed seedlings using a multi-class SVM that produces the best probabilistic output. GA was used to select the features and fine-tune the classifier parameters, followed by which SVMs were used for classification purposes. The



weeds involved in the study were: chamber bitter (*Phyllanthus Urinuria* L.); goatweed (*Agerantum Conyzoides* L.); palmer amaranth, and other dicotyledonous and monocotyledonous weeds. Three SVMs were trained to distinguish monocotyledonous weeds, goatweed and palmer amaranth from other weeds. The following features were selected: single-leaf/overall leaf shape; elliptical Fourier descriptors; regional shape parameters; fractal; Hu moment invariants; skeleton stats; boundary to the centroid; area, and color stats. The data consisting of 400 feature rows were divided into training and verification data in the ratio of 50:50 following which the SVMs were both trained and verified on it. The GA-optimized SVMs were then tested with unseen/external data consisting of 240 datasets in which 100 belonged to palmer amaranth and another 100 belonged to other weeds (no mention of what the remaining 40 belonged to). The population size was equal to 100 and the GA was set in such a way that it would stop when the best fitness does not exceed 40 generations. The dataset used for testing the classification consisted of image samples of weeds belonging to ten species. 450 images were used for testing purposes, and it was observed that all of the categories had a high true positive value of 100%.

In work that deals with automatic spraying control, Siddiqui et al. [62], a system was developed for weed classification using wavelet transform, SWLDA, and SVMs. 46 wavelets belonging to six wavelet families were tested and decomposed up to four levels. The wavelet families included the biorthogonal wavelet family with 10 sub-wavelets, Symlet wavelet family with 10 sub-wavelets, Coiflet wavelet family with 5 sub-wavelets, reverse biorthogonal wavelet family with 10 sub-wavelets, Daubechies wavelet family with 10 sub-wavelets, and discrete Meyer wavelet family. The most meaningful features (not mentioned) were extracted using SWLDA. Finally, these features were fed to the SVMs for classification (into two categories: weeds with narrow leaves and weeds broad leaves respectively). The authors also included a pre-

processing step that eliminated lighting effects thereby ensuring high accuracies in real-life scenarios. The data collected consisted of 1200 RGB images (500 each from narrow and broad categories respectively and 200 from an unknown category) which then underwent decomposition using the wavelets families before SWLDA extracted the most relevant features (not mentioned). The training set consisted of 600 images comprising 250 images of broad leaves, 250 of narrow leaves, and 100 of unknown, and cross-validation was also done. The testing set consisted of the other 600 images comprising of 250 broad leaves, 250 of narrow, and 100 of unknown. The confusion matrix was used as the performance metric and the best result was given by Symlet-SWLDA-SVM (98.1% classification accuracy). The results for the wavelets were: biorthogonal (classification accuracy of 95.66%); Coiflet (classification accuracy of 94.66%); reverse biorthogonal (classification accuracy of 95.33%); Daubechies (classification accuracy of 95.0%), and discrete Meyer (classification accuracy of 93.33%).

Another texture-based classification of weed and crop was demonstrated by Athani and Tejeshwar in their work [90]. The texture features involved in the study were entropy, mean, intensity, smoothness, uniformity, standard deviation, and third moment. Along with texture features, color features and shape features (region descriptors and boundary descriptors) were also considered. SVM was used for classification on a dataset consisting of 1000 color images (500 of maize and 500 of weed (the type/species of weed was not mentioned) and k-fold cross-validation was used too. From this dataset, 450 images of each category were used for training while 50 from each were used for testing. The results showed that the accuracy of prediction for the SVM was 82%.

Another use of shape features for crop and weed classification was demonstrated by Satvini [91]. The following shape features were involved in the study: eccentricity; area; major

axis length; perimeter, and minor axis length. Para grass (*Brachiaria mutica* (Forssk.) Stapf), Chrysanthemum, (*Chrysanthemum indicum* L.) and nutsedge were the weeds involved in this study. SVM (with RBF and polynomial functions) was used for classification purposes. 2560 images comprised the dataset out of which, 1155 images of each class (weed and crop) were used for training purposes while 125 images of each class were used to validate the trained model. The performance of the SVM was as follows: correctly classified all 125 images of the crop as crop; correctly classified 104 out of 125 weed images of weed as weed and misclassified the remaining 21 as a crop. Table 2.1 summarizes all the above works that employed SVMs for the identification of weeds.

Table 2.1. Summary of studies that employed SVMs for the identification of weeds.

<b>Study</b>	<b>Research problem</b>	<b>Dataset</b>	<b>Accuracy</b>
[61]	Detection of weed and nitrogen stress in corn	20 data points of 9 treatments consisting of 4 replicates thereby resulting in a data set of 720 entries. 50% of the data was used for training purposes while the remaining 50% was used for testing.  <b>Hardware used:</b> A Compact Airborne Spectrographic Imager	10-fold cross-validation used (testing data set). SVM: 66% to 76% for combined weed and nitrogen application rates. 73% to 83% accuracy 83% to 93% accuracy respectively for weed and nitrogen treatments separately.
[86]	Classification of weed and corn seedlings using textural features	66 color images (30 corn seedlings, 36 weed images). 60% used for training, 40% for testing  <b>Hardware used:</b> A digital camera (resolution of 640x480 pixels).	SVM with different feature selections produced 92.31 to 100%.

Table 2.1. Summary of studies that employed SVMs for the identification of weeds (continued).

<b>Study</b>	<b>Research problem</b>	<b>Dataset</b>	<b>Accuracy</b>
[87]	Using shape parameters to identify corn/weed seedling in fields	64 color images (40-training set, 24-testing set)  <b>Hardware used:</b> A digital camera (resolution of 640x480 pixels).	SVM (Sigmoid-96.5%, RBF-67.67% and Polynomial-90% respectively)
[88]	Studying Local Binary Pattern for Automated Weed Classification	200 images (100 each of broadleaf and grass respectively). Dataset is divided into 10 subsets. 1 subset used as the testing set and 9 subsets for training.  <b>Hardware used:</b> A digital camera (resolution 1200 x 768 pixels)	SVM: 98.5%
[89]	Categorize weed seedlings into groups for spot spraying and weed scouting	400 features rows for training and verification. 240 external data sets were used for testing (100 data of palmer amaranth and 100 of other weeds).  Weed species: chamber bitter, goatweed, palmer amaranth, and other weeds (dicotyledon and monocotyledon)  <b>Hardware used:</b> Logitech c615 Webcam (resolution of 1920 x 1050 pixels)	SVM: True positive true value for all the groups (100%); for second variant group for goatweed (66.7%).

Table 2.1. Summary of studies that employed SVMs for the identification of weeds (continued).

<b>Study</b>	<b>Research problem</b>	<b>Dataset</b>	<b>Accuracy</b>
[62]	Classifying weed images using Wavelet Transform	1200 images (500 of broad category, 500 of narrow category, and 200 of unknown category respectively). Training: 600 images (250 of broad leaves, 250 of narrow and 100 unknown weeds). Testing: Remaining 600 images (250 images of broad leaves, 250 of narrow and 100 unknown weeds).	Symlet wavelet family: 98.1%
		<b>Hardware used:</b> Not mentioned	
[90]	Classification of maize and weed	1000 images (500 of crop, 500 of weed). 450 of each were used for Training, 100 for Testing.	82%
		<b>Hardware used:</b> Not mentioned	
[91]	Performance comparison of algorithms used for identifying weeds	2560 images. 1155 of each class (weed and crop) used for training and 125 images per class used to validate the trained model.	SVM: 100% for crop and 83.2% for weed
		<b>Hardware used:</b> A 10 MP digital camera	

## 2.4. Neural networks

Convolutional Neural Networks (CNNs) are a class of deep neural networks used for object/ image recognition, classification, and many other computer vision tasks. It mimics the visual cortex of the human brain in recognizing visual patterns and learning the important features and spatial connections in the images with the least amount of preprocessing possible.

Hubel and Weisel [92] 1962 discovered that complex cells in the visual cortex achieve spatial invariance by summing the output of different simple receptive cells. Inspired by their work, Fukishma [93] proposed the first-ever visual recognition model called “neocognitron”. The proposed neocognitron model consisted of two preprocessing layers called ‘S’(Simple) cells and ‘C’(complex) cells mirroring the discovery of Hubel and Weisel. Waibel [94] developed a convolutional-like neural network called Time Delay Neural Networks (TDNN) in 1987 to achieve shift-invariance in the temporal dimension [95]. However, the CNN in its present form is first introduced by Lecunn et. al. [96] in 1998. The proposed convolutional neural network called ‘LeNet-5’ was successfully applied to classify hand-written digital images. The convolutional block of LeNet-5 consisted of feature maps called ‘kernels’ or ‘filters’ and pooling layers. Even though LeNet-5 initiated a promising paradigm for computer vision, the non-availability of higher computational units and large image databases dampened its progress. But in 2012, Krizhevsky et al [97] were able to successfully scale up the LeNet to a deeper and broader network with a larger image database (Imagenet) and with the use of GPUs. Since then, many advanced neural networks have been developed, such as VGGNet [98], GoogLeNet [99], and ResNets [100].

CNNs, in general consist of two blocks: 1. Convolutional block and 2. Fully connected neural network block. The convolutional block extracts important features and spatial connections from the images with minimal computation. Images are usually represented in the form of 2-D pixel matrices with multiple channels, for instance, an RGB image has 3 channels of 2-D pixel matrices. These image input matrices are first operated upon by a convolutional block, and the extracted information is flattened into a single column feature vector. This flattened feature vector is then fed into a fully connected neural network and trained using a

backpropagation algorithm. In the convolutional block, image matrices are first subjected to convolution, followed by pooling. Convolution is mainly performed for feature extraction, and it is done using filters or kernels in the form of matrices. Kernel matrices are of a considerably smaller dimension and are chosen appropriately based on the nature of the problem. Convolved features are obtained by taking Hadamard product between the image and the kernel matrices. As the kernel matrices of smaller dimensions compared to image matrices, convolved features are generated by sliding the kernel matrices from left to right and top to bottom and taking the Hadamard product at each position of the kernel matrix on the image matrix. The sliding of the kernel matrix is defined in terms of 'strides'; for example, a stride of 1 allows the kernel filter to shift one column left and one row down. In addition to striding, convolution also involves padding, which adds additional rows and columns of zeros to the input matrices so that the pixel information present in the edges of image matrices is not lost. The features extracted from convolution are sensitive to the location, and to achieve a translation invariance (less sensitive to the location) of these features, a down sampling operation called 'pooling' is carried out. Like the kernel filter, the pooling filter is also of smaller size compared to the feature maps. The size of the feature maps is usually halved when using pooling filters. For example, the size of  $4 \times 4$  will be converted to  $2 \times 2$ . Max pooling and average pooling include the two most common types of pooling filters used in CNN. Average pooling involves the extraction of the average value of map features, whereas max-pooling extracts the maximum value. The choice of pooling depends upon the nature of the given data. Average pooling tends to smoothen the image, whereas max-pooling tends to brighten or select bright pixels from the image. After pooling, a fully connected layer is formed as a single column vector for each example and fed into the neural networks, and,

trained using a backpropagation algorithm. For classification problems, CNNs commonly use ReLU, eLU, and tanH for hidden layers and SoftMax activation functions for the output layer.

Moshou et al. [101] proposed a new neural network architecture, SOM where the neurons are associated with local linear mappings for the classification of crop and weed from their near-infrared reflectance spectra which were obtained with the help of an imaging spectrograph. The dataset consisted of 88 corn samples, 77 samples of the buttercup (*Ranunculus repens* L.), 79 samples of Canada thistle (*Cirsium arvense* (L.) Scop.), 75 samples of charlock (*Sinapis arvensis* L.), 73 samples of chickweed (*Stellaria media* (L.) Vill.), 76 samples of dandelion (*Taraxacum officinale* (L.) Webber), 80 samples of meadow grass (*Poa annua* L.), 78 samples of redshank (*Poligonum persicaria* L.), 75 samples of stinging nettle (*Urtica dioica* L.), 78 samples of wood sorrel (*Onalis europaea* L.) and 75 samples of yellow trefoil (*Medicago lupulina* L.) resulting in a dataset of 766 and 88 reflectance spectra for weed and corn respectively. A separability index was used to obtain five principal components and the following wavelengths: 539; 540; 542; 545; 549; 557; 565; 578; 585; 596; 605; 639; 675; 687; 703; 814, and 840. Cross-validation divided the data into 10 equal sets and the neural network was trained and tested with 90% and 10% of the data respectively for all the 10 sets. The classification accuracy (obtained by averaging the classification rates for all the test sets) was 96% for corn and 90% for weeds. The network also fared better when compared with other classifiers such as PNN (classification accuracy of 85% for corn and 77% for weeds), Multi-layer Perceptron (95% and 70% for corn and weed respectively), SOM (85% and 77% for corn and weeds, respectively), and Linear Vector Quantization (85% and 77% for corn and weeds, respectively).

The work by Yang et al. [102] demonstrated an approach to classifying weeds in cornfields using ANN. The weeds studied in this work were: common lambsquarters; yellow



nutsedge; quackgrass, (*Agropyron repens* L.), and velvetleaf (*Abutilon theophrasti* Medik.). The original images (number/size not mentioned) were rotated by 90, 180, and 270 degrees, respectively thereby resulting in a larger dataset comprising 1,736 color images of corn, 772 of velvetleaf, 672 of quackgrass, 752 of common lambsquarters, and 1480 of yellow nutsedge. The greenness method was used to extract green content from the images followed by which the images were converted to grayscale images. Cross-validation was only supposed to be used when it was learned that the ANN was found to not be getting thorough training in the first case. ANN performed the best for corn with a recognition rate of 100%. The results for the weeds were: velvetleaf (92%); quackgrass (62%), and yellow nutsedge (80%).

The work by Wu et al. [86] was also an earlier mentioned one that deals with the classification of weeds and corn seedlings using textural features. The same author demonstrated other research, Wu et al. [103] based on wavelet features and fractal dimensions aiming at the classification of weed and corn. The weeds studied were the monocotyledonous weeds (goosegrass and rice galangale) and the dicotyledonous weeds (copperleaf, common carpesium (*Carpesium abrotanoides* L.), and yerbadetajo). The dataset consisted of 84 digital color images (35 of corn and 49 of weed). These images were then converted to gray-level images with the use of the color index, ExG – ExR followed by which wavelet transform was used to extract features. Two-level wavelet transform was performed to extract the following components: approximation component; A2; detail components namely, H1, V1, D1, H2, V2, D2, and energy values namely, eA2, eH1 eV1 eD1 eH2, and eD2. These energy values were then input to a BP network which was able to separate the weeds species with an accuracy of 100% but not the corn and weeds. When the energy features were used as input vectors, it resulted in a classification accuracy of 77.14%, whereas when the fractal dimensions of the images were used, it resulted in a

classification accuracy of 80%. Interestingly, when both the fractional dimensions and energy features were input to the network, they obtained an improved classification accuracy of 94.28%. The same author also demonstrated another application of the BP network in the identification of weeds and has been mentioned earlier, Wu et al. [87]. The work used shape parameters to accomplish this.

Chen et al. [104] proposed a method to classify monocotyledonous and dicotyledonous weeds (species not mentioned) in a corn seedling using shape features. The dataset used for the task included 60 images of corn and 280 images of weeds, the nature or format (RGB or grayscale) of the image was not mentioned. The background was removed using Otsu's threshold based on the Excess green method. 20 images of corn and 80 of weed were used for training a PNN while 40 images of corn and 200 of weed were used for testing purposes. The PNN made use of the following shape features: area ratio; aspect ratio; eccentricity, and roundness. From the confusion matrix, it was evident that 37 images of corn and 190 of weed were correctly classified, resulting in an accuracy of 92.5% for corn and 95% for weeds. The authors cited the time of image gathering as a possible reason for the misclassification i.e., gathering of images in the early stages of growth could have yielded better results. The performance of the PNN when compared with that of a BP network trained and tested on the same dataset, remained superior as the BP network could only yield accuracies of 87.5% and 93% respectively for corn and weeds.

Another wavelet-based application was demonstrated by Sajad et al. [105] where wavelet analysis using a two-dimensional DWT extracted the appropriate features for classification (identifying weed in corn) using an ANN. The dataset consisted of 35 corn images and 50 weed images. The weeds involved in the study were: common lambsquarters; camelthorne (*Alhagi maurorum* Medik.); field bindweed (*Convolvulus arvensis* L.), and *Amaranthus* sp. For training

purposes, 20 corn and 30 weed images respectively were used while for testing purposes, 15 corn and 20 weed images were used. The images were segmented using Excess green index followed by which DWT was used to extract the following features: energy; entropy; inertia; contrast, and local homogeneity. The ANN produced a classification accuracy of 98.8%.

Andrea et al. [63] demonstrated the use of CNNs for maize and weed (the types/species of weed were not mentioned) classification. The CNN architectures used were AlexNet, sent, cNet, and LeNet, and their performances were analyzed. The dataset consisted of 2835 RGB images of maize and 800 of weed. These images were segmented through Otsu's thresholding to remove the unwanted elements like soil and other non-plants elements thereby separating the plant i.e., the target object from the background. To reduce overfitting and improve precision, the images were rotated every 30 degrees thereby resulting in an increased dataset of 34020 images of maize and 10560 images of weed. 25965 images of maize and 8560 of weed were used for training while 8325 of maize and 2000 of weed were used for validation purposes. When the training performances of all four CNN architectures were compared, cNet gave the best performance with an accuracy of 96.40%. Further, when cNets with 64 filters and 16 filters, respectively, were compared with each other, cNet with 16 filters gave a superior performance of 97.26%. Another dataset (information not mentioned) consisting of 202 images of maize and 202 images of weeds was used for testing purposes. The performances of both the cNets were compared on the following hardware: CPU; CPU with Raspberry Pi 3, and GPU. cNet with 16 filters gave the best accuracy of 92.08% for maize and 89.11% for weeds, respectively, and an average classification time of 1.58 milliseconds for GPU. It gave exactly similar accuracies for the other two hardware too.

Another application of CNN was demonstrated by Dellia et al. [106] where CNN was used to discriminate i.e., object detection between weeds and maize using the context surrounding the images. The weeds studied were grass (foxtail) and grass-like (yellow nutsedge). 224 aerial images of maize fields comprised the dataset which was divided into three categories: training (158); validation (33), and testing (33). The next step was to split the images into smaller ones of size 300 x 300 pixels by placing a grid of 300 x 300 pixels over the larger images. This was followed by manually labeling them as weed and non-weed thereby resulting in 8 times more images of non-weed than weed. Therefore, a data augmentation technique (not mentioned) was used to augment the existing weed images (number not mentioned). The dataset was then re-split into training, validation, and testing respectively. Based on the idea of adding context (adding a 300-pixel border to the surrounding of the central square image of  $300 \times 300$  pixels), two more datasets were created namely, a dataset consisting of rectangular images with full-stretched context and a dataset consisting of square images with edge-stretched context. While the former was created by looking at the central image of  $300 \times 300$  pixels and stretching any of its sides that did not possess a border of 300 pixels to the edge of the full-sized image, the latter was created by stretching the sides to 300 pixels only. Therefore, the former comprised rectangular images while the latter comprised square images. CNNs were implemented 3 times on each of the 3 datasets and each set of the three runs was averaged and their validation accuracies were compared. The results read: validation accuracy of 94.6% for no context; 97.1% for edge-stretched, and 96.3% full-stretched respectively. The best performing model was the edge-stretched context model which was tested on the test dataset and its performance was compared with the no-context model. The results read: accuracy (92.9% for no-context model and 95.7% for edge-stretched context model); precision (61.9% for no-context model and 75.5%

for edge-stretched context model), and recall (88.5% for no-context model and 88.6% for edge-stretched context model). Heatmaps of the original drone images were created using the trained model following which the ES-context model was subject to a comparison with a human baseline (created by the Turkers drawing boxes around all the weeds detected by them in the image). A comparison was made between these responses and the heat maps created by the CNN. It was observed that the CNN could detect 150% more weed patches than the Turkers.

Drymann et al. [107] demonstrated a pixel-wise classification of crops and weeds by using a CNN which is a modified version of VGG16. The crop involved in the study was maize and the type/species of weed were not mentioned but it was stated that the weeds belonged to 23 different species. By randomly placing segmented plants on top of soil images, simulated field images were created and used for training a fully convolutional neural network. Ground truth segmented images where each pixel is labeled as a weed (marked as blue), soil (marked as red), or plant (marked as green) were used for creating simulated images. 8340 and 301 images of the segmented plants and soil respectively were used for generating modeled images. Training data was generated by using 80% of the plants' images while testing data was generated by using the remaining 20%. The images were then resized to  $800 \times 800$  pixels thereby resulting in a dataset of 3463 images for training and 123 for verification. The performance of this plant segmented method was evaluated on 2 real images which were segmented by hand, one gathered in a healthy maize field, where the plant overlap is little and, another from a maize field possessing smaller maize plants and a higher weed coverage. For both the images, the algorithm successfully detected both the crop and weeds, with the classification accuracy for the first image being 98.3% and for the second, being 94.4%. Citing that this accuracy does not consider that there are a lot more soil pixels than that of crop or weed, the authors considered a metric, IOU,

for each class. For the first image, IOU was 0.93, 0.98, and 0.79 for the crop, soil, and weeds, respectively, and for the second image, IOU was 0.71, 0.93, and 0.70 for the crop, soil, and weeds, respectively. Table 2.2 summarizes all the above works that employed neural networks for the identification of weeds.

Table 2.2. Summaries of studies that employed Neural networks for the identification of weeds.

<b>Study</b>	<b>Research problem</b>	<b>Dataset</b>	<b>Accuracy</b>
[101]	A plant classifier based on neural networks	88 corn samples, 77 samples of the buttercup, 79 samples of canada thistle, 75 samples of charlock, 73 samples of chickweed, 76 samples of dandelion, 80 samples of meadow grass, 78 samples of redshank, 75 samples of stinging nettle, 78 samples of wood sorrel, and 75 samples of yellow trefoil.	PNN: 93% accuracy for corn and 85% for weed, Multi-layer Perceptron: 96% for corn and 71% for weed, SOM: 89% for corn and 77% for weed, Linear Vector Quantization: 92% for corn and 84% for weed.
		<b>Hardware used:</b> Not mentioned	
[102]	Identifying weeds in corn fields using ANN	1,736 color images of corn, 772 of velvetleaf, 672 of quackgrass, 752 of common lambsquarters, and 1480 of yellow nutsedge.	ANN gave accuracies of 100% for corn, 92% for velvetleaf, 62% for quackgrass and 80% for yellow nutsedge.
		<b>Hardware used:</b> A digital camera (Kodak DC50)	
[86]	Using textural features for classification of weeds corn	66 color images (30 corn seedlings, 36 weed images). 60% used for training, 40% for testing	SVM with different feature selections produced 92.31 to 100%.  BP: 80%
		<b>Hardware used:</b> A digital camera (resolution of 640 × 480 pixels).	

Table 2.2. Summaries of studies that employed Neural networks for the identification of weeds (continued).

<b>Study</b>	<b>Research problem</b>	<b>Dataset</b>	<b>Accuracy</b>
[103]	Identifying weed or corn using wavelet features and fractal dimension	35 images of corn and 49 of weed. Training: 49 images (20 images of corn and 29 images of weed). Testing: 35 images (15 images of corn and 20 images of weed).	BP network with seven wavelet energy parameters: 77.14%  BP network with wavelet energy parameters and fractal dimension as input: 94.28%.
		<b>Hardware used:</b> A digital camera with a resolution of 640 × 480 pixels	
[87]	Using shape parameters to identify single corn or weed seedlings in fields	200 images (100 each of broadleaf and grass respectively). Dataset was divided into 10 subsets. 1 subset used as the testing set 9 subsets for training.	SVM (96.5%, 67.67% and 90% respectively), ANN (83.2%)
		<b>Hardware used:</b> A digital camera (resolution 1200 × 768 pixels)	
[104]	Identification of weeds in corn seedlings field	60 color images of corn and 300 of weed. Training: 120 (20 of corn and 100 of weed). Testing: 240 (40 and 200 of corn and weed respectively)	PNN: 92.5% recognition rate for corn seedlings and 95% recognition rate for weeds.
		<b>Hardware used:</b> A digital camera with a resolution of 640 × 480 pixels	
[105]	Wavelet-based crop detection and classification	20 images of corn and 30 of weeds (all vegetation without corn) were used to build the ANN model. 15 images of corns and 20 of weeds were used to evaluate it.	98.8% classification accuracy.
		<b>Hardware used:</b> A digital camera (Canonixus) used to obtain digital images.	

Table 2.2. Summaries of studies that employed Neural networks for the identification of weeds (continued).

<b>Study</b>	<b>Research problem</b>	<b>Dataset</b>	<b>Accuracy</b>
[63]	Precise classification of maize and weed	44,984 images (34,222- Maize, 10,762- Weed). Training (25,695- maize, 8,560- weed), Validation (8,325- maize, 2,000- weed) and Test (202- maize, 202- weed).	cNET of 16 filters: maize (92.08%) and weed (89.11%) respectively.
		<b>Hardware used:</b> A Raspberry Pi 3 with a V2.1 Pi camera	
[106]	Automated weed detection in aerial imagery	224 aerial images. The dataset was divided into 3 categories: No context, Full stretched and Edge stretched data.	Vallidation accuracy: 97.1% for edge-stretched, 94.6% for no context and 96.3% for full-stretched.
		<b>Hardware used:</b> Sony A6000 mounted on a drone.	
[107]	CNN-based pixel-wise classification of crop and weeds	8340 and 301 images of the segmented plants and soil respectively. 80% of the plant images were used to generate training data while 20% was used to generate testing data.	First image: IOU was 0.93, 0.98 and 0.79 for crop, soil and weeds respectively.  Second image: IOU was 0.71, 0.93 and 0.70 for crop, soil and weeds respectively.
		<b>Hardware used:</b> No hardware used	

## 2.5. Miscellaneous models for identification of weeds

Apart from SVM and NNs, other ML approaches were also made use of for the identification of weeds in corn, this section describes all such works. The same authors [61] used DA and DT for the same classification problem [108]. Here again, the 72nd waveband was not considered. Among the 71 wavebands available, the most important bands were extracted using SAS software's STEPDISC feature. Here again, there were three classification problems involved: just the three nitrogen application rates, just the three weed treatments, and the nine



weed and nitrogen treatment combinations. The STEPDISC approach was applied for all the three classification problems thereby resulting in the following sequence of bands for the three growth stages namely, early stage of growth, tasseling stage, and fully-grown stage: bands 34-42-42; bands 26-32-31, and bands 28-19-19, respectively. DT chose a smaller number of wavebands for each of the three classification problems. Risk estimate values were derived by dividing the number of instances that were categorized incorrectly by the number of cases that were used in the classification. A lower risk estimate denoted a high categorization accuracy. When the performances of DA and DT were compared with that of ANN, it was observed that the DA provided a classification accuracy of 75% while ANN and DT only gave 58% and 60% respectively for the first classification problem. For the second problem, the classification accuracies were: 87%; 76%, and 68% respectively while for the third problem, the accuracies were: 83%; 81%, and 69%, respectively. While DT produced the greatest classification accuracy of 71% for the first classification problem at the tasseling stage, the ANN approach produced the most accurate results of 88% each for the other two classification problems. DA produced the best results for the combined case at the fully-grown stage (79%). Furthermore, the ANN gave the best results for the other two cases: weeds (85%), and nitrogen (88%). And for the early stage of growth, DA performed best for all three classification problems.

An early work by Hossein et al. [109] demonstrated the real-time classification of the weed, Amaranth (pigweed) in corn with the use of FFT. The images were obtained from cornfields containing the weed. They were then preprocessed for color segmentation (Euclidean distance algorithm was applied to the red and green values of each pixel), conversion to grayscale, and detection of edges based on the difference in gray intensities between two adjacent pixels. The segmented images were divided into the background, crop, and weed based

on frequency, and density using two-dimensional FFT. Followed by this was the post-processing stage where regions of the images were re-checked to check for misclassifications and finally combined into a single image. The above stages were performed for the removal of the background and classification of the plant. When the performance of the proposed method was tested on 80 cornfield images, the results showed that FFT produced a classification accuracy of 92.8%. The authors also mentioned the possibility of using the proposed method on a cultivator robot that would be equipped with a digital camera to capture images following which the classification would be performed and finally the weeds will be removed by the use of herbicide sprayers, cutting blades, etc.

Gee et al. [110] proposed a method for real-time weed control by discriminating between crop and weed and estimating the inter-row WIR. The crops involved in the study were sunflower, maize, and wheat while the type/species of weed was not mentioned. Two types of images were involved in the study: 300 agronomic images (50 images each with WIRs of 0%, 10%, 20%, 30%, 40%, and 50%, respectively) which were created by using a simulation engine and, 100 plus wide-view angle RGB images acquired from fields of sunflower (35 images), wheat (35 images), and maize (30 images) followed by processing in Matlab 6.5 software. On the RGB images, Excess Green thresholding was performed. Neither the angle of the light source with respect to its target surface nor its intensity seemed to affect the normalized RGB coordinates thereby resulting in just the green channel being considered. This was followed by the detection of crop rows using a DHT to detect only the crop rows present in the picture. Classical blob coloring analysis, a region-based segmentation technique was then used to discriminate between crop and weed. Based on spatial similarity and color, it grouped the linked pixels into areas. Given that identified lines were classified as crop, it was determined that if a

pixel of a straight line was observed to be belonging to an area, it should be classified as crop, otherwise it should be classified as weed. When the algorithm was tested on simulated images, it gave the following results: 100%, 100%, 94%, 92%, 89%, 82% crop row recognition rates for WIRs of 0%, 10%, 20%, 30%, 40% and 50%, respectively. When tested on in-filed images, the algorithm was able to recognize crop rows that had low WIRs i.e., 0 to 10% with an accuracy of 88%. To differentiate between crops and weeds, a comparison was made between the detected WIR and the WIR initially fixed in the images that were simulated and the in-filed images that were segmented manually. When the algorithm was tested on 5 images of maize with medium WIR, the detected WIRs were 32.47, 18.74, 22.97, 15.96, and 12.47, respectively, while the manual WIRs that were estimated were 22.8, 19.16, 18.17, 17.36 and 29.24. respectively.

The same authors proposed an approach based on wavelet transforms for the discrimination between crops and weeds [111]. Again, two types of images were involved in the study: 1530 grey synthetic images created by using a simulation engine and RGB images (number not mentioned). The following three possible image configurations were modeled for synthetic images based on the distinct weed spatial distributions: Punctual (Poisson process); Aggregative (Neyman-Scott process), and a combination of both thereby resulting in thirty series of images. Followed by this, 17 synthetic images were created for each series using different WIRinter-row (inter-row WIR) values ranging from 0% to 80%. The RGB images were then binarized using k-means clustering. 33 wavelet transforms from 6 wavelet basis functions (Daubechies, Symlet, Coiflet, biorthogonal, reverse biorthogonal, Meyer) were analyzed following which, the best two (Daubechies 25 and the Meyer) and the worst one (Biorthogonal 3–5) wavelets were chosen. Crop rows were detected using a real bi-dimensional Gabor filter (a cosine signal modulating a Gaussian function). Through analysis of the confusion matrix and

comparison between the resulting and initial WIRs, a comparison was made between Gabor filtering and the three wavelet transforms. The terminologies used with respect to the confusion matrix were: False Crop (FC), True Crop (TC), False Weed (FW), and True Weed (TW). Using these terminologies, the followed were calculated: Initial WIR (Initial WIR<sub>inter-row</sub>); Initial Crop Rate (Initial CR); Detected WIR<sub>inter-row</sub>; Detected CR; True Weed Detection Rate (TWDR); True Crop Detection Rate (TCDR), and the error rates for the false detection of crop and weeds. For the synthetic images, the best results were obtained for the punctual image configurations: Meyer (overall accuracy of 89.4% and weed error percentage of 2.8); Daubechies 25 (overall accuracy of 89.7% and weed error percentage of 2.8), and Gabor filtering (overall accuracy of 83.3% and weed error percentage of 14.9) thereby implying the superior performance of wavelet transforms. For the real images (i.e., the ones captured in RGB and binarized using K-means), the results read: Meyer (overall accuracy of 80.6% and weed error percentage of 5.8); Daubechies 25 (overall accuracy of 80.7% and weed error percentage of 5.8), and Gabor filtering (overall accuracy of 76.3% and weed error percentage of 18.5) thereby implying the superior performance of wavelet transforms again.

The work by Asif et al. [112] presented a vision guidance system for an automated robot that is used for weed detection. Images were acquired from open sources and the type of crop/weed was not mentioned. k-means was then used for color segmentation followed by which ROI was automatically selected, the images were converted to grayscale, and edges were detected using Sobel edge detection. Hough Transform was then used to detect the crop boundaries and depending on its success, the robot was assisted in following the crop boundaries. If the HT did not detect the crop boundaries a certain number of times, then the ROI was widened. The tracking parameters, which indicated the orientation and location of the crop

borders with respect to the image's center, were obtained with the aid of HT. The developed system also aided in the successful detection and tracking of the crop boundaries. The errors on the synthetic images were less than  $\pm 5$  pixels and  $\pm 10$  degrees for translation (the robot's current displacement with respect to the reference position) and orientation respectively. The authors also mentioned that the errors can be minimized further with the use of appropriate estimators like the Kalman filter algorithm and particle filtering algorithm.

Longchamps et al. [113] investigated the ability of LDA to classify maize and weeds using their UV-induced fluorescence. The plants studied were corn hybrids namely, Monsanto DKC 26-78, Syngenta N2555 and Elite 60T05, and monocot/grass hybrids namely, barnyardgrass, smooth crabgrass (*Digitaria ischaemum* (Schreb.) ex Muhl.), green foxtail (*Setaria glauca* (L.) P. Beauv.), and witchgrass (*Panicum capillare* L.), and dicot hybrids namely, common ragweed (*Ambrosia artemisiifolia* L.), common lambsquarters, shepherd's purse (*Capsella bursa-pastoris* (L.) Medik.) and redroot pigweed. 1,440 spectral signatures of fluorescence were obtained from three experiments that were similar, performed at three different times. Some spectra were missing and hence, only 1,361 spectra were available and the most important information from these was obtained using PCA. Using the plant species, the first five principal components as inputs, and cross-validation, LDA was performed. The output was a confusion matrix with a prediction error of 37%. A second classification was performed by combining the hybrids into groups thereby resulting in a confusion matrix with a prediction error of 8.2%, indicating a classification accuracy of 91.8%. 388 spectra of grasses were correctly classified as grasses, 9 and 49 were misclassified as dicots and corn, respectively. 423 spectra of dicots were correctly classified as dicots while 17 were misclassified as grasses. 439 spectra of corn were correctly classified as corn while 36 were misclassified grasses. The author cited the

reason for the prediction error as the confusion between corn hybrid Pioneer 39Y85 and *Setaria glauca* L. (Beauv.) as corn and grasses belong to the same taxonomic family, *Poaceae*.

Xavier et al. [114] demonstrated a Computer Vision system that uses real-time image processing to identify (classify and detect) weeds in maize. The weeds involved in the study were: devil's trumpet (*Datura Stramonium* L.); fierce thornapple (*Datura. Ferox* L.); Johnson grass (*Sorghum Halepense* (L.) Pers.), and common cocklebur (*Xanthium Strumarium* L.) The data used in the study consisted of 6 videos with each one having an average duration of 12 seconds or 300 frames thereby resulting in a total of 1,800 frames. Segmentation according to the threshold was done to obtain binary images where the pixels corresponding to the vegetation were separated from the ones corresponding to non-vegetation. The real-time image processing method/system involved two sub-systems namely, RCRD and FIP that were independent of each other but worked simultaneously. RCRD was used to detect pixels corresponding to the crop rows pixels. Using an AND operation i.e., producing an image with only the persisting vegetation pixels being retained, RCRD merged all the binary frames thereby resulting in a single image. And for the ones (images containing large patches of weed) for which the AND alone was not enough, the RCRD created crop rows to be used by the FIP. The crop row pixels of the image i.e., of crop rows that coincided with the group of positions that were marked by the FIP was preserved while the rest were discarded. The system was tested on many videos of maize obtained from different fields over different years, detecting an average of 85% of weed and 69% of the crop. It not only performed well under different conditions like varied illumination, soil humidity, and blurred conditions but also when it was presented with very difficult growth stages of crop and weed. When tested on good images i.e., the ones that had clearly visible crop rows, the system performed well by producing an average classification

accuracy of 95% for weed and a classification accuracy of 80% for crop. It also always maintained a very low rate of false negatives for weed (1%).

The work by Liu et al. [115] was an object detection problem that used SVDD for the recognition of weed or corn. Seventy-five sub-images (256×256 pixels) of corn and 43 sub-images (256 × 256 pixels) of weed were extracted from originally gathered RGB images. The type/species of weeds were not mentioned. The excess green index was used to convert these into grey and binary ones following which the next task was to perform wavelet decomposition to extract morphological features and energy-based features. In order to do so, a two-dimensional multi-resolution analysis which is based on a Matlab algorithm was performed on the images to separate frequency components (both low and high). Discrete didactic wavelet transform was used to decompose images into the following four component groups: high-frequency components namely, H1, D1 (in x,y, and xy directions), and low-frequency component A1. Further decomposing A1 resulted in four more components of lower resolution namely, A2, V2, D2, and H2. The energy percentages of these 7 components were considered and the energy features were derived. 3 morphological features: Shape complexity indicator (C); Elongation factor (D), and Thickness (T) were selected. To further select better features, single-features SVDD models with these 10 features were constructed on the following dataset: 40 images of corn and 10 of weeds in the training set and 35 images of corn and 10 of weeds in the test set. The model's performance was evaluated by using RATE as the metric where RATE was defined as the number of correctly classified objects divided by the total number of objects. The SVDD obtained when T is the input vector, gave the best performance with a testing rate of 88.2%. For further analysis, the three morphological characteristics and five wavelet-based features associated with a RATE>60% were chosen, and every possible combination of these features

was utilized to create SVDD models. The four-best performing SVDD models were: SVDD (eV2, T), SVDD (eH2, eV2, T); SVDD (eH2, eV2, C, D), and SVDD (eH2, eV2, C, D, T) with RATES of 94.12%, 95.59%, 94.12% and 95.59%. respectively. SVDD (eH2, eV2, T), and SVDD (eH2, eV2, C, D, T) performed the best but considering the fact that the accuracy might be reduced if more features are considered, SVDD (eH2, eV2, T) was chosen as the best multi-feature based SVDD. This model when compared with SVM and FLDA, proved superior in terms of performance even when the number of weed samples for training was gradually reduced from 25 to 5. The results read: SVM (75.17%); FLDS (66.04%), and SVDD (94.34%).

The work by Montalvo et al. [116] demonstrated a method for the detection of crop rows in maize fields that contained high weed pressure (the type/species of weed was not mentioned). The image data consisted of 300 RGB images of maize (the first set of 200 images with high weed densities and the second set of 100 images where the weed density is exceptionally high). These images were transformed to grayscale using Excess green index following which a double Otsu approach was applied to separate the crop and weeds. The equations of straight lines associated with the crop rows were then computed using a linear regression technique that was based on total least squares. The performance of LR was compared with that of HT over images of various resolutions ( $1390 \times 1044$  (first set of images),  $696 \times 522$  (first set of images),  $720 \times 576$  (second set of images), and  $360 \times 288$  (second set of images)). The former outperformed the latter for every resolution mentioned above, with the best performance (percentage of effectiveness) being: LR (95.5%) over HT (89.3%) for the images with a resolution of  $1,390 \times 1,044$ .

Rainville et al. [66] presented a computer vision-based weed/crop classification using morphological analysis. The crops considered were corn and soybean and the type/species of



weed was not mentioned. The dataset consisted of 149 RGB images of corn and soybean. The images were segmented using PCA (used to extract the components that are associated with the vegetation) and Otsu thresholding (used to find the threshold to discriminate between the vegetation and soil). The crop rows were first identified using HT followed by which row borders were determined by analysis of the plants/vegetation that crosses the center lines of the row (these plants were considered a weed). Based on the data provided by these, PDFs of the weeds' morphological characteristics (area, compactness, major axis) were computed.

Considering that the plants that were present inside the rows were a mixture of both weed and crop, PDFs were deduced by utilizing the data from inside the rows. Following this, Naïve Bayes was used to discriminate the crop and weed that were present inside the rows. The data that was classified as the crop was then sent to GMM, another classifier that identified any leftover weed i.e., the weeds that were wrongly classified as crop. Any newly identified weeds were added to the list of previously classified weeds. As a measure of demonstrating classification accuracy, the authors worked on the sub-set of images (129 of the 149 images) for which the row positioning using Hough Transform was a success. The combination of the Bayesian classifier and GMM gave the following global classification performance average for the three morphological characteristics: area (90.8%); compactness (89.9%), and major axis (90.8%) with standard deviations of 4.4, 5.1, and 4.5, respectively.

The potential of a LIDAR sensor to detect crop rows, as well as maize and weeds was evaluated by Dionisio et al. [117]. The weeds involved in the study were: catchweed (*Galium aparine* L.); red dead-nettle (*Lamium purpureum* L.); winter speedwell (*Veronica persica* Poir.), and barnyardgrass. The distance and reflection measurements for the vegetation were gathered using the LIDAR sensor followed by which the real heights of the plants were evaluated.

Compared with the RGB images collected from the same plants, a strong correlation of 0.75 was observed between the heights measured by the LIDAR sensor and the real height of the plants. The system's ability to distinguish between plant and soil was determined using regression analysis for which the following two scenarios were considered: (i) the LIDAR's geometrical reliability, and (ii) the system's capacity to distinguish between the presence and absence of vegetation (logistic binary regression was used for this purpose as the presence/absence of vegetation is a binary variable). For the LIDAR measurements, the logistic regression performed very well, demonstrating a high level of accuracy in predicting the presence/absence of vegetation. For a total of 1,558 sample units, it was observed that the predicted accuracies for logistic regression read: vegetation (95.3%), and soil (82.2%). CDA was used to distinguish between soil and vegetation and also between plants and weeds. Although the CDA was more successful than the logistic regression in separating the plant from the soil, it had a lower success rate. With an overall accuracy of 72.2 %, CDA was able to distinguish between the following four sorts of classes: monocots; dicots; maize, and soil. The accuracies were: 92.4% for soil; 64.5% for dicots; 34.5% for monocots (accuracy was low since it was classified as crop), and 74.3% for maize.

The work by Amir and Ali [118] introduced a weed control robot capable of identifying weeds in cornfields by classifying pixels into corn and weed. The dataset consisted of 73 images taken in a cornfield, the type/species of weed was not mentioned. In order to extract plant pixels from the original images, the Excess green method was used followed by a clustering method (not mentioned). The hue plane of the image was extracted following which the clustering method was applied to it, and some morphological operation (not mentioned) was then performed. The features (not mentioned) were extracted by using wavelet transform and were

further used for classification. The entire method was implemented in LabVIEW software, which classified 70 of the 73 images thereby resulting in an accuracy of 95.89%. After the weed regions were identified, a hardware interface was used to send commands to the nozzles of the robot to spray herbicides.

Shubham [119] demonstrated a method for the classification of weeds in a maize field. The dataset involved in the study consisted of 60 RGB images of a maize field, the type/species of weed was not mentioned. These RGB images were transformed to gray ones using Excess green index followed by which the weeds and crops were separated using a double thresholding Otsu approach. It was then extended across each crop row for the weed present in that crop using the PCA technique to identify crops from weed in high-density regions. PCA was able to classify 55 of the 60 images correctly as weed or crop thereby resulting in an accuracy of 91.67%.

Pantazi et. Al. [120] proposed a new active learning approach to discriminate between maize and different species of weed based on the variations in their spectral reflectance. The weeds involved in the study were: creeping buttercup (*Ranunculus repens* L.); common nettle (*Urtica dioica* L.); black medick (*Medicago lupulina* L.); annual meadow grass (*Poa annua* L.); canada thistle; sheep weed (*Oxalis europaea* L.); winterweed (*Stellaria media* (L.) Vill.); charlock (*Sinapis arvensis* L.); dandelion, and redshank (*Polygonum persicaria* Gray). Spectral features were extracted using a hyperspectral optical sensor that was mounted on a robotic platform. Through reflectance calculation, plant selection, NDVI, and spatial resolution and, spectral analysis, the following spectral bands were chosen: 550 nm; 580 nm; 660 nm, and 830 nm. The weeds were recognized and rendered outliers using the one-class classifiers and then added to a new multi-class classifier that detected any new species of weed that appeared. This procedure was repeated until the multiple class classifier had all weed classes i.e., all the weed

classes were augmented in the multi-class classifier. The rest of the method was repeated for the following weed type, ensuring that the suggested technique can learn and enhance any new weed species forever. SVMs, autoencoders, MOG, and SOM were the ML methods used. Feature selection was performed on 110 spectra pertaining to maize plants thereby resulting in a dataset of 110 samples each of which had a vector of 4 features. The one-class classifiers were then tested to recognize the new species as outliers by using a total of 54 additional samples belonging to maize plants and 54 from a single weed species. Crop and the outlier spectra obtained from one species of weed were used as the baseline set in the next phase. The process of outlier detection was a repetitive one involving the addition of the first weed species to the data samples pertaining to the crop. Following that, the one-class classifiers were fed with a new weed species as well as the data from the already existing crop and weed species. If a new sample was discovered to be from one of the baseline set's crop or weed species, the outlier detection procedure had to be run for each class inside the baseline set, and the sample was classed as belonging to one of the baseline sub-classes. This process was iteratively repeated for every newly appearing weed species. While for crop recognition, the one-class MOG and one-class SOM achieved a rate of 100%, the best recognition rates for weed species read: 98.15% (MOG) and 98.44% (SOM) for canada thistle; 90.74% (SOM) for charlock; 94.44% (MOG) and 92.59% (SOM) for winterweed; 90.74% (SOM) for dandelion; 94.44% (SOM) for annual meadow grass; 94.44% (SOM) for redshank; 94.44% (SOM) for common nettle, and 94.44% (SOM) for black medick. Good recognition rates of 83.33%, 79.63%, and 85.19% were also obtained for annual meadow grass, dandelion, and black medick respectively while SOM provided a good rate of 85.19% for sheep weed and the autoencoder gave a good rate of 83.33% for black medick.

The integration of texture, shape, and spectral characteristics to classify crops and different species of weed was investigated by Zhang et al. [121]. The crop studied was corn and the weeds were dicotyledonous weeds namely, lobed leaf pharbitis (*Pharbitis nil* (L.) Choisy), redroot amaranth, leaf pharbitis (*Pharbitis purpurea* (L.) Voigt) and purslane (*Portulaca oleracea* L.) and monocotyledonous weeds namely, green foxtail, and goose grass (*Eleusine indica* L.). SPCA was used to select the following relevant wavelengths: 710 nm; 516 nm; 843 nm; 677 nm, and 749 nm. For classification, the following texture, shape, and spectral characteristics were employed using C 5.0 algorithm: texture features namely, homogeneity, entropy, and contrast for the wavelengths 677 nm, 843 nm, and 516 nm; shape features namely length, width, shape index and area, and spectral features namely, ratio of the bands 677 nm and 710 nm, normalized difference index between the bands 749 nm and 710 nm, red index, and ratio vegetation index. The model produced both a global accuracy and kappa coefficient of over 95% when spectral and shape features were used.

The work by Gao et al [122] investigated the potential of classifying weed and maize using hyperspectral imaging. The weeds in the study were: field bindweed; *Rumex* species, and Canada thistle. The dataset consisted of 24 hyperspectral images of each of the three weeds and 25 of maize. ROIs of the leaves of the plants involved in the study were used and consisted of 79, 80, 80, and 84 for field bindweed, *Rumex* spp., Canada thistle, and maize, respectively. For each band, the calibrated reflectance of ROIs was calculated followed by which 80 NDVIs (ranging between 0 and 1) and 80 RVIs were calculated and used for feature construction. When these were subject to PCA, the redundancy was reduced and only the first five principal components were used for further analysis. Classifiers with different combinations of spectral features were built using RF. Following feature construction, importance scores determined the

30 most important features to be chosen by an accuracy-oriented feature reduction technique. Five-fold cross-validation (one set for testing and four for training) was used to evaluate RF. The results read: Maize (94% precision and 100% recall); Rumex (70.3% precision); Canada thistle (65.9% precision), and field bindweed (95.9% precision). When the performance of RF was compared to that of KNN using a McNemar test, the optimal RF model performed better than KNN at a significance level of 0.05.

Zheng et al. [123] developed an efficient method to classify maize and weeds by using color features. RGB images of weeds (species not mentioned) and maize were gathered for the three consecutive years 2011, 2012, and 2013 and consisted of three classes: maize; weed, and soil. The images were then preprocessed for background removal using Excess Green followed by Otsu's thresholding. PCA aided in the extraction of the following color features: single-color indices namely, Rn and Gn; two-color indices, ExR, and three-color indices namely, ExR, ERI, Gray, EGI, and CIVE. SVDD was used for classification and was trained on 197 image samples from the year 2011. 4333 samples of maize, 5730 of weed from 2011, 3573 samples of maize and 7976 of weed from 2012, and 1465 samples of maize and 7878 of weed from 2013 were chosen for testing purposes. When compared with LS-SVM, SVDD models performed better on the data for all three years based on the results evident from the confusion matrix. The results read: LS-SVM (accuracies of 89.08%, 87.87% and 90.44% respectively), and SVDD (accuracies of 90.19%, 92.36% and 93.87%, respectively). Citing lower sensitivity to canopy overlap, wind effect, leaf orientation, etc., the authors concluded that the use of color indices for classification is more practical than the use of shape/texture features. Table 2.3. summarizes all the above works that employed ML techniques other than SVMs or neural networks for the identification of weeds.

Table 2.3. Summaries of studies that employed miscellaneous models for the identification of weeds.

<b>Study</b>	<b>Research problem</b>	<b>Dataset</b>	<b>Accuracy</b>
[108]	Detection of weed and nitrogen stress in corn	20 data points of 9 treatments consisting of 4 replicates thereby resulting in a data set of 720 entries. 50% of the data was used for training purposes while the remaining 50% was used for testing.  <b>Hardware used:</b> A Compact Airborne Spectrographic Imager (CASI)	DT: 71% for first classification problem at tasseling stage  DA: 79% for third classification problem at full growth stage  ANN: 71% for first classification problem at tasseling stage
[109]	Use of FFT to classify weed and corn	<b>Hardware used:</b> Robotic cultivators with a digital camera to capture images and pre-processing was done to obtain RGB images.	80 corn field images were used to test classification accuracy. 5927 blocks of size 1024 x 768 were detected as weed, 3217 as crop, and 8579 correctly classified.  Accuracy was 92.8%
[110]	Discriminating crop and weed in agronomic images	300 simulated images, 100 in-field images (35 of wheat, 35 of sunflower, and 30 of maize)	Simulated images: 100% each for crops with low WIR, 94% and 92% respectively for medium, 89% and 82% respectively for high.  100 in-field RGB images: 88%.for 30 images of maize with low WIR
[111]	Discriminate between crop and weed using wavelet transform	1530 images  <b>Hardware used:</b> A digital camera (CANON Ixus 330)	Daubechies 25: 80.7% Discrete approximation Meyer wavelets: 80.6%.
[112]	Vision-based autonomous weed detection	No information about data  <b>Hardware used:</b> Not mentioned	Error $< \pm 5$ and $\pm 10$ pixels for translation and degrees for orientation respectively.

Table 2.3. Summaries of studies that employed miscellaneous models for the identification of weeds (continued).

<b>Study</b>	<b>Research problem</b>	<b>Dataset</b>	<b>Accuracy</b>
[113]	Crop and weeds classification based on their UV-induced fluorescence spectral signature	No information about data  <b>Hardware used:</b> Not mentioned	LDA over PCA: 91.8%
[114]	Discrimination of crop and weed by using real-time image processing	6 video segments (each having an average 12 second duration i.e. 300 frames) thereby resulting in a total of 1800 frames  <b>Hardware used:</b> Sony DCR PC110E and JVC GR-DV700E (resolution of 720×576 pixels).	Successfully detecting an average of 95% for weeds and 80% of crops under different environmental conditions.
[115]	Recognizing images of weed and corn using SVDD	118 color images. 40 images of corn and 10 of weed for used for training. 35 images of corn and 33 of weed were used for testing.  <b>Hardware used:</b> Olympus FE-280 digital camera with a resolution of 1280x960 pixels.	SVDD (eH2, eV2, T): 95.59% SVDD (eH2, eV2, C, D, T): 95.59%
[116]	Detection of crop rows in maize fields containing high weed pressure	No information about data  <b>Hardware used:</b> Basler scA 1400-17fc camera (resolution: 1392 x 1044 pixels) for first 200 images. Sony commercial DCR PC110E camera (resolution: 720 x 576 pixels) for second set of 100 images	Images with resolution of 1392 x 1044: HT (89.3%), LR (95.5%) Images with resolution of 696 x 522: HT (86.4%), LR (92.9%) Images with resolution of 720 x 576: HT (82.4%), LR (89.6%) Images with resolution of 360 x 288: HT (80.1%), LR (88.1%)



Table 2.3. Summaries of studies that employed miscellaneous models for the identification of weeds (continued).

<b>Study</b>	<b>Research problem</b>	<b>Dataset</b>	<b>Accuracy</b>
[66]	Using Bayesian classification to isolate weeds in row crops	149 images of crops (corn and soybean) and weeds  <b>Hardware used:</b> Not mentioned	An average of 94 % of corn and soybean plants were classified and 85 % of the weeds were classified
[117]	Using LIDAR to discriminate between maize and weeds	1,558 sampling units  <b>Hardware used:</b> Not mentioned	CDA overall accuracy: 72.2%. Accuracy for dicots: 64.5%, and Accuracy for crop: 74.3%.
[118]	Automatic classification of weeds and corn	73 images <b>Hardware used:</b> Digital camera (normal webcam). RGB images were captured with a size of 640 x 480 pixels	95.89%. 3 images were misclassified
[119]	Detection of crop row and distinguishing between crop and weed in field with high weed pressure	60 RGB images  <b>Hardware used:</b> Not mentioned	91.67%, 5 images misclassified
[120]	Recognizing and discriminating between weed and maize using hyperspectral imaging	110 samples derived through feature selection from 110 spectra pertaining to maize plants. The one-class classifiers were tested to recognize the new species as outliers by using 54 additional samples of maize plants and 54 from a single weed species.  <b>Type of imaging:</b> Hyperspectral  <b>Hardware used:</b> Inspector V9, a 10-bit integration charge-coupled device	100% for both MOG and SOM. MOG based one-class classifier: between 31% to 98%. SOM based one-class classifier: between 53% to 94%.

Table 2.3. Summaries of studies that employed miscellaneous models for the identification of weeds (continued).

<b>Study</b>	<b>Research problem</b>	<b>Dataset</b>	<b>Accuracy</b>
[121]	Texture, space and spectral features-based classification of weeds and corn	No information about data  <b>Hardware used:</b> Field Imaging Spectrometer System (FISS), CCD camera	Over 95%
[122]	Hyperspectral imaging-based classification of maize and weed	Maize: 25 images, 24 each for <i>C. arvensis</i> , <i>C. arvensis</i> and <i>Rumex</i> spp.  <b>Type of imaging:</b> Hyperspectral  <b>Hardware used:</b> Snapshot mosaic hyperspectral camera and sensor.4 OSRAM Halogen lamps	Maize (94% precision and 100% recall), <i>Rumex</i> spp. (70.3% precision), <i>C. arvensis</i> (95.9% precision) and <i>C. arvensis</i> (65.9% precision).
[123]	Identification of weed and using color indices	Training data: 197 RGB image samples from 2011, 4333 samples of maize, 5730 of weed from 2011, 3573 samples of maize and 7976 of weed from 2012 Testing data: 1465 samples of maize and 7878 of weed from 2013 were  <b>Hardware used:</b> E450 Olympus (resolution = 3648 x 2736 pixels, focal length = 16 mm).	Accuracies of LS-SVM for three years: 89.08%, 87.87% and 90.44%  Accuracies of SVDD for three years: 90.19%, 92.36% and 93.87%.

## 2.6. Dataset size, data augmentation, transfer learning, and performance metrics

Training a new classification model with the desired accuracy may require huge amounts of data and sophisticated computational tools to process the collected data. The size and quality of the dataset have a major impact on the image classification performance of ML models. In

general, smaller datasets result in poor classification accuracy. This has been shown in numerous previous studies [124–129]. The size of the dataset necessary for the desired accuracy is determined by a variety of criteria, including the number of classification categories, the complexity of the features present in the images that are to be classified, and class imbalance. For example, Luo et al showed that an image dataset size of 6,000 was required when the number of classification categories were three and when the categories was increased to eight, a dataset size of 40,000 was required to obtain 90% accuracy [130]. Smaller datasets also result in the overfitting of the model [131]. Overfit models tend to memorize the variance along with the underlying relationships and perform poorly on the testing and unseen future datasets [132]. Yet, in our domain, it is often too expensive or not viable to build a large dataset for training.

The problem caused by the smaller datasets (especially overfitting) can be partially mitigated through data augmentation [133]. Data augmentation expands the original dataset through image manipulations, feature space augmentation, and adversarial training [134]. Image manipulations include geometric transformations, color space transformations, random erasing, introducing corruptive noises, and image mixing. Geometric transformations involve the modification of geometrical features through flipping, translation, rotation, and cropping of images [135]. Color space transformations use filters to modify the RGB space of images [136]. Random erasing is about randomly removing some of the image features [137]. In image mixing, new images are formed by combining the pixel values of pair of images [138, 139]. In contrast to all the image-based approaches discussed above, Devries and Taylor introduced a novel way of augmenting data in the feature space [140]. Instead of applying transformations to the input, they have applied transformations to the encoded versions of the inputs. Another interesting approach to data augmentation is the use of GANs [141]. GANs consist of two different competing

networks called generator and discriminator. The role of the generator is to confuse the discriminator that the artificially generated image is real whereas the discriminator's role is to differentiate the real images from the synthetic images created by the generator. The simultaneous training of these two networks generates artificial images which share similar characteristics to original images.

Though data augmentation offers a way to increase the size of the dataset to mitigate the overfitting of the model, it is computationally expensive and time-consuming. Another popular approach that allows us to bypass the requirement of a larger dataset is transfer learning [142, 143]. Instead of developing a neural network (say for image classification) from the ground up, we can utilize the learned parameters of a neural network trained on different yet related domain tasks to train our new task of interest. This approach is successfully applied in many domains including precision agriculture. For instance, Espejo-Garcia et al leveraged the trained neural network parameter of ImageNet for weed classification [144]. Suh et al again utilized the pre-trained network on ImageNet dataset for the classification of sugar beet (*Beta vulgaris* L.) and volunteer potato (*Solanum tuberosum* L.) [145]. Kaya et al compared four different transfer learning models with the one developed from scratch for plant classification [146]. Currently there are various approaches available in transfer-learning and can be found elsewhere [147–153].

We have discussed the importance of larger datasets for higher classification accuracy. But classification accuracy is just one of the parameters to evaluate the model's performance and in many situations, accuracy alone is not sufficient enough to quantify the performance of an ML model. The other commonly used performance metrics are F1-score, precision, confusion matrix, recall, log-loss, and ROC-AUC [154]. The accuracy of a classifier is defined as the ratio of the

number of correct predictions to the total number of predictions. But it gives misleading performance evaluation when the dataset is imbalanced. In order to understand how to utilize other performance metrics, we need to understand some basic terminologies involved such as true positives, false positives, true negatives, and false negatives. The definitions of these terms are summarized in Table 2.4.

Table 2.4. Definitions of a classifier predictions.

<b>Terminology</b>		<b>Definition</b>
True Positive	TP	Correctly identified an instance to a particular class
False Positive	FP	Incorrectly identified an instance to a particular class
True Negative	TN	Correctly identified an instance does not belong to a particular class
False Negative	FN	Incorrectly identified an instance does not belong to a particular class

The mathematical definitions of commonly used performance metrics are given in Table 2.5.

Table 2.5. Mathematical definitions of performance metrics.

<b>Performance metric</b>	<b>Definition</b>
Precision (P)	$TP/(TP+FP)$
Recall (R) / True Positive Rate (TPR)	$TP/(TP+FN)$
Specificity (S) / True Negative Rate (TNR)	$TN/(TN+FP)$
Miss Rate / False Positive Rate (FPR)	$FN/(TP+FN)$
F1 Score	$2PR/(P+R)$
Log Loss (for one-hot coded vectors)	$-\log p$

Note:  $p$  – probability of an instance belonging to a class

Though the confusion matrix is not strictly a performance metric, it gives an overview of positives and negatives predicted by the classifier. An illustration of the confusion matrix for binary classification is given in Fig.2.

		Predicted Class	
		-	+
Actual Class	-	No. of True Negatives	No. of False Positives
	+	No. of False Negatives	No. of True Positives

Fig. 2.2. Confusion matrix for a binary classification.

Precision measures the correctly predicted positives out of the total positives predicted. Higher precision indicates a smaller number of false positives in the model and is used in situations where the false positives in a model are highly undesirable. Recall or sensitivity or true positive rate talks about the ability of the model to predict the true positives out of total real positives. A higher recall is important in the identification of diseases. F1 measure gives equal weightage to the false positives and false negatives and a harmonic mean of recall and precision. Miss rate or false positive rate is the additive inverse of sensitivity and measures the proportion of correctly identified negatives with respect to the total predicted negatives. Log-loss measures the deviation of the predicted probability of an instance belonging to a class to that of the actual probability (in general 1) and is commonly used in binary classifications. The receivers operating characteristics (ROC) curve is an excellent performance standard used for binary classification models with imbalanced datasets [155]. It's a plot between the true positive rate (on Y-axis) and false positive rate (on X-axis) for different classification thresholds (probability thresholds) as shown in Fig. 3.

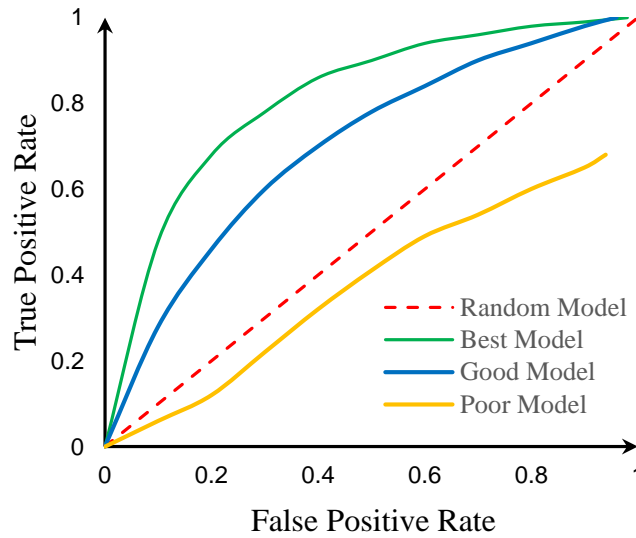


Fig. 2.3. Receiver-Operating characteristic (ROC) curves.

It is considered that a classifier model has a trade-off between true positives and false positives. A random model tuned to generate a higher number of true positives also may equally generate false positives. So, a random classifier, in this case, follows a 45° straight ROC line with 0.5 as the area under the curve (AUC). A poor classifier falls below this straight line and has an AUC value less than 0.5. Hence, any good classifier should have a ROC curve above this straight line with an AUC value of more than 0.5. A Perfect classifier has a true positive rate of 1 for all classification thresholds. It is to be noted that unlike other performance measures ROC-AUC is an index measure. Though ROC is mainly developed for binary classification, it can be extended to multi-class classification by clubbing the rest of the categories as one class. A detailed review of error metrics can be found here [156, 157].

## 2.7. Conclusion and future research directions for the identification of weeds in corn

This review surveyed 35 articles featuring ML approaches with full technical details. Twenty-seven of the presented articles were intended at solving a classification problem while seven were intended at solving the problem of object detection. There were also two articles that

solved both these problems. Figure 4 presents the distribution of these articles according to the type of ML problem.

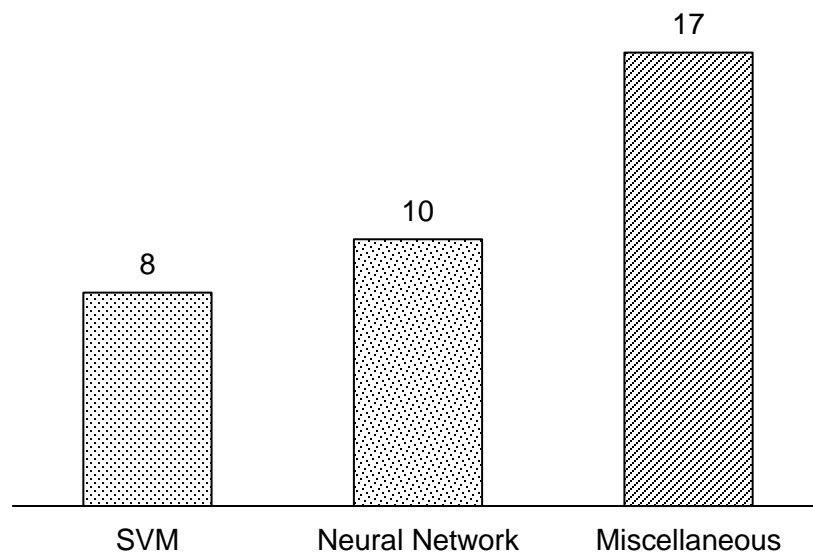


Fig. 2.4. Frequency distribution of different ML approaches used in the reviewed articles.

Three ML approaches were used namely, SVM, Neural Networks and Miscellaneous (Bayesian networks, Decision Trees, Genetic Algorithms etc.). Eight of the presented articles used SVM as the ML approach, ten used Neural Networks, and seventeen used Miscellaneous approaches (Bayesian networks, Decision Trees, Genetic Algorithms etc.). Figure 5 depicts the distribution of these articles according to the ML approach used.



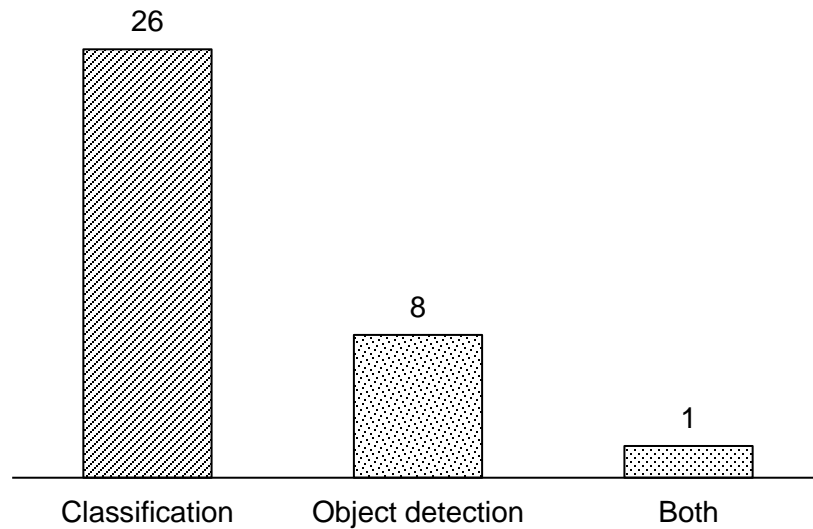


Fig. 2.5. Frequency distribution of different ML problems focused on the reviewed articles.

It was found that the SVM with RBF kernel function was the most used type of SVM while BP network was the most used Neural Network, although CNNs were also commonly used. Among the Miscellaneous approaches, wavelet transforms were the popular ones while DT, PCA, customized Computer Vision systems etc., were also used. The most popular type of data that was used by these approaches was color data (images and videos) comprising twenty-eight of the presented articles while in eight articles, spectral data (hyperspectral data, reflectance spectra, fluorescence spectra etc.) was also used. The distribution of articles based on the type of data involved is shown in Figure 6.

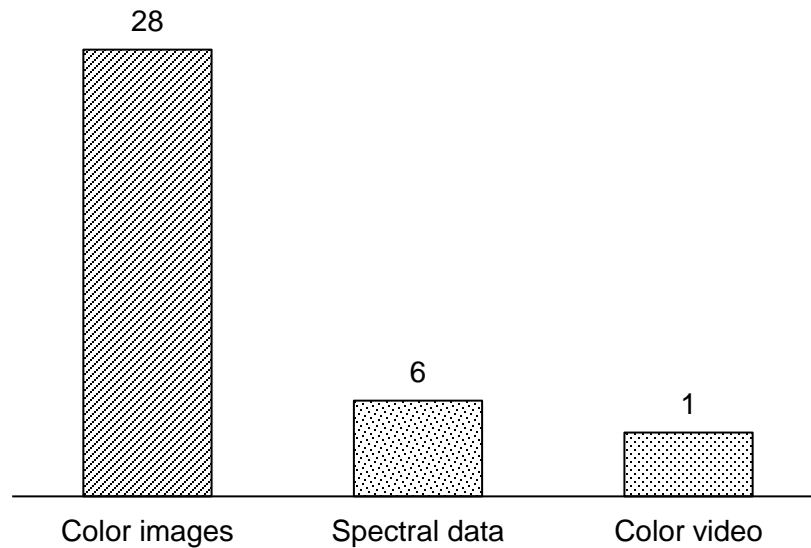


Fig. 2.6. Frequency distribution of different data types used in the reviewed articles.

A variety of weeds belonging to different categories namely, broadleaf, narrow leaves, grassy, dominant grassy, dominant broad-leaves, monocotyledonous, dicotyledonous, etc., were involved in the articles.

Industry, university academics, and the USDA (United States Department of Agriculture) are all working together to advance the identification of weeds in corn. More effort should be directed to the following areas, based on our review:

1) Data acquisition and augmentation: Data plays an important role in aiding in the identification of weeds. Some works in this review made use of minimal to very little data to train the ML algorithms, and only two works among made use of data augmentation. This might not suffice for the task of identifying weeds, and most importantly, the results obtained by using low amounts of data do not justify the predictions of the trained algorithms.

2) Early identification of weeds: Although most works in this review dealt with the data acquired when the weeds were in the early growth stages, some works dealt with data that was collected when the weeds were in the later stages of growth i.e., three weeks, six weeks or more.

This is a drawback because, at three to six weeks, weeds will display distinguishable features that can aid in manual identification relegating the need for identification through algorithmic means.

3) Sanity checks: The need to check for model overfitting as well as to validate the model in various lighting conditions/environments cannot be undermined and falls under the realm of sanity checks. The models trained on the data should be tested on different modifications of the original data. Commonly used simple sanity checks include testing the trained model on cropped and resized images, images with altered brightness and contrast, and the addition of noise.

4) Transfer learning: Transfer learning involves initializing the current neural network with the use of learned parameters of already trained neural networks employed for a different but related task. Transfer learning helps the network to achieve the generalizing ability with a smaller dataset. They also reduce the time required for the network training. There are several studies which utilize transfer learning for weed identification in crops [158–161], yet more research is required to address the pitfalls of transfer learning especially a phenomenon called ‘negative transfer’ where the network performs poorly after the transfer.

5. Interpretability: ML algorithms act as black-box models and offer little explanation on how the predictions are made. This lack of transparency questions the reliability of the predictions or conclusions made by the ML models. Hence, the interpretability of ML models used for the identification of weeds is highly desired to understand the embedded biases in the network and also to identify the important input features and conditions that led to the ML decision. Although some research [162, 163] focused on interpretability of neural networks employed for identification of weeds, more works are needed to understand the bias in the

network and the important input features responsible for the weed identification and classification.

### **3. DISTINGUISHING PALMER AMARANTH FROM WATERHEMP IN THE FIRST TWO WEEKS**

Palmer amaranth (*Amaranthus palmeri* S. Watson) is an annual broadleaf weed native to the arid southwestern United States and northwestern Mexico. Palmer amaranth can grow rapidly, consuming useful nutrients and towers over the crops, drastically reducing crop yields. Palmer amaranth was recently found in several counties of North Dakota and Minnesota, concerning the farmers, and threatening the agrarian economy of North Dakota. For this reason, Palmer amaranth was named the weed of the year in 2014 and 2015 by NDSU Plant Sciences department faculty. Early detection and eradication are considered the best strategy to mitigate the damage caused by Palmer amaranth. However, Palmer amaranth is visually similar to other pigweed species including waterhemp (*Amaranthus tuberculatus*) (Moq.) J. D. Sauer Powell amaranth (*Amaranthus powellii* S. Watson), and redroot pigweed (*Amaranthus retroflexus* L.) in the early stages of its growth and development. The goal of this research is to automatically distinguish Palmer amaranth from waterhemp in the first two weeks after germination.

Palmer amaranth and waterhemp were grown in a controlled environment for over two weeks after emergence. Approximately 2,000 digital images of both weeds were acquired between 8-14 days after emergence (DAE). These images were utilized to track the morphological characteristics including length, width, area, perimeter, aspect ratio, circularity, and roundness of Palmer amaranth and waterhemp leaves. Several popular Machine Learning (ML) algorithms were trained on the estimated morphological features to classify the weed as either Palmer amaranth or waterhemp. A deep learning approach using a Convolutional Neural Network (CNN) was adopted to improve the classification accuracy. To this end, data

augmentation techniques were used to generate 14,000 additional images from the original 2,000 images. A CNN was trained using 100% of the available data. The trained CNN was validated using the original 2,000 images embedded with Gaussian noise. Finally, YOLO V5, an object detection algorithm based on transfer learning, was successfully prepared and tested for the detection of Palmer amaranth in a set of synthetically generated images consisting of both Palmer amaranth and waterhemp.

The rest of the dossier was organized as follows: image acquisition and pre-processing are explained in palmer amaranth and waterhemp image acquisition; quantification of morphological characteristics of palmer amaranth and waterhemp was described in Morphological Characteristics; a description of ML techniques used to distinguish palmer amaranth from waterhemp is discussed in Machine Learning; a description of CNN for the same purpose is provided in Deep Learning; Transfer Learning is explained in Object Detection and Transfer Learning; and the results of the study are discussed in Results.

### **3.1. Palmer amaranth and waterhemp image acquisition**

Fifty palmer amaranth and waterhemp plants were grown in pots in a controlled greenhouse environment at North Dakota State University (NDSU), Fargo, North Dakota. The pots were continually irrigated and image acquisition was performed using a high-resolution camera (24.2 MP Canon EOS Rebel T7i DSLR) established on a stable platform perpendicular to the surface of the pots. The details of the experiment are provided in Table 2. RGB images pertaining to 27 days from the date of emergence were acquired between 1:00 PM and 3:00 PM on a daily basis. RGB images of size 4020 × 6024 pixels were acquired at three different orientations (first, 25 centimeters from the level of the soil, second, 20 centimeters from the level

of the soil, and third, close-up shots) as shown in Figure 3.1 and Figure 3.2, respectively, while the details of the experiment are provided in Table 3.1. Note that the lighting inside the greenhouse was turned off so as to ensure the light did not interfere with the process and care was also taken to ensure the samples were not affected/harmed in any way during the process i.e., neither the hands nor the camera touched/caused any damage to the plants.



Fig. 3.1. Palmer amaranth captured 8 days after emergence: (a) 25 centimeters from the soil surface; (b) 20 centimeters from the soil surface, and (c) close to the soil surface.

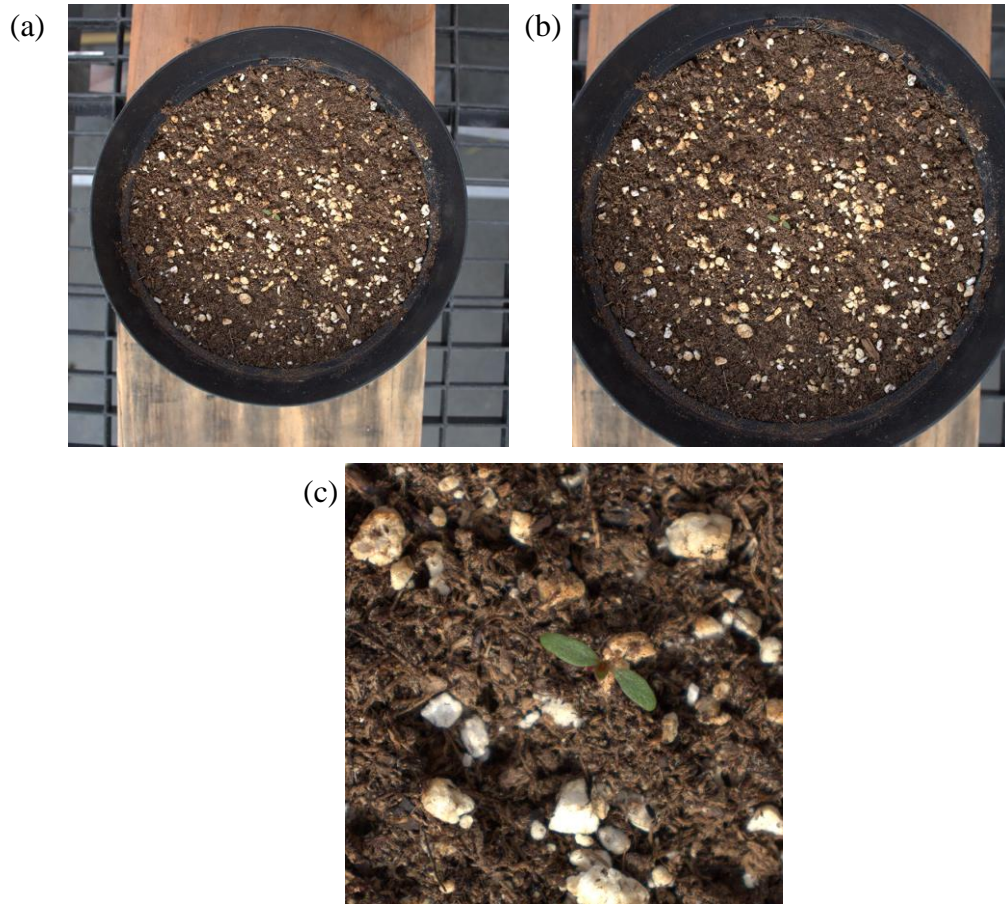


Fig. 3.2. Waterhemp captured 8 days after emergence: (a) 25 centimeters from the soil surface; (b) 20 centimeters from the soil surface, and (c) close to the soil surface.

Table 3.1. Experiment details.

<b>Experimental data</b>	<b>Value</b>
Number of pots involved	50
Number of pots of palmer amaranth	25
Number of pots of waterhemp	25
Start date of experiment	01/19/2021
End date of experiment	02/23/2021
Time of image gathering	1 p.m. to 3 p.m.
Date of emergence of palmer amaranth	01/28/2021
Date of emergence of waterhemp	02/05/2021

The pre-processing of images and their augmentation is described next.



### 3.1.1 Pre-processing of images

The images corresponding to the second week of growth i.e., 8 to 14 DAE were selected for pre-processing owing to the small size of the weeds during the first week of growth. A total of 2,000 images (1,000 each of palmer amaranth and waterhemp, respectively) were processed for background removal using the Image Segmenter tool in MATLAB. Background removal dealt with the removal of the soil (potted mix) and any other objects from the image to ensure that the sample (weed) is the only object present in the image thereby making it the region of interest (Figures 3.3 and 3.4).

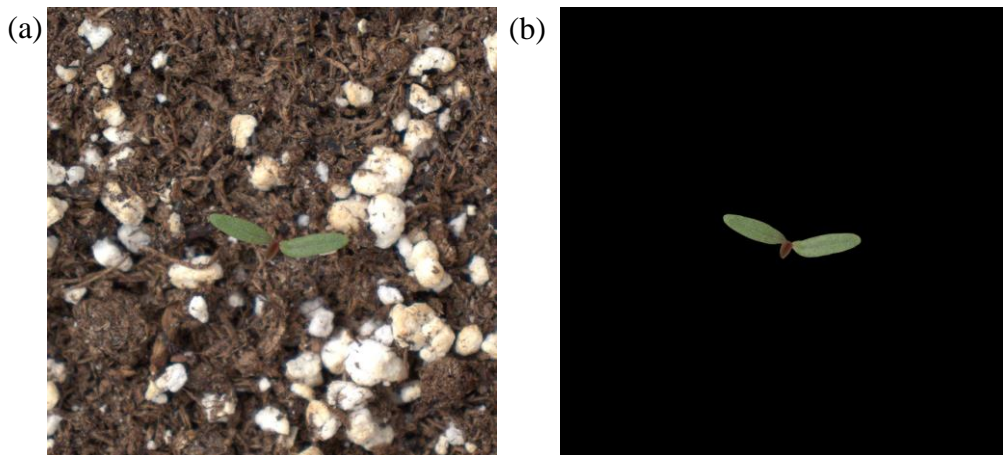


Fig. 3.3. (a) Original image of palmer amaranth, (b) Palmer amaranth after background removal.

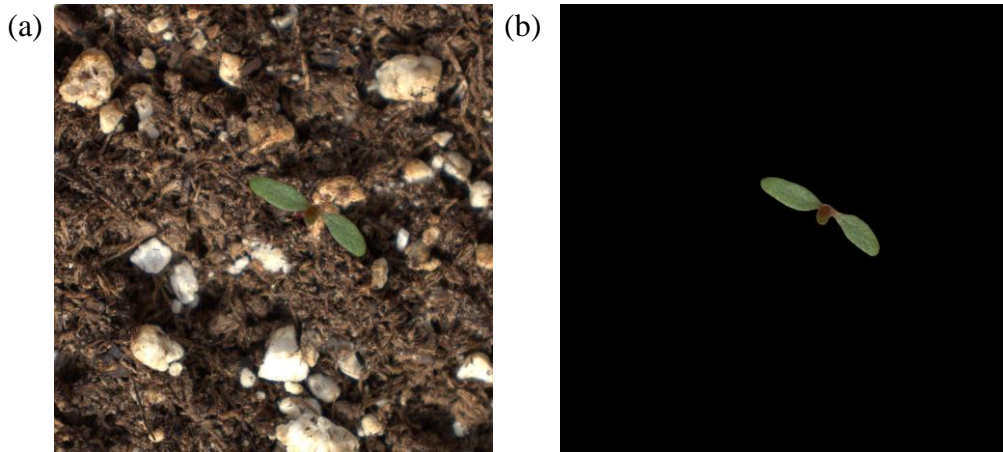


Fig. 3.4. (a) Original image of waterhemp, (b) Waterhemp after background removal.

### 3.2. Morphological characteristics

A select set of 36 leaves corresponding to each weed species from the above-mentioned dataset were randomly chosen and their morphological characteristics were extracted using a pixel-count method. This was performed by placing a grid of  $1 \times 1$  pixel on each image and counting the number of pixels corresponding to the morphological characteristic.

The following characteristics were extracted:

- Length (L) – the number of pixels corresponding to the length of the leaf i.e., the major axis
- Width (W) – the number of pixels corresponding to the width of the leaf i.e., the minor axis
- Area (A) – the number of pixels that correspond to the leaf in the image
- Perimeter (P) – the number of pixels that outline the leaf in the image

These parameters in turn, were used to estimate the following dimensionless characteristics namely, Aspect Ratio, Circularity, and Roundness.

Figures 3.5 to 3.10 visualize the evolution of these dimensionless characteristics between days 8 to 14 for both the weed species.

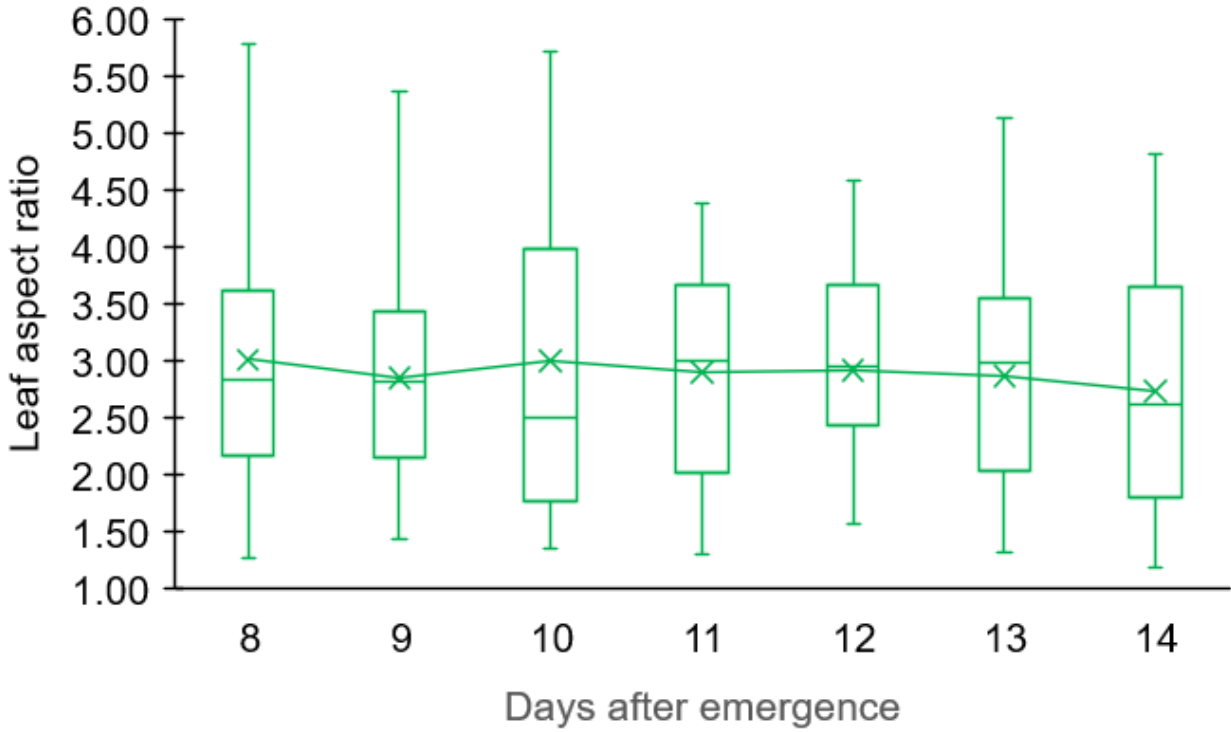


Fig. 3.5. Evolution of aspect ratio for palmer amaranth (8 to 14 DAE).

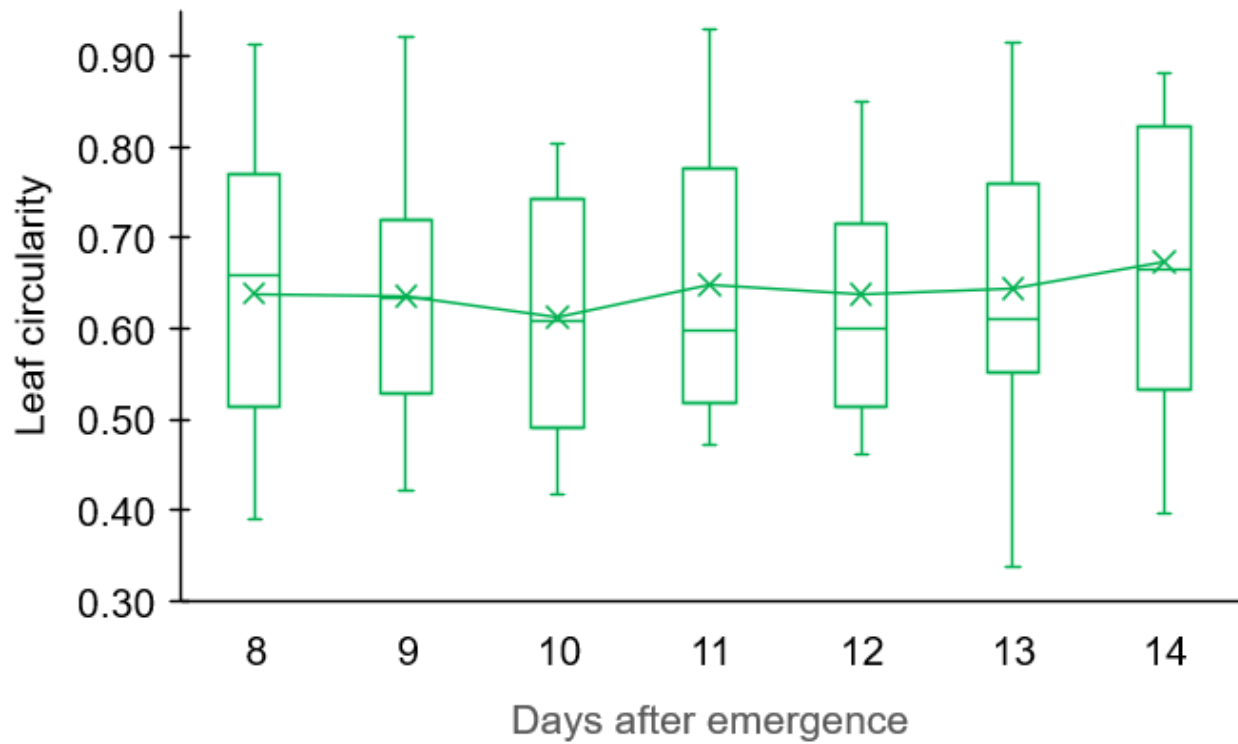


Fig. 3.6. Evolution of circularity for palmer amaranth (8 to 14 DAE).

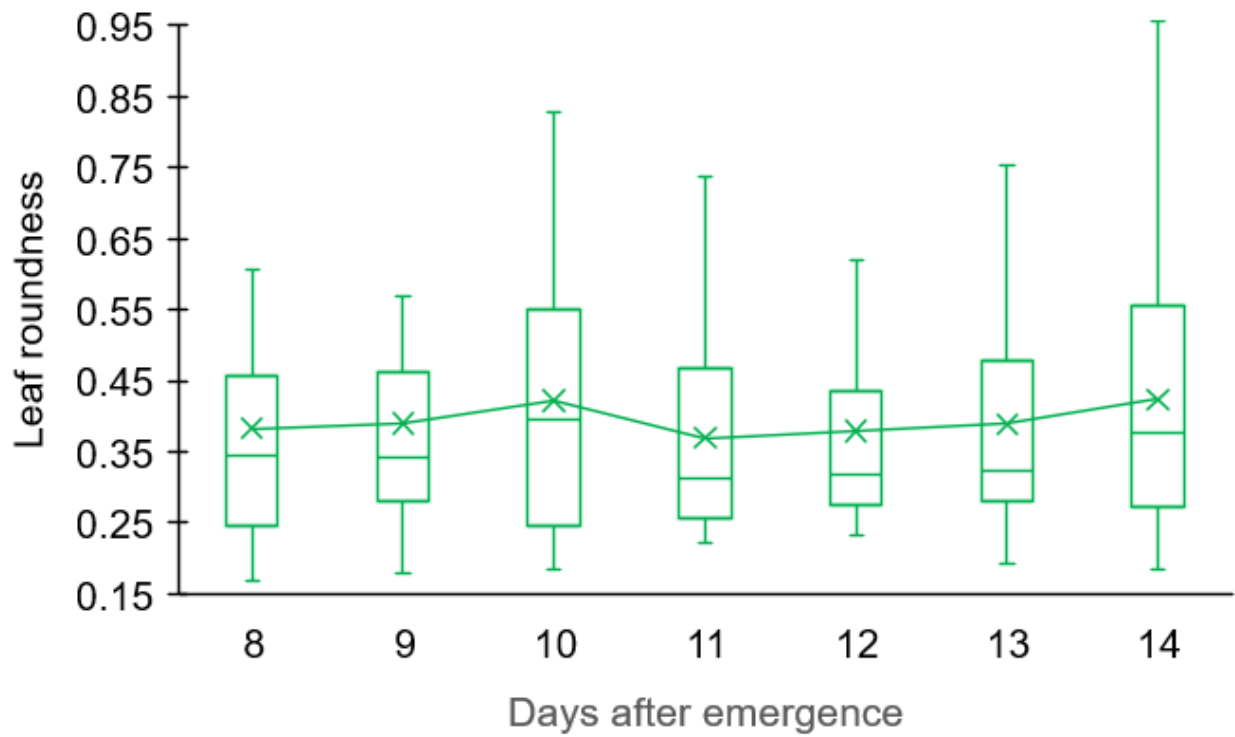


Fig. 3.7. Evolution of roundness for palmer amaranth (8 to 14 DAE).

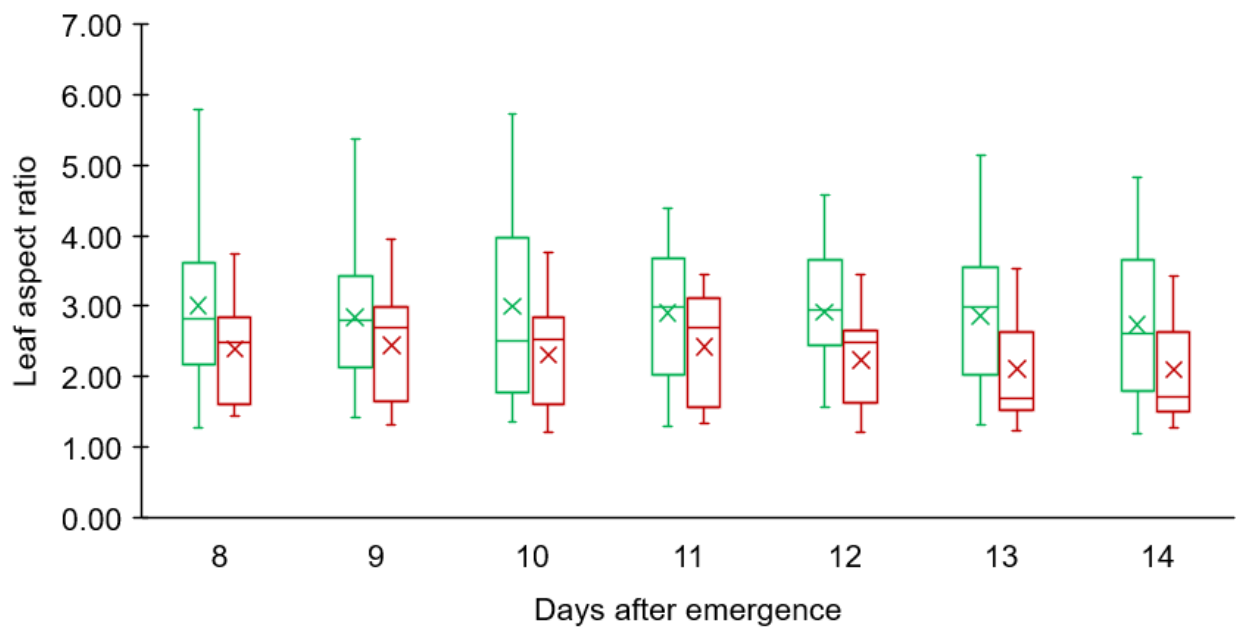


Fig. 3.8. Comparison of evolution of aspect ratio of palmer amaranth with that of waterhemp (8 to 14 DAE).

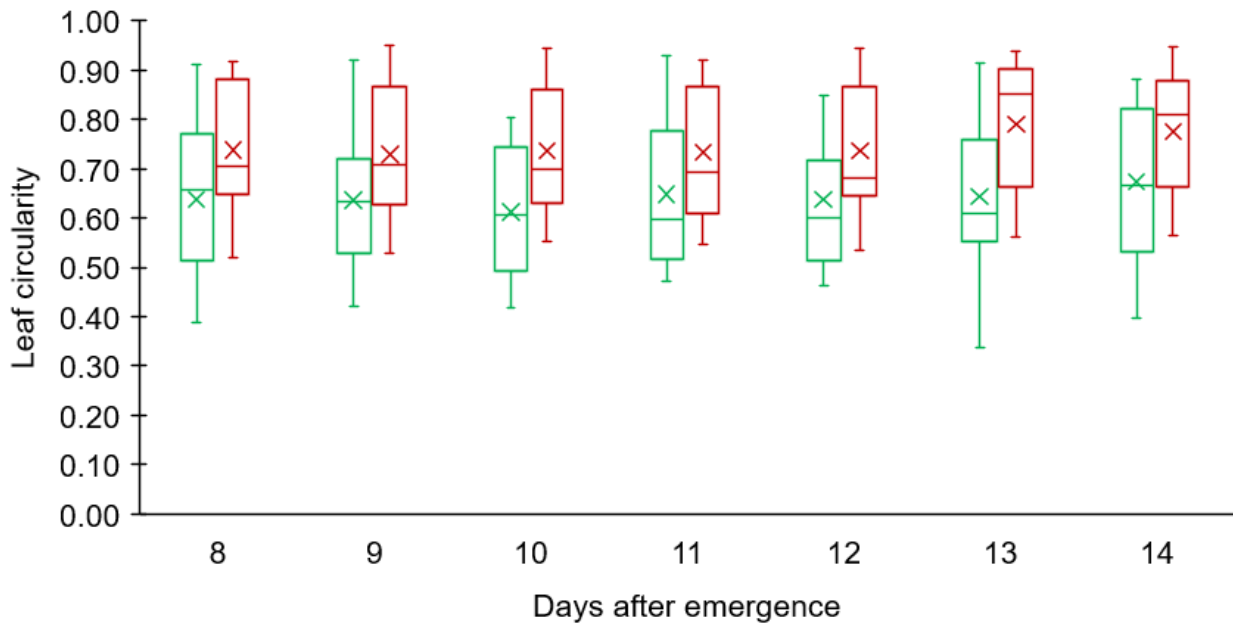


Fig. 3.9. Comparison of evolution of circularity of palmer amaranth with that of waterhemp (8 to 14 DAE).

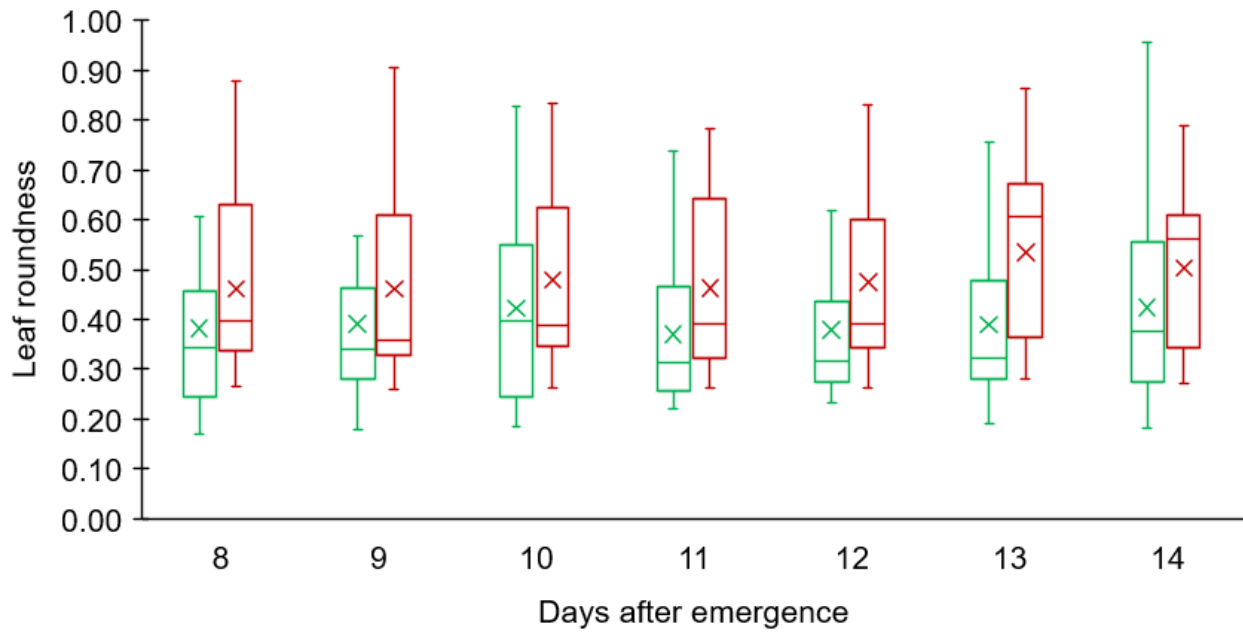


Fig. 3.10. Comparison of evolution of roundness of palmer amaranth with that of waterhemp (8 to 14 DAE).

Dimensionless characteristics were averaged and plotted against time with an aim of distinguishing palmer amaranth from waterhemp within the first two weeks of emergence.

Figures 3.11 to 3.13 visualize the three dimensionless parameters (averaged for 36 leaves) for days 8 to 14 DAE.

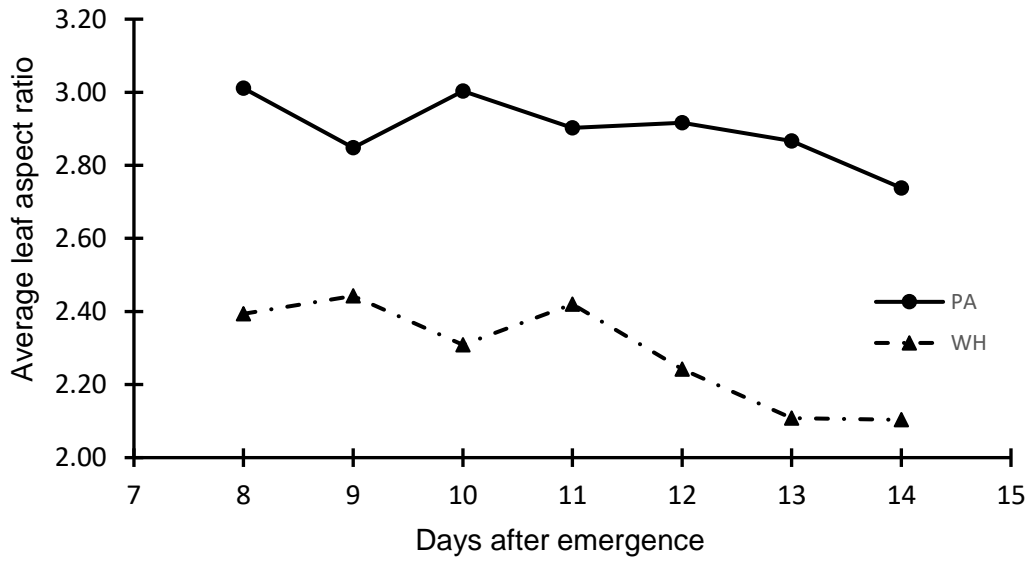


Fig. 3.11. Aspect ratios of palmer amaranth and waterhemp (8 to 14 DAE).

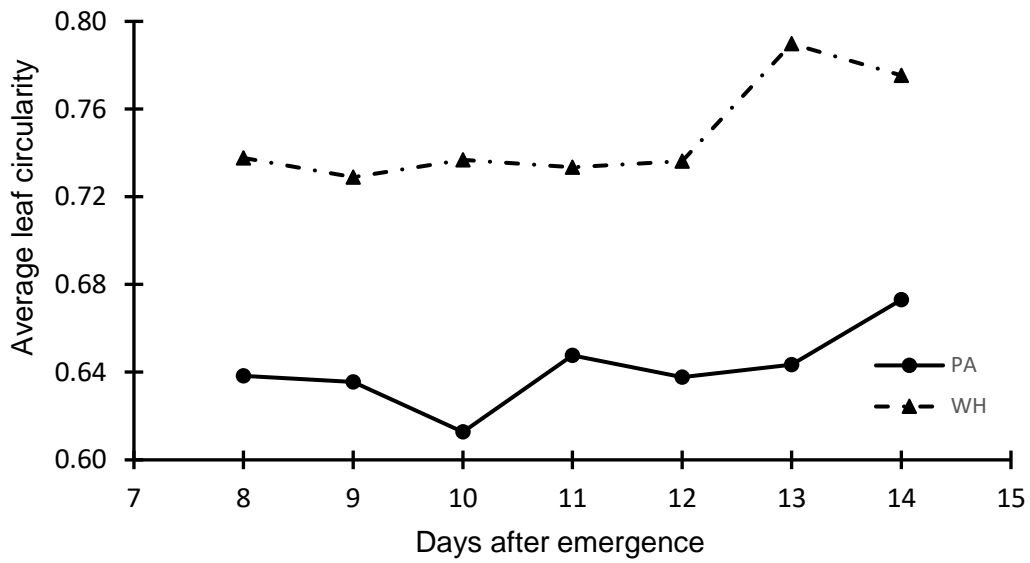


Fig. 3.12. Circularity of palmer amaranth and waterhemp (8 to 14 DAE).

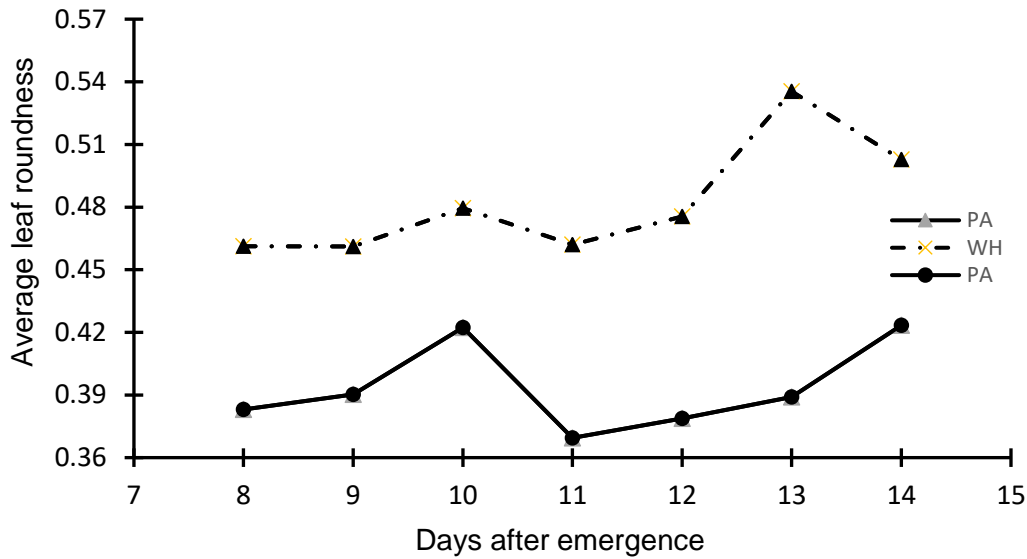


Fig. 3.13. Roundness of palmer amaranth and waterhemp (8 to 14 DAE).

### 3.3. Machine Learning

ML algorithms learn from the data provided and use statistical methods to make predictions. Moreover, ML is known to be a less data hungry approach i.e., it is known to operate even with a small number of data points [164] thereby resulting in lesser training times. A dataset to train classical ML models was created using the above extracted morphological characteristics to help draw inferences from them and make predictions so as to successfully classify the weeds into either category. The dataset comprised 9 columns (length, width, area, perimeter, aspect ratio, circularity, roundness, day #, and species of weed) and 7 rows (day 8, day 9, day 10, day 11, day 12, day 13, and day 14) thereby resulting in a dataset of 312 data points (156 each of palmer amaranth and waterhemp, respectively). This dataset was further divided into Training and Test sets in the ratio, 80:20. The following ML algorithms were used for classification purposes: Support Vector Machines; K-Nearest Neighbors; Random Forest, and Logistic Regression.



### **3.3.1. Support Vector Machines**

Support Vector Machines (SVMs) is one of the most widely used supervised ML algorithm, classifying the data through the construction of hyperplanes that maximize the margin between support vectors. A hard margin is used for linearly separable data while a soft margin is used in case of non-linear data. SVM also uses 'kernel trick' to deal with non-linear data, Linear, Polynomial, Radial Basic Function (RBF), Sigmoid etc. are some of the kernels used. In this study, an SVM with linear kernel was used.

### **3.3.2. Random Forest**

A Random Forest classifier is comprised of a group of decision tree classifiers, also called estimators. Each estimator is generated by randomly sampling a vector from the input vector and classifies an input vector by casting a vote to a class thereby producing its own prediction [165]. Random Forest then predicts the output based on the class that is most voted by these estimators.

### **3.3.3. K-Nearest Neighbors (KNN)**

For a given dataset, KNN uses distance functions to find a group of k instances that are closest to the unknown samples. Euclidean Distance, Minkowski Distance, Manhattan Distance, and Cosine Distance etc. include some of the distance functions that are used by KNN among which Euclidean Distance is the widely used one. KNN with a k value of 5 was used in this study.

### **3.3.4. Logistic Regression**

Logistic regression models the input data using the sigmoid function and uses a loss function, Maximum Likelihood Estimation which is based on conditional probability. The

predictions of the model will be classified as belonging to classes 0 and 1 if the probability is greater and lesser than 0.5, respectively.

Confusion matrix was used to evaluate the performance of the above algorithms. Table 3.2 summarizes and compares the performances of each of these algorithms.

Table 3.2. Performance comparison of different ML algorithms employed in the study.

ML method	Confusion Matrix			Classification report			
	Actual class label	Predicted class label		Precision	Recall	F1-score	
Random Forest			PA	WH	PA	0.81	0.53
	PA	17	15	WH	0.65	0.88	0.75
	WH	4	28				
	<b>Accuracy (%): 70.31</b>						
SVM		PA	WH	PA	0.64	0.66	0.65
	PA	21	11	WH	0.65	0.62	0.63
	WH	12	20				
	<b>Accuracy (%): 64.06</b>						
Logistic Regression		PA	WH	PA	0.69	0.56	0.62
	PA	18	14	WH	0.63	0.75	0.69
	WH	8	2				
	<b>Accuracy (%): 68.62</b>						
kNN		PA	WH	PA	0.75	0.56	0.64
	PA	18	14	WH	0.65	0.81	0.72
	WH	6	26				
	<b>Accuracy (%): 68.75</b>						

It was observed that a significant number of datapoints corresponding to palmer amaranth were misclassified as waterhemp, particularly in the case of Random Forest where 15 datapoints were misclassified. Interestingly, Random Forest also yielded a classification accuracy of 70.31% which was the maximum among all the algorithms. The process of hand-crafting the features i.e., extracting the morphological characteristics and engineering them for further classification by ML models is labor-intensive and time-consuming. Moreover, the accuracies of each of the algorithms were not adequate.

### 3.4. Convolutional Neural Networks (CNN)

CNN is a widely used deep neural network that is popularly used for the analysis of visual data. A typical CNN (as shown in Fig. 3.14) consists of the following layers:

Convolutional layer; Pooling layer, and Fully-connected layer.

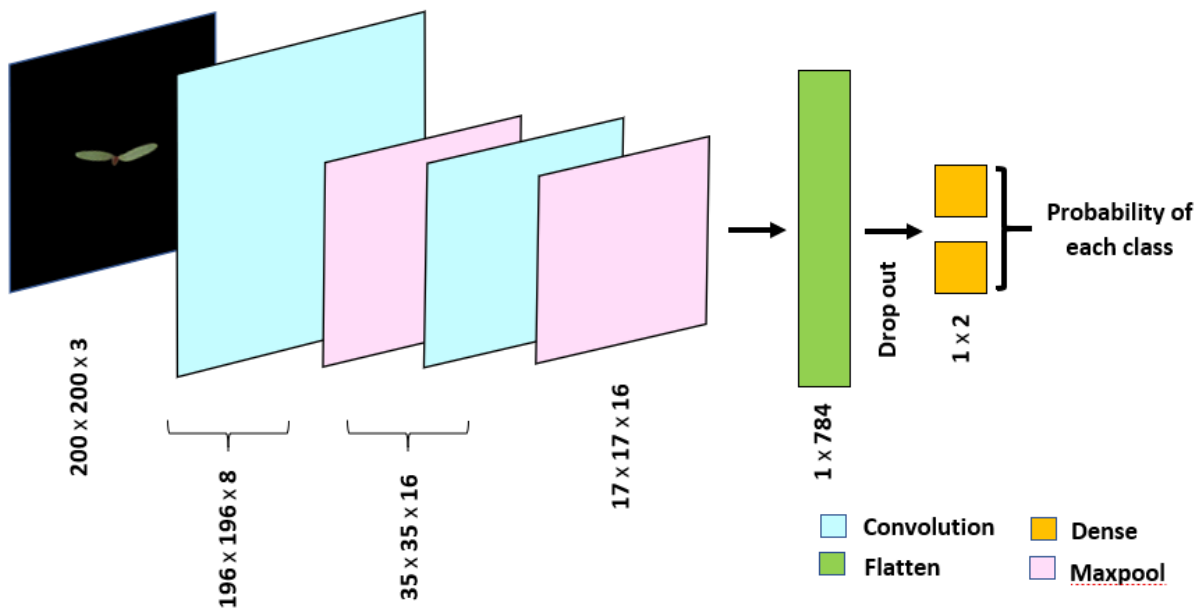


Fig. 3.14. Architecture of CNN employed in the study for the classification of palmer amaranth and waterhemp.

The convolution layer is the first layer in a CNN and is responsible for autonomously identifying features from the input image. The convolution process is concerned with extracting and preserving essential information from the image. It is a mathematical process that is carried out between the input image and a filter (of a specific size). By sliding the filter over the image, the dot product between the two is produced with respect to the filter's size, resulting in a feature map. The feature map contains information about the image (edges and corners) and is passed to the subsequent layers to learn additional features of the image. The pooling layer receives several such feature maps and applies pooling operation on them. Pooling decreases the spatial size of the convoluted feature by combining the output of one layer's neuron cluster into a single neuron in the following layer. Pooling comprises two types namely, max pooling and average pooling. The greatest value from each cluster of neurons from the preceding layer is used in max pooling, whereas the average value is used in average pooling. In our study, max pooling operation was used. These pooling operations are shown in Fig. 3.15.

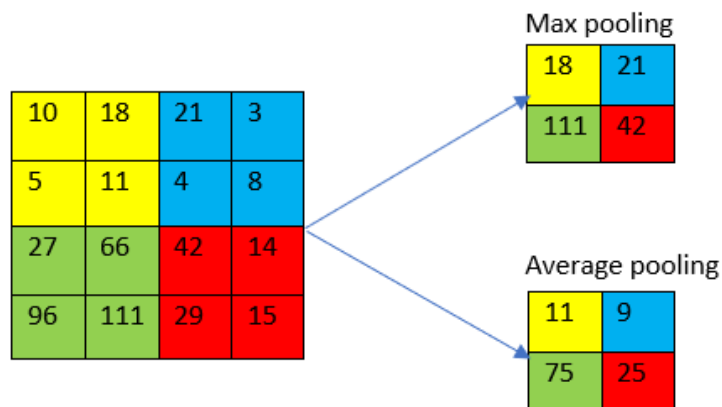


Fig. 3.15. Types of pooling operations used after convolution operations.

The final output is supplied to the fully connected layer which is trained using a backpropagation technique following numerous layers of convolution and pooling. ReLU, tanH,

and eLU include commonly used activation functions for hidden layers and for output layers, SoftMax is used.

A dataset consisting of 2,000 images (1,000 each of palmer amaranth and waterhemp, respectively) was created from the pre-processed images mentioned previously in palmer amaranth and waterhemp image acquisition. But Deep Learning models, especially, CNN requires large amounts of data for it to be generalizable. We employed several data augmentation techniques in order to increase the size of our data.

### 3.4.1. Data augmentation

Data augmentation was performed using MATLAB to significantly increase the diversity of the available data without collecting new data. The types of data augmentation that were performed on the original images of palmer amaranth are described in Table 3.3. Similar techniques were also applied to images of waterhemp.

Table 3.3. Augmentation techniques applied to original images of palmer amaranth.

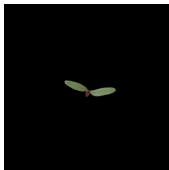
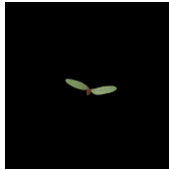
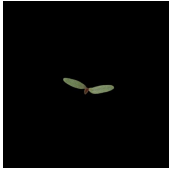
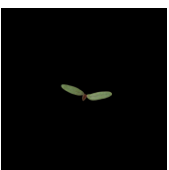
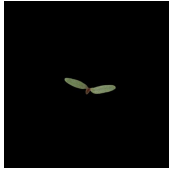

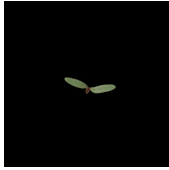


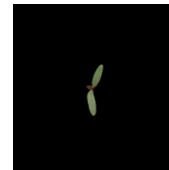
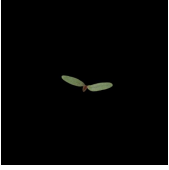
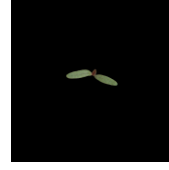
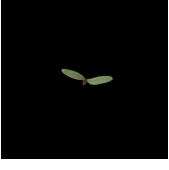
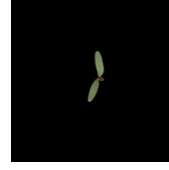
Augmentation technique	Technique description	Original image (palmer amaranth)	Augmented image (palmer amaranth)
Change in brightness	Slight increase the brightness of the image		
Change in contrast	Slight increase the contrast of the image		

Table 3.3. Augmentation techniques applied to original images of palmer amaranth (continued).

<b>Augmentation technique</b>	<b>Technique description</b>	<b>Original image (palmer amaranth)</b>	<b>Augmented image (palmer amaranth)</b>
Conversion to black and white	Convert the image to black and white		
Scaling	Scaling the weed sample (palmer amaranth or waterhemp) by 2.0		
90-degree rotation	Rotating the image by 90 degrees		
180-degree rotation	Rotating the image by 180 degrees		
270-degree rotation	Rotating the image by 270 degrees		

This combined with the pre-processed 2,000 images that were acquired resulted in a large dataset of 16,000 images (8,000 each of palmer amaranth and waterhemp, respectively) and was further used for training the CNN. In order to make the make the deep learning model robust,

Gaussian noise of noise intensity 0.04 was applied on the pre-processed 2000 images (1,000 each of palmer amaranth and waterhemp, respectively) and comprised the test set. Fig 3.16 shows the images following the application of Gaussian noise.

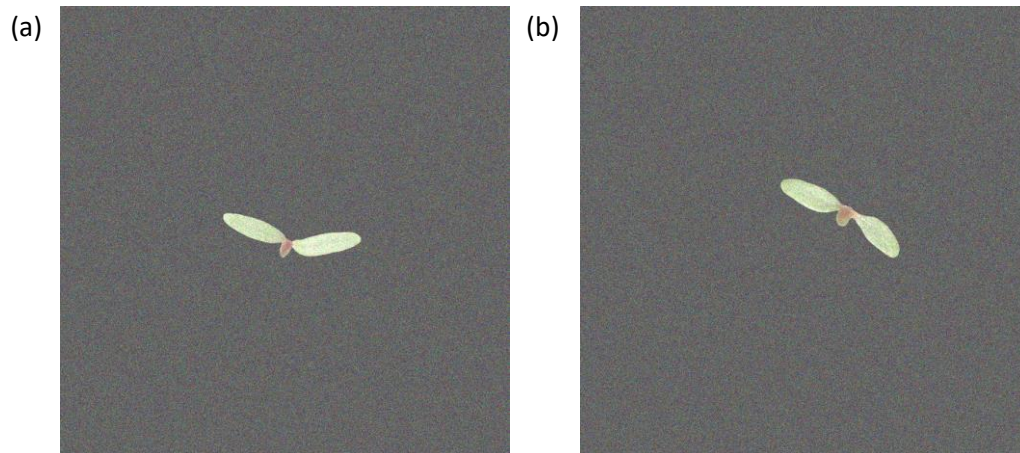


Fig. 3.16. (a) Palmer amaranth after addition of Gaussian noise, (b) Waterhemp after addition of Gaussian noise.

The combination of the training set and the test set comprised DATASET 1 and was used for image classification by CNN. In order to reduce training time of the CNN, the images comprising DATASET 1 were reduced to  $200 \times 200$  pixels. CNN and its ability to classify between the weeds into either category are described next.

The CNN with the following network structure (Table 3.4) was built and trained on the training set. of DATASET 1.

Table 3.4. The network structure of CNN configured for the classification of palmer amaranth and waterhemp.

<b>Layer (type)</b>	<b>Output Shape</b>	<b>No. of trainable parameters</b>
conv2d (Conv2D)	(None, 196, 196, 8)	608
activation (Activation)	(None, 196, 196, 8)	0
max_pooling2d (Max_Pooling2D)	(None, 39, 39, 8)	0
conv2d_1 (Conv2D)	(None, 35, 35, 16)	3216
activation_1 (Activation)	(None, 35, 35, 16)	0
max_pooling2d_1 (Max_Pooling2D)	(None, 17, 17, 16)	0
flatten (Flatten)	(None, 784)	0
dropout (Dropout)	(None, 784)	0
dense (Dense)	(None, 2)	1570
Activation_2 (Activation)	(None, 2)	
Total params: 5,394		
Trainable parameters: 5,394		
No Non-trainable parameters: 0		

Table 3.5 lists the hyperparameters used for training the network.



Table 3.5. Tuned hyperparameters for the employed CNN model.

<b>Parameter</b>	<b>Value</b>
CNN filter size	5 x 5
CNN pooling size	5 x 5
Number of layers	8
Number of training images	16,000
Number of epochs	100
Batch size	64
Optimizer for network	Adam
Learning rate of Adam	0.001

Table 3.6 shows the performance of the employed CNN model.

Table 3.6. Actual and predicted class labels of palmer amaranth and waterhemp.

		<b>Predicted class label</b>	
		<b>PA</b>	<b>WH</b>
<b>Actual class label</b>	<b>PA</b>	855	145
	<b>WH</b>	0	1,000

Table 3.6. PA denotes palmer amaranth and WH denotes waterhemp.

Observations indicted all the images of waterhemp were correctly classified while 145 images of palmer amaranth were misclassified as waterhemp. However, to identify and distinguish the weeds in more realistic scenarios, particularly, when they are spread across agronomic fields in a random fashion (both close and distant proximities), pertaining to different age groups etc., it is important to localize each object i.e., weeds in an image and distinguish it from other categories rather than just classifying an object contained in an image i.e., image classification. Hence, there is a need for identification of multiple objects in an image through Object Detection.

### 3.5. Object detection and transfer learning

Object detection is a Computer Vision technique that determines the location of objects in an image i.e., object localization and its corresponding category i.e., classification [166]. Through the process of drawing bounding boxes around the objects detected, it locates the objects in the image.

The various stages involved in the process of object detection include:

- Informative region selection – scanning the entire image through a multiscale sliding window to find all the possible regions of objects
- Feature extraction – extracting visual features of the objects in the image in order to recognize
- Classification – distinguishing a target object from other categories of objects in the image

Object detection models require a huge amount of data [167], comprised of lot of varieties to train, however, availability of such amounts of data might not be practically feasible. However, Transfer learning helps solve this problem. Transfer learning is an ML method that involves the use of knowledge learned from a task to improve the learning of a different but related task. The concept of transfer learning was first addressed by Stevo Bozinovski in [168] who explained it during the training process of a neural network. Ever since, numerous discussions have been made on the ML method namely, Meta Learning [169], Knowledge-based inductive bias [170], Learning to learn [171], Multi-tasking Learning [172], Incremental Learning [173], Life-long Learning [174], Context-sensitive Learning [175], Inductive transfer [176], Knowledge Transfer [177] and Knowledge Consolidation [178]. [180–182] defined

transfer learning as a combination of two concepts namely, domain and task. The domain,  $D$  is further comprised of a feature space,  $X$  and a marginal distribution,  $P(X)$  such that  $X = \{x_1, x_2, \dots, x_n\}$  where  $x_i \in X$ , here represents a sample data point while  $x_i$  is the  $i^{\text{th}}$  term vector corresponding to some data point and  $X$  represents the space of all data points.

The task,  $T$  is a combination of  $Y$ , the set of all labels (True, False) and a conditional probability  $P(Y|X)$  which is learned from the label pairs  $(x_i, y_i)$  where  $x_i \in X$  and  $y_i \in Y$ .

Given the following:

A source domain  $D_S$

A target domain  $D_T$

A source task  $T_S$  and

A target task  $T_T$

Transfer learning aims at utilizing the knowledge gained from  $D_S$  and  $T_S$  where  $D_S$  or  $T_S$  are not equal to  $D_T$  and  $T_T$  respectively to help us learn the target conditional probability  $P(Y_T|X_T)$  in  $D_T$ . Transfer learning in the context of deep learning (Fig. 3.17) refers to the transfer of knowledge that was previously used to train a model for a certain task  $A$  to another model for a relatively similar task  $B$ .

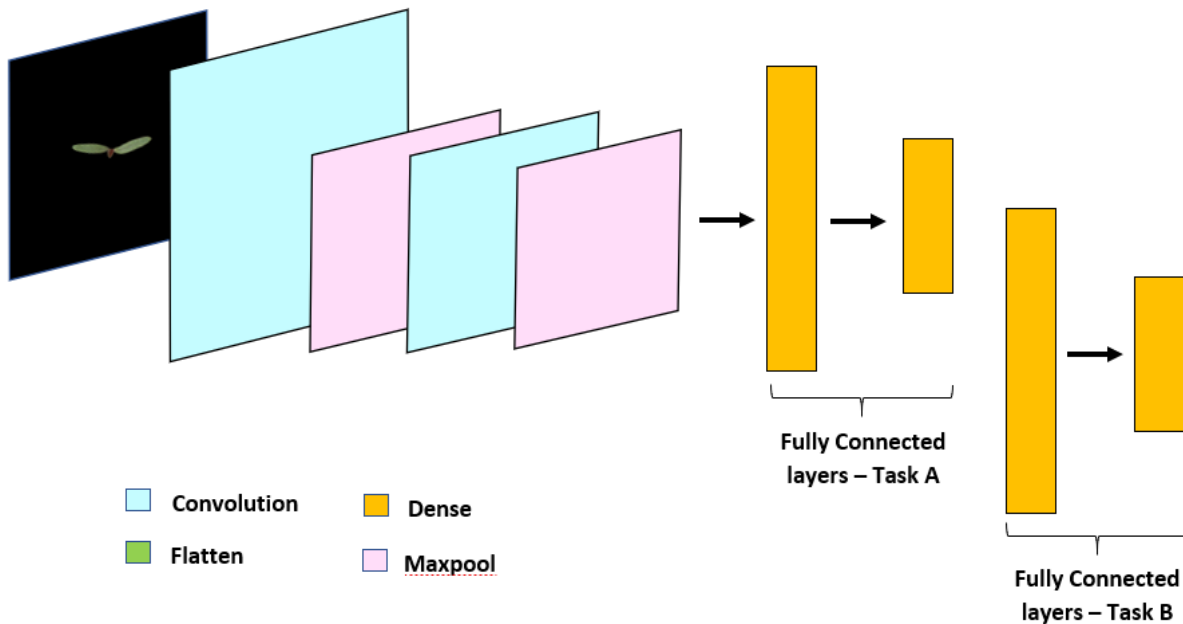


Fig. 3.17. General architecture of Transfer learning.

Most of the inner layers of the model remained untouched while the ones that are close to the output layers are altered. Also, the datasets on which the two models are trained may be similar or entirely different from one another.

A simulated dataset for object detection, DATASET 2 was created by using the training set of DATASET 1 and annotating it in this study. Annotation was performed by creating bounding boxes around the objects i.e., weeds in the image, class labels created using Labelling thereby resulting in 16,000 image labels and their corresponding coordinates. For testing purposes, a total of 132 RGB images of palmer amaranth and waterhemp, respectively, that were not part of the original 2000 images (DATASET 1) were used. These images were preprocessed using MATLAB for background removal following which the objects in the images i.e., palmer amaranth and waterhemp were carefully selected, cropped, and placed in a different image of a larger size. As a result, 12 images of size  $4,000 \times 4,000$  were constructed by selecting samples of

palmer amaranth and waterhemp from the original images (pertaining to various ages ranging between 8 to 14 days) and randomly distributing them across the image. This was done in order to generalize to a real-world scenario where the weeds would occur in corn fields, spread out in a random fashion (both close and distant proximities) and pertaining to different ages. Two such constructed images are shown in Figure 3.18.

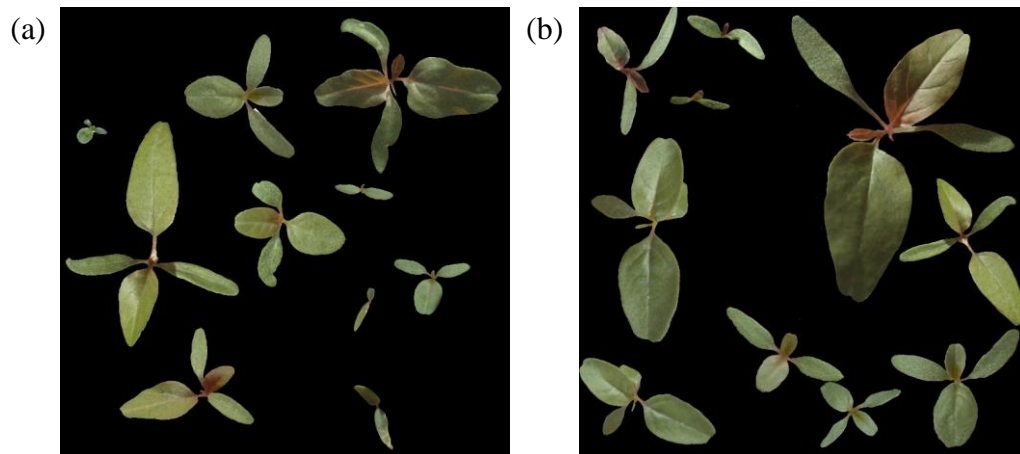


Fig. 3.18. Samples of palmer amaranth and waterhemp from original images randomly distributed to construct images for object detection.

A YOLO V5 model pre-trained on the COCO dataset, a large dataset consisting of bounding boxes, segmentation masks, labels for approx. 330,000 images pertaining to 80 different general object categories (dog, cat, boat, airplane etc.) was used for object detection. YOLO V5 with the weights corresponding to this dataset was trained on a subset of the training set of DATASET 2 (consisting of 3,200 images with their bounding boxes and labels) formed by selecting 200 images each from the original set of 2,000 images as well as 200 each from each of the augmented sets pertaining to each weed category. Post training, the newly obtained weights were used to test the model's performance on the 12 simulated images. Figure 3.19 shows the bounding boxes created by YOLO V5 around samples of palmer amaranth and waterhemp. The

bounding boxes in red represent the detection of palmer amaranth and the pink ones, waterhemp. It was observed that the model could also detect these objects irrespective of their age and proximity to each other thereby proving to be successful in a real-world like scenario.

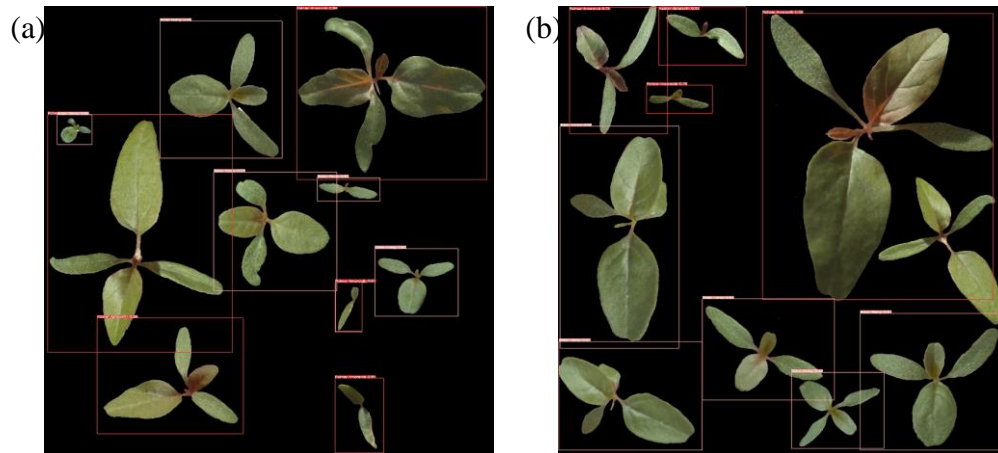


Fig. 3.19. Labelled images of individual samples of palmer amaranth and waterhemp obtained from the trained YOLO V5 model. YOLO V5 uses bounding boxes to localize individual image objects.

The results of the object detection approach using YOLO V5 are summarized in Tables 3.7 and 3.8, respectively.

Table 3.7. Summary of results obtained for Object detection using YOLO V5.

<b>Image No.</b>	<b>No. of samples of palmer amaranth</b>	<b>No. of samples correctly classified</b>	<b>No. of samples of waterhemp</b>	<b>No. of samples correctly classified</b>	<b>Total no. of samples</b>	<b>Total no. of samples correctly classified</b>
1	5	5	5	5	10	10
2	5	5	5	5	10	10
3	5	4	5	2	10	6
4	5	4	5	5	10	9
5	5	4	5	4	10	8
6	5	5	5	4	10	9
7	7	6	5	5	12	11
8	6	4	5	4	11	8
9	5	4	5	5	10	9
10	5	4	5	5	10	9
11	9	8	8	4	17	12
12	6	5	6	5	12	11
					<b>132</b>	<b>112</b>

Table 3.8. Object detection results summary.

<b>Parameter</b>	<b>Value</b>
Total no. of images	12
Total no. of objects in all images combined	132
Total no. of objects correctly classified	112
Total no. of objects undetected or wrongly classified	20

### 3.6. Results

Confusion matrix was the performance metric used for the evaluation of the model's performances. A confusion matrix measures the correctness of the model and its accuracy for binary or multi-class classification problems. In a binary class classification problem, the expected values are the actual values i.e., two values (for example, 0 and 1, or True and False)

while the ones that the model predicts represent the predicted values. The confusion matrix visualizes the classifier's (in this case, CNN) performance by showing expected vs predicted values in the form of a matrix. The expected values are represented by rows whereas the predicted ones, by columns. The diagonal values represent items where the predicted values were identical to the anticipated values i.e., expected values, while the off-diagonal values represent items where the classifier predicted incorrectly. The elements of the matrix include true positives, true negatives, false positives, and false negatives. True Positives represent the number of cases where both the actual and predicted values of a data sample is 1. True Negatives represent the number of cases where the actual value as well as the predicted value of a data sample is 0. On the other hand, False Positives represent the number of cases where the actual value 0 and the predicted value of the data sample is 1. False Negatives represent the number of cases where the actual value is 1 and the predicted value of the data sample is 0. From the above stated terminologies, it can be understood that the performance of the model is considered to be good if the number of True Positives and True Negatives respectively are higher and the number of False Positives and False Negatives respectively are lower. Therefore, a model needs to be trained so as to maximize the number of True Positives and True Negatives respectively and minimize the number of False Positives and False Negatives respectively.

The performances of the various ML algorithms used i.e., Random Forest, SVM, Logistic Regression, and k-NN, along with their hyperparameters are provided in Table 3.2. From the table, it can be inferred that 17 and 28 datapoints of palmer amaranth and waterhemp, respectively, were correctly classified by Random Forest while 15 datapoints of palmer amaranth were misclassified as waterhemp and four datapoints of waterhemp were misclassified as palmer



amaranth resulting in a classification accuracy of 70.31%. Twenty-one and 20 datapoints of palmer amaranth and waterhemp, respectively, were correctly classified by SVM while 11 datapoints of palmer amaranth and waterhemp were misclassified as waterhemp and 12 datapoints of waterhemp were misclassified as palmer amaranth resulting in a classification accuracy of 64.06%. Logistic Regression correctly classified 18 and 24 datapoints of palmer amaranth and waterhemp, respectively, while it misclassified 14 and 8 datapoints of palmer amaranth and waterhemp, respectively, resulting in a classification accuracy of 65.62%. kNN fared the best after Random Forest, correctly classifying 18 and 26 datapoints of palmer amaranth and waterhemp, respectively, while wrongly classifying 14 datapoints of palmer amaranth and waterhemp, resulting in a classification accuracy of 68.75%. Table 3.6 shows the confusion matrix for the CNN model described in the previous section. From the table, it can be inferred that all the images of waterhemp were correctly classified while 145 images of palmer amaranth were misclassified as waterhemp thereby resulting in a classification accuracy of 92.75%.

The performance of the YOLO V5 model was evaluated on the 12 manually created test images consisted of both the weeds i.e., objects scattered all across the frame in a random manner. Manual evaluation revealed that the model was able to successfully detect 112 of the total 132 objects present in all the 12 images combined. The details such as the number of weeds i.e., objects of either category in each image, the number of objects successfully detected in each image, total number of successfully detected objects are summarized in tables 3.7 and 3.8, respectively.

#### 4. CONCLUSIONS

The ability of automated approaches for the early-stage distinguishing of palmer amaranth from waterhemp were demonstrated in this experiment. The following conclusion are drawn based on the analyses conducted in the study:

1. The morphological characteristics namely, length, width, area, perimeter, aspect ratio, circularity, and roundness of the leaves of palmer amaranth and waterhemp pertaining to days 8 to 14 DAE were extracted and later, compared. Visualization of these characteristics revealed that the aspect ratio of palmer amaranth was greater than that of waterhemp. However, the circularity and roundness were greater for waterhemp than palmer amaranth. Palmer amaranth could be clearly distinguished from waterhemp, through the visualization of morphological characteristics, however, the process of extracting the morphological characteristics is a laborious and time-consuming process, requiring immense focus. Moreover, as the size of the data increases i.e., the number of leaves increases, it becomes harder to extract these characteristics.

2. A dataset of 312 datapoints comprising the morphological characteristics of palmer amaranth and waterhemp was created to train ML algorithms. Classical ML algorithms namely, Random Forest, SVM, KNN, and Logistic Regression etc. were trained using 80% of the available data. The trained algorithms were validated using the remaining 20% data. A significant number of datapoints corresponding to palmer amaranth were misclassified as waterhemp, particularly in the case of Random Forest where 15 out of 32 datapoints were misclassified. Interestingly, Random Forest also fared the best among all the classical algorithms

with an accuracy of 70.31%. Eleven, 14, and 14 datapoints of palmer amaranth were misclassified by SVM, Logistic Regression, and KNN, respectively.

3. A deep learning approach using a CNN was adopted to increase the classification accuracy in categorizing a weed as either palmer amaranth or waterhemp. The CNN was trained on a dataset of 16,000 images and validated using 2,000 images embedded with Gaussian noise. The CNN correctly classified 855 of palmer amaranth and all 1,000 images of waterhemp while misclassifying 145 images of palmer amaranth thereby yielding a classification accuracy of 92.75%. A possible reason for the misclassification could have been the similarities in terms of appearance of both palmer amaranth and waterhemp in the first few days (day 8 and 9). Although misclassifications of palmer amaranth were observed in case of both ML and the CNN, a significantly higher classification accuracy was achieved in the case of CNN.

4. A YOLO V5 object detection model with pre-trained weights was re-trained on a subset (3200) of the image dataset which was annotated to distinguish palmer amaranth from waterhemp in more realistic scenarios, for example, when the weeds are spread across an agronomic field in a random manner. The model was then tested on 12 synthetic images consisting of a total of 132 objects of palmer amaranth and waterhemp. One hundred twelve of the 132 samples of the weeds were correctly detected.

The results from the object detection performed in this study can play an important role in successfully distinguishing between palmer amaranth from waterhemp in their early stage, particularly when they exhibit similar morphological characteristics. These results also establish a convenient approach to detect these weeds in real-life scenarios where they occur together in the same field and in proximity of one another.

## 5. FUTURE RESEARCH DIRECTION

While the early-stage distinguishing of palmer amaranth from waterhemp is advantageous, it was performed in cases where the background was eliminated after pre-processing in the research. However, the proposed methodology could be extended to work in real corn fields which would constitute a more realistic scenario. In addition, considering palmer amaranth and waterhemp are *Amaranthus* species, the possibility of distinguishing palmer amaranth from other pigweed species namely redroot pigweed, smooth pigweed, powell amaranth etc. could also be explored as an extension to the work conducted in this research.

Images of palmer amaranth and waterhemp were acquired in a greenhouse with controlled lighting settings in this research. Also, data augmentation was performed for the diversification of existing data i.e., preprocessed and augmented images following which there were used for distinguishing palmer amaranth from waterhemp. However, the proposed method does not account for the distinguishing in different conditions that are uncontrollable, for example, tilt angle of the device used for image acquisition, overlapping of the weeds' leaves, and environmental conditions namely, light, temperature, weather etc. Hence, this method could be extended to distinguish palmer amaranth from waterhemp in such conditions.

The only reliable way to differentiate palmer amaranth and waterhemp at this stage would be the use of genetic testing since they possess a striking similarity in the early stages of growth and look identical to an untrained eye. Genetic testing involves collecting seed samples of palmer amaranth and other related species, performing genomic sequencing on them, searching for specific genetic differences, and designing genetic markers to distinguish palmer amaranth from the other species based on DNA. Studies have shown genetic testing to be the

most reliable way for the process of distinguishing palmer amaranth from other species [183] with accuracies ranging between 99.7 to 99.9%. However, the process of genetic testing (both leaf tissue testing and seed sample testing) is expensive, with the testing of a single seed/tissue sample costing about \$75 per sample [184]. Moreover, hundreds of samples are required for the purpose. The proposed method in this study could be extended to analyze ML as a possible, reliable, and cost-effective alternative to genetic testing that can provide similar or better efficacies in distinguishing palmer amaranth from other pigweed species including waterhemp in the early stages.

The presence of palmer amaranth and waterhemp uncontrolled in cornfields reduces yields, causing economic losses. However, the proposed approaches provide effective solutions to this problem. Moreover, the financial benefits of distinguishing palmer amaranth from waterhemp in the early stage using the proposed approaches in cornfields is yet to be quantified and could be pursued in the near future.

## REFERENCES

- [1] Franssen, Aaron S., Daniel Z. Skinner, Kassim Al-Khatib, Michael J. Horak, and Peter A. Kulakow. (2001). Interspecific hybridization and gene flow of ALS resistance in *Amaranthus* species. *Weed Science*, vol. 49, no. 5, pp. 598–606.
- [2] Sauer, J.D. (1957). Recent migration and evolution of the dioecious amaranths. *Evolution*, pp 11–31.
- [3] Massinga, R.A., Randall S. Currie, Michael J. Horak, and John Boyer. (2001). Interference of Palmer amaranth in corn. *Weed Science*, vol. 49, no. 2, pp. 202–208.
- [4] Dillon, T. L., Baldwin, F. L., & Becton, C. M. (1989). Palmer amaranth control in sandy soil in northeast Arkansas. In *Proc. South. Weed Sci. Soc*, vol. 42, p. 113.
- [5] Bradley, K. W., Smeda, R. J., & Massey, R. E. (2008). Management of Glyphosate-Resistant Waterhemp in Corn and Soybean (2008).
- [6] Nordby, D. E., & Hartzler, R. G. (2004). Influence of corn on common waterhemp (*Amaranthus rudis*) growth and fecundity. *Weed science*, vol. 52, no. 2, pp. 255–259.
- [7] Ward, S. M., Webster, T. M., & Steckel, L. E. (2013). Palmer amaranth (*Amaranthus palmeri*): a review. *Weed Technology*, vol. 27, no. 1, pp. 12–27.
- [8] Hartzler, B. (2013). Palmer amaranth: ID, biology and management.
- [9] Steckel, L. E., & Sprague, C. L. (2004). Late-season common waterhemp (*Amaranthus rudis*) interference in narrow-and wide-row soybean. *Weed Technology*, vol. 18, no. 4, pp. 947–952.
- [10] Waterhemp. Take Action Pesticide-Resistance Management.
- [11] Keeley, P. E., Carter, C. H., & Thullen, R. J. (1987). Influence of planting date on growth of Palmer amaranth (*Amaranthus palmeri*). *Weed Science*, vol. 35, no. 2, pp. 199–204.
- [12] Herbicide Resistant Waterhemp Is Here How Do We Manage It? (2018) River Country Coop Waterhemp-Bulletin.
- [13] Jill Loehr. (2016). Waterhemp drains nutrients from plants. *PrairieFramer*.
- [14] Massinga, R. A., Currie, R. S., & Trooien, T. P. (2003). Water use and light interception under Palmer amaranth (*Amaranthus palmeri*) and corn competition. *Weed Science*, vol. 51, no. 4, pp. 523–531.
- [15] Legleiter, T. R., & Johnson, B. (2013). Palmer amaranth biology, identification, and management (pp. 1-2). West Lafayette, IN: Purdue Extension.
- [16] Kevin Bradley. (2019). Waterhemp Management in Soybean. *Mizzou Weed Science*.
- [17] D. Nordby, B. Hartzler, and K. Bradley. *Waterhemp*.

- [18] Modderman, C. (2020). Palmer amaranth Seeds in Manure—What Can You Do?.
- [19] Schwartz, L. M. (2015). A comparative study of the population dynamics of four Amaranthaceae species. Southern Illinois University at Carbondale.
- [20] Anderson, M. (2015). Waterhemp's big, bad brother is back this spring.
- [21] Anderson, M., Hartzler, B., & Jha, P. (2021). Scout now for Palmer amaranth.
- [22] Palmer Amaranth Management in Soybeans. (2013). Take Action.
- [23] Cordes, J. C., Johnson, W. G., Scharf, P., & Smeda, R. J. (2004). Late-emerging common waterhemp (*Amaranthus rudis*) interference in conventional tillage corn. *Weed technology*, vol. 18, no. 4, pp. 999–1005.
- [24] Hager, A. G., Wax, L. M., Stoller, E. W., & Bollero, G. A. (2002). Common waterhemp (*Amaranthus rudis*) interference in soybean. *Weed science*, vol. 50, no. 5, pp. 607–610.
- [25] Kohrt, J. R., & Sprague, C. L. (2017). Herbicide management strategies in field corn for a three-way herbicide-resistant Palmer amaranth (*Amaranthus palmeri*) population. *Weed Technology*, vol. 31, no. 3, pp. 364–372.
- [26] Chahal, P. S., Aulakh, J. S., Jugulam, M., & Jhala, A. J. (2015). Herbicide-resistant Palmer amaranth (*Amaranthus palmeri* S. Wats.) in the United States—mechanisms of resistance, impact, and management. *Herbicides, Agronomic Crops and Weed Biology*. Rijeka, Croatia: InTech, pp. 1–29.
- [27] Heap, I. (2020). The international herbicide-resistant weed database.
- [28] L. Steckel. (2019). Weed control manual for Tennessee. Knoxville: University of Tennessee. Extension publication PB 1580.
- [29] Grichar, W. J., Besler, B. A., & Palrang, D. T. (2005). Flufenacet and isoxaflutole combinations for weed control and corn (*Zea mays*) tolerance. *Weed technology*, vol. 19, no. 4, pp. 891–896.
- [30] Wiggins, M. S., McClure, M. A., Hayes, R. M., & Steckel, L. E. (2015). Integrating cover crops and POST herbicides for glyphosate-resistant Palmer amaranth (*Amaranthus palmeri*) control in corn. *Weed Technology*, vol. 29, no. 3, pp. 412–418.
- [31] Crow, W. D., Steckel, L. E., Mueller, T. C., & Hayes, R. M. (2016). Management of large, glyphosate-resistant Palmer amaranth (*Amaranthus palmeri*) in corn. *Weed Technology*, vol. 30, no. 3, pp. 611–616.
- [32] Janak, T. W., & Grichar, W. J. (2016). Weed control in corn (*Zea mays* L.) as influenced by preemergence herbicides. *International Journal of Agronomy*, vol. 2016.

- [33] Steckel, L. E., & Sprague, C. L. (2004). Common waterhemp (*Amaranthus rudis*) interference in corn. *Weed Science*, vol. 52, no. 3, pp. 359–364.
- [34] Ritchie, S. W., Hanway, J. J., & Benson, G. O. (1993). How a corn plant develops, special report no. 48. Ames, IA: Iowa State University of Science and Technology Cooperative Extension Service.
- [35] Anderson, D. D., Roeth, F. W., & Martin, A. R. (1996). Occurrence and control of triazine-resistant common waterhemp (*Amaranthus rudis*) in field corn (*Zea mays*). *Weed Technology*, vol. 10, no. 3, pp. 570-575.
- [36] Shoup, D. E., & Al-Khatib, K. (2004). Control of protoporphyrinogen oxidase inhibitor-resistant common waterhemp (*Amaranthus rudis*) in corn and soybean. *Weed technology*, vol. 18, no. 2, pp. 332–340.
- [37] Schuster, C. L., & Smeda, R. J. (2007). Management of *Amaranthus rudis* S. in glyphosate-resistant corn (*Zea mays* L.) and soybean (*Glycine max* L. Merr.). *Crop Protection*, vol. 26, no. 9, pp. 1436–1443.
- [38] Sarangi, D., & Jhala, A. J. (2017). Biologically effective rates of a new premix (atrazine, bicyclopyrone, mesotrione, and S-metolachlor) for preemergence or postemergence control of common waterhemp [*Amaranthus tuberculatus* (Moq.) Sauer var. *rudis*] in corn. *Canadian Journal of Plant Science*, vol. 97, no. 6, pp. 1075–1089.
- [39] Legleiter, T. R., & Bradley, K. W. (2009). Evaluation of herbicide programs for the management of glyphosate-resistant waterhemp (*Amaranthus rudis*) in maize. *Crop Protection*, vol. 28, no. 11, pp. 917–922.
- [40] Travis Legleiter. (2020). Palmer Amaranth and Waterhemp Control in Corn and Soybean. University of Kentucky College of Agriculture, Food and Environment Cooperative Extension Service.
- [41] Amit Jhala. (2017). How to Differentiate Common Waterhemp and Palmer Amaranth Seedlings. University of Nebraska-Lincoln, Institute of Agriculture and Natural Resources CROPWATCH.
- [42] Ikley, J., & Jenks, B. (2019). Identification, Biology and Control of Palmer Amaranth and Waterhemp in North Dakota. NDSU Extension, North Dakota State University.
- [43] Waterhemp vs. Palmer Amaranth. (2017). Dow AgroSciences.
- [44] World of Corn. (2021). National Corn Growers Association.
- [45] salt Corn-based, R. (2020). CORN-BASED DEICERS.



- [46] Sajid, H. U., Kiran, R., Qi, X., Bajwa, D. S., & Battocchi, D. (2020). Employing corn derived products to reduce the corrosivity of pavement deicing materials. *Construction and Building Materials*, vol. 263, p. 120662.
- [47] Yusuf, T. A., Gundu, D. T., Oseni, M. I., Bolaji, B. O., & Ismaila, S. O. (2013). Evaluation of corn water for corrosion inhibitors extract.
- [48] Sajid, H. U., Kiran, R., & Bajwa, D. S. (2022). Soy-protein and corn-derived polyol based coatings for corrosion mitigation in reinforced concrete. *Construction and Building Materials*, vol. 319, p. 126056.
- [49] Sajid, H. U., Kiran, R., & Bajwa, D. S. (2022). Soy-protein and corn-derived polyol based coatings for corrosion mitigation in reinforced concrete. *Construction and Building Materials*, vol. 319, p. 126056.
- [50] Palviainen, P., Heinämäki, J., Myllärinen, P., Lahtinen, R., Yliruusi, J., & Forssell, P. (2001). Corn starches as film formers in aqueous-based film coating. *Pharmaceutical development and technology*, vol. 6, no. 3, pp. 353–361.
- [51] Alam, M., & Alandis, N. M. (2014). Corn oil based poly (ether amide urethane) coating material—Synthesis, characterization and coating properties. *Industrial Crops and Products*, vol. 57, pp. 17–28.
- [52] Economic Impact of Corn Refining. (2020). Corn Refiners Association.
- [53] Soltani, N., Dille, J. A., Burke, I. C., Everman, W. J., VanGessel, M. J., Davis, V. M., & Sikkema, P. H. (2016). Potential corn yield losses from weeds in North America. *Weed Technology*, vol. 30, no. 4, pp. 979–984.
- [54] J. B. Langemeier. (2021). 2021 Purdue Crop Cost.
- [55] Samuel, A. L. (1988). Some studies in machine learning using the game of checkers. II—recent progress. *Computer Games I*, 366-400.
- [56] Mitchell, T. M. (1999). Machine learning and data mining. *Communications of the ACM*, vol. 42, no. 11, pp. 30-36.
- [57] Treveil, M., Omont, N., Stenac, C., Lefevre, K., Phan, D., Zentici, J., ... & Heidmann, L. (2020). *Introducing MLOps*. O'Reilly Media.
- [58] Mäkinen, S., Skogström, H., Laaksonen, E., & Mikkonen, T. (2021, May). Who needs MLOps: What data scientists seek to accomplish and how can MLOps help?. In *2021 IEEE/ACM 1st Workshop on AI Engineering-Software Engineering for AI (WAIN)*, pp. 109-112. IEEE.
- [59] Gift, N., & Deza, A. (2021). *Practical MLOps*. O'Reilly Media, Inc.

- [60] Alla, S., & Adari, S. K. (2021). What is mlops?. In *Beginning MLOps with MLFlow*. Apress, Berkeley, CA., pp. 79–124.
- [61] Karimi, Y., Prasher, S. O., Patel, R. M., & Kim, S. H. (2006). Application of support vector machine technology for weed and nitrogen stress detection in corn. *Computers and electronics in agriculture*, vol. 51, no. 1–2, pp. 99–109.
- [62] Siddiqi, M. H., Lee, S. W., & Khan, A. M. (2014). Weed Image Classification using Wavelet Transform, Stepwise Linear Discriminant Analysis, and Support Vector Machines for an Automatic Spray Control System. *Journal of Information Science & Engineering*, vol. 30, no. 4.
- [63] Andrea, C. C., Daniel, B. B. M., & Misael, J. B. J. (2017, October). Precise weed and maize classification through convolutional neuronal networks. In *2017 IEEE Second Ecuador Technical Chapters Meeting (ETCM)*. pp. 1-6. IEEE.
- [64] Davis, R. L., Greene, J. K., Dou, F., Jo, Y. K., & Chappell, T. M. (2020). A practical application of unsupervised machine learning for analyzing plant image data collected using unmanned aircraft systems. *Agronomy*, vol. 10, no. 5, pp. 633.
- [65] Comba, L., Biglia, A., Aimonino, D. R., & Gay, P. (2018). Unsupervised detection of vineyards by 3D point-cloud UAV photogrammetry for precision agriculture. *Computers and Electronics in Agriculture*, vol. 155, pp. 84-95.
- [66] Rainville, D., Durand, A., Fortin, F. A., Tanguy, K., Maldague, X., Panneton, B., & Simard, M. J. (2014). Bayesian classification and unsupervised learning for isolating weeds in row crops. *Pattern Analysis and Applications*, vol. 17, no. 2, pp. 401–414.
- [67] De Rango, F., Potrino, G., Tropea, M., Santamaria, A. F., & Fazio, P. (2019). Scalable and lighthway bio-inspired coordination protocol for FANET in precision agriculture applications. *Computers & Electrical Engineering*, vol. 74, pp. 305-318.
- [68] Uyeh, D. D., Basse, B. I., Mallipeddi, R., Asem-Hiablie, S., Amaizu, M., Woo, S., ... & Park, T. (2021). A reinforcement learning approach for optimal placement of sensors in protected cultivation systems. *IEEE Access*, vol. 9, pp. 100781-100800.
- [69] Zhang, Z., Boubin, J., Stewart, C., & Khanal, S. (2020). Whole-field reinforcement learning: A fully autonomous aerial scouting method for precision agriculture. *Sensors*, vol. 20, no. 20, pp. 6585.
- [70] Vapnik, V. N. (1964). A note on one class of perceptrons. *Automat. Rem. Control*, vol. 25, pp. 821-837.
- [71] C. Cortes and V. Vapnik, "Support-vector networks," *Mach Learn*, vol. 20, no. 3, pp. 273–297, 1995.

- [72] B. E. Boser, I. M. Guyon, and V. N. Vapnik, “A training algorithm for optimal margin classifiers,” in Proceedings of the fifth annual workshop on Computational learning theory, 1992, pp. 144–152.
- [73] Drucker, H., Burges, C. J., Kaufman, L., Smola, A., & Vapnik, V. (1996). Support vector regression machines. Advances in neural information processing systems, vol. 9.
- [74] Weston, J., & Watkins, C. (1998, May). Multi-class support vector machines. Technical Report CSD-TR-98-04, Department of Computer Science, Royal Holloway, University of London, pp. 98-04.
- [75] Bennett, K., & Demiriz, A. (1998). Semi-supervised support vector machines. Advances in Neural Information processing systems, vol. 11.
- [76] Mangasarian, O. L., & Musicant, D. R. (2001, Mar). Lagrangian support vector machines. Journal of Machine Learning Research, vol. 1, pp. 161–177.
- [77] Collobert, R., & Bengio, S. (2001, Feb). SVM-Torch: Support vector machines for large-scale regression problems. Journal of machine learning research, vol. 1, pp. 143-160.
- [78] Lee, Y. J., & Mangasarian, O. L. (2001, April). RSVM: Reduced support vector machines. In Proceedings of the 2001 SIAM International Conference on Data Mining. Society for Industrial and Applied Mathematics, pp. 1–17.
- [79] Waibel, A., Hanazawa, T., Hinton, G., Shikano, K., & Lang, K. J. (1989). Phoneme recognition using time-delay neural networks. IEEE transactions on acoustics, speech, and signal processing, vol. 37, no. 3, pp. 328–339.
- [80] DeCoste, D., & Schölkopf, B. (2002). Training invariant support vector machines. Machine learning, vol. 46, no. 1, pp. 161–190.
- [81] Hsu, C. W., & Lin, C. J. (2002). A comparison of methods for multiclass support vector machines. IEEE transactions on Neural Networks, vol. 13, no. 2, pp. 415–425.
- [82] Zhu, J., Rosset, S., Tibshirani, R., & Hastie, T. (2003). 1-norm support vector machines. Advances in neural information processing systems, vol. 16.
- [83] Cervantes, J., Garcia-Lamont, F., Rodríguez-Mazahua, L., & Lopez, A. (2020). A comprehensive survey on support vector machine classification: Applications, challenges and trends. Neurocomputing, vol. 408, pp. 189–215.
- [84] Cervantes, J., Garcia-Lamont, F., Rodríguez-Mazahua, L., & Lopez, A. (2020). A comprehensive survey on support vector machine classification: Applications, challenges and trends. Neurocomputing, vol. 408, pp. 189–215.
- [85] Chih-Chung, C. (2011, Apr). LIBSVM: a library for support vector machines. ACM transactions on intelligent systems and technology, vol. 2, pp. 27-1.

- [86] LanLan, W., & Youxian, W. (2009). Weed/corn seedling recognition by support vector machine using texture features. *African Journal of Agricultural Research*, vol. 4, no. 9, pp. 840-846.
- [87] Lanlan, W., & Youxian, W. (2010, December). Application of support vector machine for identifying single corn/weed seedling in fields using shape parameters. In *The 2nd International Conference on Information Science and Engineering*. IEEE, pp. 1-4.
- [88] Ahmed, F., Bari, A. H., Shihavuddin, A. S. M., Al-Mamun, H. A., & Kwan, P. (2011, November). A study on local binary pattern for automated weed classification using template matching and support vector machine. In *2011 IEEE 12th International Symposium on Computational Intelligence and Informatics (CINTI)*. IEEE, pp. 329–334.
- [89] Wong, W. K., Chekima, A., Mariappan, M., Khoo, B., & Nadarajan, M. (2014, December). Probabilistic multi svm weed species classification for weed scouting and selective spot weeding. In *2014 IEEE International Symposium on Robotics and Manufacturing Automation (ROMA)*. IEEE, pp. 63-68.
- [90] Athani, S. S., & Tejeshwar, C. H. (2017, January). Support vector machine-based classification scheme of maize crop. In *2017 IEEE 7th International Advance Computing Conference (IACC)*. IEEE, pp. 84–88.
- [91] Sarvini, T., Sneha, T., GS, S. G., Sushmitha, S., & Kumaraswamy, R. (2019, April). Performance comparison of weed detection algorithms. In *2019 International Conference on Communication and Signal Processing (ICCSP)*. IEEE, pp. 843–847.
- [92] Hubel, D. H., & Wiesel, T. N. (1962). Receptive fields, binocular interaction and functional architecture in the cat's visual cortex. *The Journal of physiology*, vol. 160, no. 1, p. 106.
- [93] Fukushima, K., & Miyake, S. (1982). Neocognitron: A self-organizing neural network model for a mechanism of visual pattern recognition. In *Competition and cooperation in neural nets*. Springer, Berlin, Heidelberg, pp. 267–285.
- [94] Waibel, A., Hanazawa, T., Hinton, G., Shikano, K., & Lang, K. J. (1989). Phoneme recognition using time-delay neural networks. *IEEE transactions on acoustics, speech, and signal processing*, vol. 37, no. 3, pp. 328–339.
- [95] Waibel, A., Hanazawa, T., Hinton, G., Shikano, K., & Lang, K. J. (1989). Phoneme recognition using time-delay neural networks. *IEEE transactions on acoustics, speech, and signal processing*, vol. 37, no. 3, pp. 328–339.
- [96] LeCun, Y., Bottou, L., Bengio, Y., & Haffner, P. (1998). Gradient-based learning applied to document recognition. *Proceedings of the IEEE*, vol. 86, no. 11, pp. 2278–2324.
- [97] Krizhevsky, A., Sutskever, I., & Hinton, G. E. (2017). Imagenet classification with deep convolutional neural networks. *Communications of the ACM*, vol. 60, no. 6, pp. 84-90.

- [98] Simonyan, K., & Zisserman, A. (2014). Very deep convolutional networks for large-scale image recognition. arXiv preprint arXiv:1409.1556..
- [99] Szegedy, C., Liu, W., Jia, Y., Sermanet, P., Reed, S., Anguelov, D., ... & Rabinovich, A. (2015). Going deeper with convolutions. In Proceedings of the IEEE conference on computer vision and pattern recognition, pp. 1–9.
- [100] He, K., Zhang, X., Ren, S., & Sun, J. (2016). Deep residual learning for image recognition. In Proceedings of the IEEE conference on computer vision and pattern recognition, pp. 770–778.
- [101] Moshou, D., Vrindts, E., De Ketelaere, B., De Baerdemaeker, J., & Ramon, H. (2001). A neural network based plant classifier. *Computers and electronics in agriculture*, vol. 31, no. 1, pp. 5-16.
- [102] Yang, C. C., Prasher, S. O., & Landry, J. A. (2002). Weed recognition in corn fields using back-propagation neural network models. *Canadian Biosystems Engineering*, vol. 44, pp. 7–15.
- [103] Wu, L., Wen, Y., Deng, X., & Peng, H. (2009). Identification of weed/corn using BP network based on wavelet features and fractal dimension. *Scientific research and essay*, vol. 4, no. 11, pp. 1194–1200.
- [104] Chen, L., Zhang, J. G., Su, H. F., & Guo, W. (2010, July). Weed identification method based on probabilistic neural network in the corn seedlings field. In *2010 international conference on machine learning and cybernetics*. IEEE., vol. 3, pp. 1528–1531.
- [105] Kiani, S., Azimifar, Z., & Kamgar, S. (2010, May). Wavelet-based crop detection and classification. In *2010 18th Iranian Conference on Electrical Engineering*. IEEE., pp. 587–591.
- [106] Bullock, D., Mangeni, A., Wiesner-Hanks, T., DeChant, C., Stewart, E. L., Kaczmar, N., ... & Lipson, H. (2019). Automated Weed Detection in Aerial Imagery with Context. *arXiv preprint arXiv:1910.00652*.
- [107] Dyrmann, M., Mortensen, A. K., Midtiby, H. S., & Jørgensen, R. N. (2016, June). Pixel-wise classification of weeds and crops in images by using a fully convolutional neural network. In *Proceedings of the International Conference on Agricultural Engineering, Aarhus, Denmark*, pp. 26–29.
- [108] Karimi, Y., Prasher, S. O., McNairn, H., Bonnell, R. B., Dutilleul, P., & Goel, P. K. (2005). Classification accuracy of discriminant analysis, artificial neural networks, and decision trees for weed and nitrogen stress detection in corn. *Transactions of the ASAE*, vol. 48, no. 3, pp. 1261–1268.

- [109] Nejati, H., Azimifar, Z., & Zamani, M. (2008, October). Using fast fourier transform for weed detection in corn fields. In *2008 IEEE International Conference on Systems, Man and Cybernetics*. IEEE., pp. 1215-1219.
- [110] Gée, C., Bossu, J., Jones, G., & Truchetet, F. (2008, Jan). Crop/weed discrimination in perspective agronomic images. *Computers and Electronics in Agriculture*, vol. 60, no. 1, pp. 49–59.
- [111] Bossu, J., Gée, C., Jones, G., & Truchetet, F. (2009, Jan). Wavelet transform to discriminate between crop and weed in perspective agronomic images. *computers and electronics in agriculture*, vol. 65, no. 1, pp. 133–143.
- [112] Asif, M., Amir, S., Israr, A., & Faraz, M. (2010). A vision system for autonomous weed detection robot. *International Journal of Computer and Electrical Engineering*, vol. 2, no. 3, p. 486.
- [113] Longchamps, L., Panneton, B., Samson, G., Leroux, G. D., & Thériault, R. (2010). Discrimination of corn, grasses and dicot weeds by their UV-induced fluorescence spectral signature. *Precision Agriculture*, vol. 11, no. 2, pp. 181–197.
- [114] Burgos-Artizzu, X. P., Ribeiro, A., Guijarro, M., & Pajares, G. (2011). Real-time image processing for crop/weed discrimination in maize fields. *Computers and Electronics in Agriculture*, vol. 75, no. 2, pp. 337–346.
- [115] Liu, X., Li, M., Sun, Y., & Deng, X. (2010). Support vector data description for weed/corn image recognition. *Journal of Food, Agriculture and Environment*, vol. 8, no. 1, pp. 214–219.
- [116] Montalvo, M., Pajares, G., Guerrero, J. M., Romeo, J., Guijarro, M., Ribeiro, A., ... & Cruz, J. M. (2012, Nov). Automatic detection of crop rows in maize fields with high weeds pressure. *Expert Systems with Applications*, vol. 39, no. 15, pp. 11889–11897.
- [117] Andújar, D., Rueda-Ayala, V., Moreno, H., Rosell-Polo, J. R., Escolà, A., Valero, C., ... & Griepentrog, H. W. (2013). Discriminating crop, weeds and soil surface with a terrestrial LIDAR sensor. *Sensors*, vol. 13, no. 11, pp. 14662-14675.
- [118] Shirzadifar, A. M. (2013, February). Automatic weed detection system and smart herbicide sprayer robot for corn fields. In *2013 First RSI/ISM International Conference on Robotics and Mechatronics (ICRoM)*. IEEE., pp. 468-473.
- [119] Lavania, S., & Matey, P. S. (2015, February). Novel method for weed classification in maize field using Otsu and PCA implementation. In *2015 IEEE International Conference on Computational Intelligence & Communication Technology*. IEEE., pp. 534–537.
- [120] Pantazi, X. E., Moshou, D., & Bravo, C. (2016). Active learning system for weed species recognition based on hyperspectral sensing. *Biosystems Engineering*, vol. 146, pp. 193–202.

- [121] Lin, F., Zhang, D., Huang, Y., Wang, X., & Chen, X. (2017, Aug). Detection of corn and weed species by the combination of spectral, shape and textural features. *Sustainability*, vol. 9, no. 8, pp. 1335.
- [122] Gao, J., Nuyttens, D., Lootens, P., He, Y., & Pieters, J. G. (2018). Recognising weeds in a maize crop using a random forest machine-learning algorithm and near-infrared snapshot mosaic hyperspectral imagery. *Biosystems engineering*, vol. 170, pp. 39–50.
- [123] Zheng, Y., Zhu, Q., Huang, M., Guo, Y., & Qin, J. (2017). Maize and weed classification using color indices with support vector data description in outdoor fields. *Computers and Electronics in Agriculture*, vol. 141, pp. 215–222.
- [124] Figueroa, R. L., Zeng-Treitler, Q., Kandula, S., & Ngo, L. H. (2012). Predicting sample size required for classification performance. *BMC medical informatics and decision making*, vol. 12, no. 1.
- [125] Durden, J. M., Hosking, B., Bett, B. J., Cline, D., & Ruhl, H. A. (2021, Aug). Automated classification of fauna in seabed photographs: The impact of training and validation dataset size, with considerations for the class imbalance. *Progress in Oceanography*, vol. 196, pp. 102612.
- [126] Beleites, C., Neugebauer, U., Bocklitz, T., Krafft, C., & Popp, J. (2013, Jan). Sample size planning for classification models. *Analytica chimica acta*, vol. 760, pp. 25–33.
- [127] Alwosheel, A., van Cranenburgh, S., & Chorus, C. G. (2018, Sep). Is your dataset big enough? Sample size requirements when using artificial neural networks for discrete choice analysis. *Journal of choice modelling*, vol. 28, pp. 167–182.
- [128] Althnian, A., AlSaeed, D., Al-Baity, H., Samha, A., Dris, A. B., Alzakari, N., ... & Kurdi, H. (2021). Impact of dataset size on classification performance: an empirical evaluation in the medical domain. *Applied Sciences*, vol. 11, no. 2, p. 796.
- [129] Caluña, G., Guachi-Guachi, L., & Brito, R. (2020, July). Convolutional neural networks for automatic classification of diseased leaves: the impact of dataset size and fine-tuning. In *International Conference on Computational Science and Its Applications*. Springer, Cham., pp. 951–966.
- [130] Luo, C., Li, X., Wang, L., He, J., Li, D., & Zhou, J. (2018, November). How does the data set affect cnn-based image classification performance?. In *2018 5th International conference on systems and informatics (ICSAI)*. IEEE., pp. 361–366.
- [131] Ying, X. (2019, February). An overview of overfitting and its solutions. In *Journal of physics: Conference series*. IOP Publishing., vol. 1168, no. 2, pp. 0222022.
- [132] Dietterich, T. (1995). Overfitting and undercomputing in machine learning. *ACM computing surveys (CSUR)*, vol. 27, no. 3, pp. 326-327.

- [133] Mikołajczyk, A., & Grochowski, M. (2018, May). Data augmentation for improving deep learning in image classification problem. In *2018 international interdisciplinary PhD workshop (IIPhDW)*. IEEE., pp. 117–122.
- [134] Shorten, C., & Khoshgoftaar, T. M. (2019, Dec). A survey on image data augmentation for deep learning. *Journal of big data*, vol. 6, no. 1, pp. 1-48.
- [135] Taylor, L., & Nitschke, G. (2018, November). Improving deep learning with generic data augmentation. In *2018 IEEE Symposium Series on Computational Intelligence (SSCI)*. IEEE., pp. 1542–1547.
- [136] Jurio, A., Pagola, M., Galar, M., Lopez-Molina, C., & Paternain, D. (2010, June). A comparison study of different color spaces in clustering based image segmentation. In *International conference on information processing and management of uncertainty in knowledge-based systems*. Springer, Berlin, Heidelberg., pp. 532–541.
- [137] Zhong, Z., Zheng, L., Kang, G., Li, S., & Yang, Y. (2020, April). Random erasing data augmentation. In *Proceedings of the AAAI conference on artificial intelligence*, vol. 34, no. 07, pp. 13001-13008.
- [138] Inoue, H. (2018). Data augmentation by pairing samples for images classification. *arXiv preprint arXiv:1801.02929*.
- [139] Summers, C., & Dinneen, M. J. (2019, January). Improved mixed-example data augmentation. In *2019 IEEE Winter Conference on Applications of Computer Vision (WACV)*. IEEE., pp. 1262–1270.
- [140] DeVries, T., & Taylor, G. W. (2017). Dataset augmentation in feature space. *arXiv preprint arXiv:1702.05538*.
- [141] Goodfellow, I., Pouget-Abadie, J., Mirza, M., Xu, B., Warde-Farley, D., Ozair, S., ... & Bengio, Y. (2020). Generative adversarial networks. *Communications of the ACM*, vol. 63, no. 11, pp. 139-144.
- [142] Zhuang, F., Qi, Z., Duan, K., Xi, D., Zhu, Y., Zhu, H., ... & He, Q. (2020). A comprehensive survey on transfer learning. *Proceedings of the IEEE*, vol. 109, no. 1, pp. 43–76.
- [143] Pan, S. J., & Yang, Q. (2009). A survey on transfer learning. *IEEE Transactions on knowledge and data engineering*, vol. 22, no. 10, pp. 1345-1359.
- [144] Espejo-Garcia, B., Mylonas, N., Athanasakos, L., Fountas, S., & Vasilakoglou, I. (2020). Towards weeds identification assistance through transfer learning. *Computers and Electronics in Agriculture*, vol. 171, pp. 105306.
- [145] Suh, H. K., Ijsselmuiden, J., Hofstee, J. W., & van Henten, E. J. (2018). Transfer learning for the classification of sugar beet and volunteer potato under field conditions. *Biosystems engineering*, vol. 174, pp. 50–65.



- [146] Kaya, A., Keceli, A. S., Catal, C., Yalic, H. Y., Temucin, H., & Tekinerdogan, B. (2019). Analysis of transfer learning for deep neural network based plant classification models. *Computers and electronics in agriculture*, vol. 158, pp. 20–29, 2019.
- [147] Zhao, W., Yamada, W., Li, T., Digman, M., & Runge, T. (2020). Augmenting Crop Detection for Precision Agriculture with Deep Visual Transfer Learning—A Case Study of Bale Detection. *Remote Sensing*, vol. 13, no. 1, pp. 23.
- [148] Thenmozhi, K., & Reddy, U. S. (2019). Crop pest classification based on deep convolutional neural network and transfer learning. *Computers and Electronics in Agriculture*, vol. 164, pp. 104906.
- [149] Sen, D., Kundu, A., & Barnwal, R. P. (2020) Transfer learning for robust paddy and weed classification in precision agriculture: A reverse approach. *International Journal of Computer Applications*, pp. 975–8887.
- [150] Lu, H., Fu, X., Liu, C., Li, L. G., He, Y. X., & Li, N. W. (2017). Cultivated land information extraction in UAV imagery based on deep convolutional neural network and transfer learning. *Journal of Mountain Science*, vol. 14, no. 4, pp. 731–741.
- [151] Li, Q., Wang, Z., Shangguan, W., Li, L., Yao, Y., & Yu, F. (2021). Improved daily SMAP satellite soil moisture prediction over China using deep learning model with transfer learning. *Journal of Hydrology*, vol. 600, pp. 126698.
- [152] Coulibaly, S., Kamsu-Foguem, B., Kamissoko, D., & Traore, D. (2019). Deep neural networks with transfer learning in millet crop images. *Computers in Industry*, vol. 108, pp. 115–120.
- [153] Bosilj, P., Aptoula, E., Duckett, T., & Cielniak, G. (2020). Transfer learning between crop types for semantic segmentation of crops versus weeds in precision agriculture. *Journal of Field Robotics*, vol. 37, no. 1, pp. 7–19.
- [154] Sokolova, M., & Lapalme, G. (2009). A systematic analysis of performance measures for classification tasks. *Information processing & management*, vol. 45, no. 4, pp. 427–437.
- [155] Fawcett, T. (2006). An introduction to ROC analysis. *Pattern recognition letters*, vol. 27, no. 8, pp. 861–874.
- [156] Naser, M. Z., & Alavi, A. H. (2021). Error metrics and performance fitness indicators for artificial intelligence and machine learning in engineering and sciences. *Architecture, Structures and Construction*, pp. 1-19.
- [157] Naser, M. Z., & Alavi, A. (2020). Insights into performance fitness and error metrics for machine learning. *arXiv preprint arXiv:2006.00887*.

- [158] Wang, J., Li, M., Zhang, J., Zeng, W., & Yang, X. (2019, April). DCNN Transfer Learning and Multi-Model Integration for Disease and Weed Identification. In *Chinese Conference on Image and Graphics Technologies*. Springer, Singapore., pp. 216–227.
- [159] Wang, S., Han, Y., Chen, J., Pan, Y., Cao, Y., & Meng, H. (2020). A transfer-learning-based feature classification algorithm for UAV imagery in crop risk management. *Desalination Water Treat*, vol. 181, pp. 330–337.
- [160] Chen, D., Lu, Y., Li, Z., & Young, S. (2022, Apr). Performance evaluation of deep transfer learning on multi-class identification of common weed species in cotton production systems. *Computers and Electronics in Agriculture*, vol. 198, pp. 107091.
- [161] Jose, J. A., Sharma, A., Sebastian, M., & Densil, R. V. F. (2022, January). Classification of Weeds and Crops using Transfer Learning. In *2022 International Conference on Advances in Computing, Communication and Applied Informatics (ACCAI)*. IEEE., pp. 1–7.
- [162] Rudin, C. (2014, August). Algorithms for interpretable machine learning. In *Proceedings of the 20th ACM SIGKDD international conference on Knowledge discovery and data mining*, pp. 1519-1519.
- [163] Nori, H., Jenkins, S., Koch, P., & Caruana, R. (2019). Interpretml: A unified framework for machine learning interpretability. *arXiv preprint arXiv:1909.09223*.
- [164] Chauhan, N. K., & Singh, K. (2018, September). A review on conventional machine learning vs deep learning. In *2018 International conference on computing, power and communication technologies (GUCON)*. IEEE., pp. 347–352.
- [165] Breiman, L. (2001). Random forests. *Machine learning*, vol. 45, no. 1, pp. 5-32.
- [166] Zhao, Z. Q., Zheng, P., Xu, S. T., & Wu, X. (2019). Object detection with deep learning: A review. *IEEE transactions on neural networks and learning systems*, vol. 30, no. 11, pp. 3212–3232.
- [167] Jeong, J., Lee, S., Kim, J., & Kwak, N. (2019). Consistency-based semi-supervised learning for object detection. *Advances in neural information processing systems*, vol. 32.
- [168] Bozinovski, S. (2020). Reminder of the first paper on transfer learning in neural networks, 1976. *Informatica*, vol. 44, no. 3.
- [169] Bengio, Y., Bengio, S., & Cloutier, J. (1990). *Learning a synaptic learning rule*. Université de Montréal, Département d'informatique et de recherche opérationnelle., pp. 969-975.
- [170] Caruana, R. (1993). Multitask learning: A knowledge-based source of inductive bias1. In *Proceedings of the Tenth International Conference on Machine Learning*, pp. 41–48.
- [171] Caruana, R., Silver, D. L., Baxter, J., Mitchell, T. M., Pratt, L. Y. & Thrun, S. (1995). Learning to learn: knowledge consolidation and transfer in inductive systems.

- [172] Caruana, R. (1997). Multitask learning. *Machine learning*, vol. 28, no. 1, pp. 41–75.
- [173] Thrun, S., & Pratt, L. (1998). Learning to learn: Introduction and overview. In *Learning to learn*. Springer, Boston, MA, pp. 3-17.
- [174] Silver, D. L., & Mercer, R. E. (2002, May). The task rehearsal method of life-long learning: Overcoming impoverished data. In *Conference of the Canadian Society for Computational Studies of Intelligence*. Springer, Berlin, Heidelberg., pp. 90–101.
- [175] Silver, D. L., & Poirier, R. (2007, May). Context-Sensitive MTL Networks for Machine Lifelong Learning. In *FLAIRS Conference*, pp. 628–633.
- [176] Rückert, U., & Kramer, S. (2008, September). Kernel-based inductive transfer. In *Joint European Conference on Machine Learning and Knowledge Discovery in Databases*. Springer, Berlin, Heidelberg., pp. 220–233.
- [177] Huang, J. T., Li, J., Yu, D., Deng, L., & Gong, Y. (2013, May). Cross-language knowledge transfer using multilingual deep neural network with shared hidden layers. In *2013 IEEE International Conference on Acoustics, Speech and Signal Processing*. IEEE., pp. 7304–7308.
- [178] Silver, D. L. (2013, March). The consolidation of task knowledge for lifelong machine learning. In *2013 AAAI Spring Symposium Series*.
- [179] Lu, J., Behbood, V., Hao, P., Zuo, H., Xue, S., & Zhang, G. (2015). Transfer learning using computational intelligence: A survey. *Knowledge-Based Systems*, vol. 80, pp. 14–23.
- [180] Weiss, K., Khoshgoftaar, T. M., & Wang, D. (2016). A survey of transfer learning. *Journal of Big data*, vol. 3, no. 1, pp. 1–40.
- [181] Tan, C., Sun, F., Kong, T., Zhang, W., Yang, C., & Liu, C. (2018, October). A survey on deep transfer learning. In *International conference on artificial neural networks*. Springer, Cham., pp. 270–279.
- [182] Sarkar, D., Bali, R., & Ghosh, T. (2018). *Hands-On Transfer Learning with Python: Implement advanced deep learning and neural network models using TensorFlow and Keras*. Packt Publishing Ltd.
- [183] Palmwer Amaranth Testing, *National Corn Growers Association*.
- [184] U of M researchers develop 99.9% accurate genetic test for early detection of Palmer Amaranth. (2021, Apr), *University of Minnesota*.